wawi

INSTITUT FÜR HYDROLOGIE UND WASSERWIRTSCHAFT

Mitteilungen Heft 109

Agro-hydrological Modelling of Regional Irrigation Water Demand

Agro-hydrological Modelling of Regional Irrigation Water Demand

Von der Fakultät für Bauingenieurwesen und Geodäsie
der Gottfried Wilhelm Leibniz Universität Hannover

zur Erlangung des akademischen Grades
Doktor-Ingenieurin
- Dr.-Ing. -

genehmigte Dissertation

von

Bhumika Uniyal, M.Tech.
geboren am 25.01.1990 in Dehradun (Indien)

Hannover, September 2019

Referent: PD. Dr.-Ing. Jörg Dietrich
Korreferentin: Prof. Dr. Nicola Fohrer

Tage der Promotion: 19.12.2019

Erklärung

Hiermit versichere ich eidesstattlich, dass ich

1. die Regeln der geltenden Promotionsordnung kenne und eingehalten habe und mit einer Prüfung nach den Bestimmungen der Promotionsordnung einverstanden bin,

2. die Dissertation selbst verfasst habe, keine Textabschnitte von Dritten oder eigener Prüfungsarbeiten ohne Kennzeichnung übernommen und alle von mir benutzten Hilfsmittel und Quellen in meiner Arbeit angegeben habe,

3. Dritten weder unmittelbar noch mittelbar geldwerte Leistungen für Vermittlungstätigkeiten oder für die inhaltliche Ausarbeitung der Dissertation erbracht habe,

4. die vorliegende Dissertation noch nicht als Prüfungsarbeit fur eine staatliche oder andere wissenschaftliche Prüfung eingereicht habe,

5. die gleiche oder eine in wesentlichen Teilen ähnliche Arbeit bei keiner anderen Hochschule als Dissertation eingereicht habe und auch keine andere Abhandlung als Dissertation habe,

6. damit einverstanden bin, dass die Dissertation auch zum Zwecke der Überprufung der Einhaltung allgermein geltender wissenschaftlicher Standards genutzt wird, insbesondere auch unter Verwendung elektronischer Datenverarbeitungsprogramme.

Hannover, 18.09.2019

Abstract

The irrigation sector accounts for over 70% of the total freshwater consumption in the world. Therefore, efficient management of irrigation water is essential to ensure water, food, energy and environmental securities in a sustainable manner; these securities are grand challenges of the 21st century. The main objective of this research is to evaluate the simulation of irrigation water demand at the catchment scale in order to develop improved tools for conducting quantitative planning and climate change studies. Irrigation water demand is mostly driven by soil moisture. It is a state variable which is used to trigger the irrigation in hydrological models. In this study, a hydrolgical model (Soil and Water Assessment Tool, SWAT) is evaluated for reliably simulating the spatial and temporal patterns of soil moisture at a catchment scale. The SWAT simulated soil moisture was compared with the indirect estimates of soil moisture from Landsat and Time-domain reflectometry (TDR). The results showed that the SWAT simulated soil moisture was comparable with the soil moisture estimated from Landsat and TDR.

Secondly, the applicability of the SWAT model was tested for simulating streamflow, evapotranspiration (ET) and irrigation water demand for four different agro-climatic zones (Mediterranean, Subtropical monsoon, Humid, and Tropical). Two different irrigation scheduling techniques were used to simulate irrigation namely, soil water deficit and plant water demand. It was seen from the results that the SWAT simulated irrigation amounts under soil moisture irrigation scheduling technique were close to the irrigation statistics provided by the state. However, the irrigation amounts simulated under the plant water demand irrigation scheduling technique were underestimated. Additionally, the two reanalysis data were also used to check the data uncertainty in simulating irrigation water demand.

SWAT model code was modified by incorporating modified root density distribution function and dynamic stress factor. The modified model was used to simulate irrigation and crop yield. It was tested against the irrigation and crop yield simulated by Soil Water Atmosphere Plant (SWAP) model and field data (Hamerstorf, Lower Saxony, Germany). It was then validated for different catchments (Germany, India and Vietnam). The results showed that the SWAT simulated irrigation water demand in case of plant water demand is comparable with the amount simulated by the model under soil water deficit irrigation scheduling technique.

This dissertation not only bridges the gap between the scales of soil moisture determination but also establishes a close connection with the actual observations and modelled soil moisture and irrigation amounts at the field, regional and global studies in agricultural water management. Additionally, the studies about simulating irrigation water requirement in data-scarce areas must address data uncertainty when using reanalysis data. It was found that rainfall is not always

the dominant variable in irrigation simulation. Therefore, it is worth checking and bias correct the other climate variables.

Zusammenfassung

Der Bewässerungswasserverbrauch macht über 70% des gesamten verfügbaren Süßwassers aus. Daher ist die Bewirtschaftung des Bewässerungswassers für ein effizientes landwirtschaftliches Wassermanagement und damit für eine nachhaltige Deckung des weltweiten Nahrungsmittelbedarfs unerlässlich. Hauptziel dieser Forschung ist die Simulation des Bewässerungsbedarfs im Einzugsgebiet, um bessere Instrumente für die Durchführung quantitativer Planungs- und Klimaänderungsstudien zu haben. Der Bedarf an Bewässerungswasser wird hauptsächlich durch die Bodenfeuchtigkeit bestimmt. Es ist eine Zustandsvariable, mit der die Bewässerung in hydrologischen Modellen ausgelöst wird. In dieser Studie wird ein hydrologisches Modell (Soil and Water Assessment Tool, SWAT) evaluiert, um die räumlichen und zeitlichen Muster der Bodenfeuchte auf einer Einzugsskala zuverlässig zu simulieren. Die mit SWAT simulierte Bodenfeuchte wurde mit den indirekten Schätzungen der Bodenfeuchte aus Landsat und Reflektometrie verglichen (TDR). Die Ergebnisse zeigten, dass die von SWAT simulierte Bodenfeuchte mit der von Landsat und TDR geschätzten Bodenfeuchte vergleichbar war.

Zweitens wurde die Anwendbarkeit des SWAT-Modells für die Simulation von abfluss, Evapotranspiration (ET) und Bewässerungswasserbedarf für vier verschiedeneAgro-Klimazonen (Mittelmeer, subtropischer Monsun, feucht und tropisch) getestet. Zwei verschiedene Bewässerungssteuerungstechniken wurden verwendet, um die Bewässerung zu simulierennämlich Bodenwasserdefizit und Pflanzenwasserbedarf. Es wurde aus den Ergebnissen gesehen, dass die von SWAT simulierte Bewässerungsmenge unter Bodenfeuchtigkeitsbewässerung in etwa der vom Staat bereitgestellten Bewässerungsstatistik entsprach. Die Bewässerungsmengen werden jedoch unter Pflanzenwasserbedarf unterschätzt. Zusätzlich wurden auch zwei Reanalysedaten verwendet, um die Datenunsicherheit bei der Simulation zu überprüfen.

Der SWAT-Modellcode wurde durch Einbeziehung der modifizierten Wurzeldichte, Verteilungsfunktion und dynamischer Spannungsfaktor verbessert. Das modifizierte Modell wurde verwendet, um Bewässerung und Ernteertrag zu simulieren. Es wurde gegen eine Modellierung mit dem Standartmodell SWAP (Soil Water Atmosphere Plant) Felddaten getestet (Hamerstorf, Niedersachsen, Deutschland) und validiert für verschiedene Einzugsgebiete (Deutschland, Indien) und Vietnam). Die Ergebnisse zeigen, dass das modifizierte SWAT mit den beiden steuerungstechniken "Bodenwasser" und "Pflanzenwasserbedarf" ahnliche Ergebnisse erzielen Kann.

Diese Dissertation schließt nicht nur die Lücke zwischen den Maßstäben der Bodenfeuchte Messungen stellen aber auch eine enge Verbindung zu den tatsächlichen Beobachtungen her und modellierte Bodenfeuchtigkeits- und

Bewässerungsmengen vor Ort, regional und global Studien in landwirtschaftlicher Wasserwirtschaft. Darüber hinaus sind die Studien über Die Simulation des Bewässerungswasserbedarfs in datenarmen Gebieten muss sich mit Daten befassen Unsicherheit bei der Verwendung von Reanalysedaten. Es wurde festgestellt, dass Regen nicht immer fällt die dominierende Variable in der Bewässerungssimulation. Daher lohnt es sich zu prüfen und Bias korrigieren die anderen Klimavariablen.

Contents

List of Tables

List of Figures

Abbreviations

ABA	Abscisic acid
AHP	Analytical Hierarchy Process
MSL	Mean Sea Level
ASCAT	Advanced SCATterometer
AVHRR	Advanced Very High Resolution Radiometer
BGR	Bundesanstalt für Geowissenschaften und Rohstoffe
BT	Brightness Temperature
CADSM	Command Area Decision Support Model
CERES	Crop Estimation through Resource and Environment Synthesis
CIMMYT	International Maize and Wheat Improvement Centre
CSIL	Corn Silage
DEM	Digital Elevation Model
DSSAT	Decision Support System for Agrotechnology Transfer
DWD	Deutscher Wetterdienst
ECMWF	European Centre for Medium-Range Weather Forecasts
EnKF	Ensemble Kalman Filter
EPIC	Erosion Productivity Impact Calculator
ERS	European Remote Sensing
ET	Evapotranspiration
FAO	Food and Agriculture Organization
FEWS-Net	Famine Early Warning Systems Network
GIS	Geographic Information System
GPR	Ground Penetrating Radar
GLUE	Generalized Likelihood Uncertainty Estimation
GRACE	Gravity Recovery and Climate Experiment
HRU	Hydrologic Response Unit
KGE	Kling-Gupta Efficieny
Landsat	Land Remote-Sensing Satellite
LBEG	Landesamt fur Bergbau, Energie und Geologie
LAI	Leaf Area Index
LST	Land Surface Temperature
LWK	Landwirtschaftskammer, Neidersachen
MAD	Management Allowable Depletion
MODIS	Moderate Resolution Imaging Spectroradiometer
NCEP	National Centres for Enviornmental Prediction
NASA	National Aeronautics and Space Administration
NOAA	National Oceanic and Atmospheric Administration
NDVI	Normalized Difference Vegetation Index
NLWKN	Niedersächsische Landesbetrieb für Wasserwirtschaft, Küsten- & Naturschutz
NSE	Nash–Sutcliffe Efficiency

PBIAS   Percentage BIAS
POTA   Potato
PREVAH   Precipitation-Runoff-Evapotranspiration-Hydrotope
RWU   Root Water Uptake
SEBAL   Surface Energy Balance Algorithm for Land
SHE   Système Hydrologique Européen
SMAP   Soil Moisture Active Passive
SMOS   Soil Mooisture Occean Salinity
SGBT   Sugar beet
SLURP   Semi-distributed, Land-Use-based, Runoff Processes
SW   Plant available water content
SWAP   Soil Water Atmosphere Plant
SWAT   Soil and Water Assessment Tool
SWAT-CUP   SWAT Calibration and Uncertainty Procedures
TDR   Time Domain Reflectometer
TRMM   Tropical Rainfall Measuring Mission
TVDI   Thermal Vegetation Difference Index
US   United States
UTC   Universal Time Coordinated
VIC   Variable Infiltration Capacity
WEAP   Water Evaluation And Planning system
WOFOST   WOrld FOod STudies
WHCNS   Water Heat Carbon Nitrogen Simulator
WUE   Water Use Efficiency
WP   Wilting Point
WWHT   Winter wheat
95PPU   95% Parameter Uncertainty

Chapter 1
Motivation and Objectives

1.1 Background

Water is one of the vital natural resources that the sustain functioning of ecosystems, human development, and economic growth of a country. Agricultural water use accounts for a major (around 70 %) portion of the world's water resources with vast variation across countries (Molden, 2013). The global demand for water is increasing at the rate of 1% per year from the past decade due to population rise, economic development, changing consumption patterns, etc. This trend is expected to surge exponentially in the future (Houngbo, 2018). Currently, the irrigated agriculture area accounts for 18% of the total agriculture which is majorly concentrated in the developing countries (Rockström and Falkenmark, 2000; Siebert et al., 2000; Scanlon et al., 2007).

Increase in irrigation water demand is generally recognized as the reason of depleting water resources in many parts of the world (Zhu et al., 2018). There are several examples around the world where improper irrigation water management has led to the depletion of available water resources. Some of these include the disappearing Aral Sea (Peachey, 2004), drying of Yellow river, China (Ongley, 2000) and Lake Urmia in Iran (Tourian et al., 2015; Nihoul et al., 2012), alarming groundwater depletion in North India (Rodell et al., 2009) and in high plains and central valley of United States (Scanlon et al., 2012). Additionally, improper reservoir water management has led to serious agricultural drought in many districts of Maharashtra, India with 26 of its major dam hitting zero water storage level on May 18, 2019 (Government of Maharashtra, Water Resources Department: `http://www.punefloodcontrol.com/krishna%20Basin.html`). In 2018 Cape Town, South Africa experienced severe drought which resulted in extremely low reservoir water level leading to shortage in the potable water supply (Maxmen, 2018).

Increase of regional irrigation water demand along with the existing water scarcity will limit the expansion of irrigated agricultural areas and might slow down the production of high water demanding crops (Rosegrant et al., 2009). Other issues like salinization, water-logging, erosion, etc., [(Joshi and Agnihotri, 1984); `http://www.fao.org/3/V8350E/v8350e09.htm`] will persist. This will not only affect agricultural production but will also threaten the future world food security. Thus, both water and food security depend on efficient water management techniques which enhance the regional water productivity in agriculture (Zhu et al., 2018). Some of the techniques include the use of deficit irrigation strategies or growing water-efficient crops. In addition, the latest World Water Development Report by the United Nations emphasizes finding nature-based solutions to the current and unforeseen future water crisis (Houngbo, 2018). Organic soil remedies, implementation of buffer strips, restoring wetlands are few examples of nature-based solutions that will not only benefit in improving the overall food production but will also help us in attaining environmental sustainability (Foley et al., 2011).

Irrigation water demand mostly depends on soil water availability and plant water demand. Soil water availability plays an important role in enhancing the water use efficiency (water productivity) in irrigated agricultural fields which further enhances the overall crop production. Soil moisture is a key state variable generally expressed as, the water present in the root zone which interacts with the atmosphere via the process of evapotranspiration (ET) and precipitation (Houser et al., 1998). Soil moisture has different roles and significance for agriculturalist, hydrologists and meteorologist etc., (Brocca et al., 2010). Soil moisture estimation plays a major role in controlling the hydrological processes that occur at the catchment scale during both extreme and average long-term conditions. It controls the partitioning of precipitation into surface runoff and infiltration (Grayson and Western, 1998; Brocca et al., 2010). Soil moisture links the water cycle and energy budget of land surfaces via regulation of latent heat fluxes. Therefore, its meticulous assessment at different spatial and temporal scales is necessary for understanding the bio-geophysical processes occurring in nature (Houser et al., 1998). A good estimation of soil moisture and plant water demand in terms of actual ET is required to quantify the irrigation amounts to be applied on a field, catchment and global scale.

Agricultural or hydrological models are the analytical tools used for water resources management, irrigation planning, and climate change adaptation. These models often use soil moisture to trigger the irrigation operations. So, in order to improve irrigation scheduling and yield forecasting, correct soil moisture information is required (Schmugge et al., 1980). Observed data is always required to calibrate these analytical tools in order to have a practical response to a specific input. The collection of observed soil moisture and irrigation water amount data is an exhaustive and time-consuming process. Furthermore, the management decisions are mostly taken at watershed/regional scale and not at point/field scale. In order to overcome these discrepancies, scientists are favouring the indirect ways of estimating soil moisture and crop growth process. This is being estimated in terms of different soil moisture indices and leaf area index using remote sensing datasets. Additionally, scientists also use advanced geo-spatial datasets to evaluate the response of different water balance components (e.g., ET and soil moisture) on crop growth. Therefore, the combination of remote sensing, field scale measurements/models and catchment scale hydrological models are preferred to bridge the gap between point/regional scale to global scale in simulating soil moisture and irrigation water demand.

1.2 Motivation and Objectives

The agro-hydrological modelling at catchment was performed to answer the following questions:

- *How good is the soil moisture simulated by catchment models?* Its correct simulation is required as it is the limiting variable for plant growth and a control variable for irrigation scheduling.

- *How good is the plant growth simulated by catchment models?* This is required as yield is an important agricultural and economic output which

depends on ET. It is an important hydrological variable in terms of water demand/consumption.

- *How good are catchment models in different regions?* This is required as irrigation water demand is a global issue and it is vital to check whether a specific catchment model is able to simulate different agro-climatic regions around the world with the same level of accuracy.

The main focus is to check *how irrigation water demand will differ with the changing climate*, which directly entails questions about existing capabilities of the hydrological models in simulating soil moisture and irrigation water demand in different agro-climates. The previous studies have revealed the relation between irrigation water demand and meteorological data (Wada et al., 2013). In this study, it was questioned *whether its estimation would be possible with less uncertainty in data sufficient and data-scarce catchments.*

To answer these questions, a hydrological model Soil and Water Assessment Tool (SWAT) is used in this study. At the beginning of this work, the literature review revealed that irrigation studies at regional scale were analyzed by very few researchers in different agro-climatic zones, in contrast to water management studies, which have been of scientific and administrative interest for quite some time. In view of the vast number of studies dealing with the impact of regional climate change on the fate of water resources, there is a need to quantify the reliable estimates of irrigation water demand, even for the humid climate (Maier and Dietrich, 2016). Knowledge about irrigation water demand in different agro-climatic zones is important for the farming community who depend heavily on irrigation for growing their crops. Automatic irrigation in SWAT is triggered by defining plant water stress or soil water deficit. It was reported in the previous literature that the irrigation amounts simulated under plant water stress irrigation scheduling technique are consistent with the amounts simulated under soil water deficit technique.

The main technical innovations of this work are to compare the regional scale agro-hydrological models using Soil and Water Assessment Tool (SWAT) in different climatic zones. Also, the SWAT simulated irrigation scheduling using plant water uptake technique is modified to bring it closer to the one simulated under soil water deficit technique. It was seen from the state statistics of all the different catchments used in this study that the irrigation amounts simulated by SWAT under soil water deficit condition were close to the observed data. Bias-corrected reanalysis data was also used to check the overall uncertainty in simulating irrigation water demand simulated by SWAT at catchment scale which is explored by very few researchers till now.

The goal of this work is to first evaluate the spatial and temporal behaviour of SWAT soil moisture using direct and indirect estimates of soil moisture obtained from the field and remote sensing data. As hydrological models are parameter sensitive, the effect of soil moisture on parameter uncertainty was also evaluated under different soil and land-use combinations. Thereafter, the application of SWAT for simulating

irrigation water requirement under four different agro-climatic zones was evaluated. MODIS ET was used to check the plant water requirement simulated by SWAT. The next step was to simulate irrigation water demand in different irrigation control scenarios by SWAT.

Later on, for better simulation of irrigation scheduling using plant water demand technique a modified version of SWAT was proposed. The objective was not to outperform the existing irrigation amounts simulated by the model under soil water deficit irrigation scheduling technique rather, it was to improve both scheduling technique by modifying the SWAT code using modified root density distribution function along with the dynamic estimation of soil water compensation factor. The selected technique is applicable irrespective of the catchment and the type of crop grown with no extra processing time. Thus, the modified model will ideally be able to better simulate the regional irrigation water demand for different agro-climatic conditions. Additionally, the study enabled the investigation of irrigation amount simulated in soil water deficit using the modified model.

Thesis Structure and Overview

This thesis deals with the agro-hydrological simulation of regional irrigation water demand. Agricultural water demand is simulated by using SWAT. For this, several irrigation scheduling techniques and different water deficit scenarios are compared and analyzed. This thesis is the result of the compilation of three papers published by the researcher as a first author during her Ph.D. period. Chapters 3-5 are scientifically complete by themselves as they consist of the introduction, state of the art, methodology, and result and discussions corresponding to the objectives described. There are two major topics covered in this research namely soil moisture and irrigation simulation. The soil moisture is a state variable used for triggering irrigation in hydrological models. Therefore, the soil moisture simulated by SWAT model was evaluated against the field and Landsat derived soil moisture estimates. A flow chart is included in this section, Fig. 1.1 to show how the workflow has been undertaken. Additionally, the soil moisture field campaign data is also put online by the authors to promote data sharing (Uniyal and Dietrich, 2019a).

The second major topic deals with evaluating the performance of SWAT in simulating irrigation water demand under different auto-irrigation scheduling techniques for different agro-climates. In SWAT, irrigation is triggered by using soil water deficit and plant water stress. The irrigation simulated under the two techniques were compared with the respective state statistics. Later on, SWAT model code was modified to better simulate the irrigation water demand under plant water stress technique (Fig. 1.2).
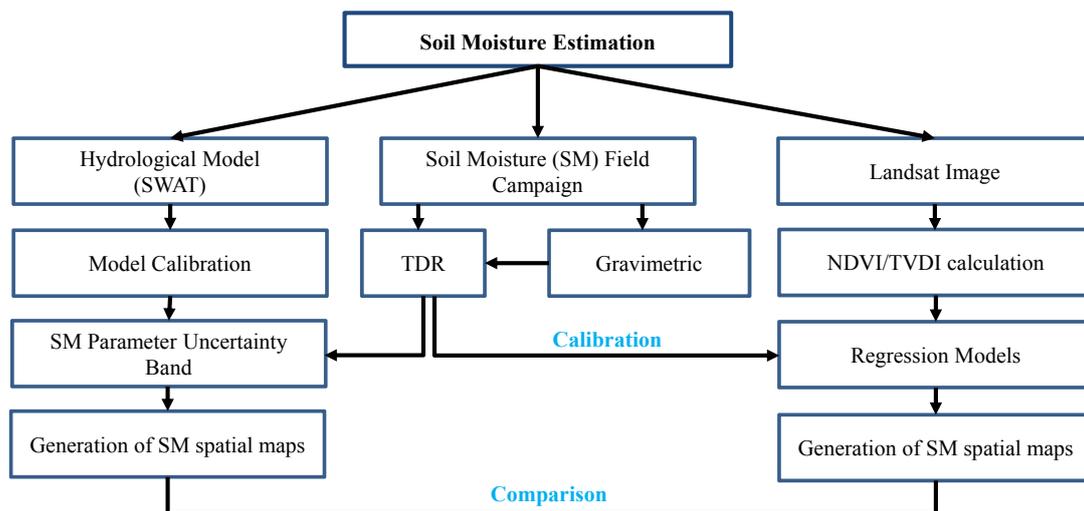
Figure 1.1: Flow chart of soil moisture evaluation.

The work is accordingly structured in the following way:

1. Chapter 1 describes the motivation behind this study and states the different objectives involved.

2. Chapter 2 provides an overview of the state of the art in the field of soil moisture measurement and simulations and simulation of irrigation water demand at field and catchment scale.

3. Chapter 3 evaluates the spatial and temporal behavior of SWAT simulated soil moisture with direct and indirect estimates of soil moisture obtained from field and remotely sensed data, respectively (Uniyal et al., 2017). In this paper, the author contributed to the soil moisture field campaign, model development and writing the manuscript.

4. Chapter 4 investigates the application of SWAT model in different agro-climatic zones of the world (Chile - Mediterranean; Germany - Humid; India - Subtropical monsoon and Vietnam - Tropical) for simulating irrigation water requirement under different irrigation control scenarios. Additionally, the use of climate reanalysis datasets like NCEP (National Centers for Environmental Prediction) and ERA-Interim for agro-hydrological studies in data scarce catchments was also invstigated (Uniyal et al., 2019). In this paper, the author contributed to the setting up of three SWAT models for Indian, German and Chilean catchments and improved the previously developed SWAT model for Vietnamese catchment. Additionally, the author wrote the manuscript and communicated it to the other co-authors.

5. Chapter 5 deals with modifying and validating the auto-irrigation scheduling under plant water stress condition using SWAT (Uniyal and Dietrich, 2019b). For the fulfillment of this objective, author contributed to the idea, coding and writing the manuscript.

6. Chapter 6 is the final chapter that concludes the results obtained and present the main findings from the three research objectives. It also summarizes the future research prospects and the area in which more research is required in the near future and also some ongoing work.
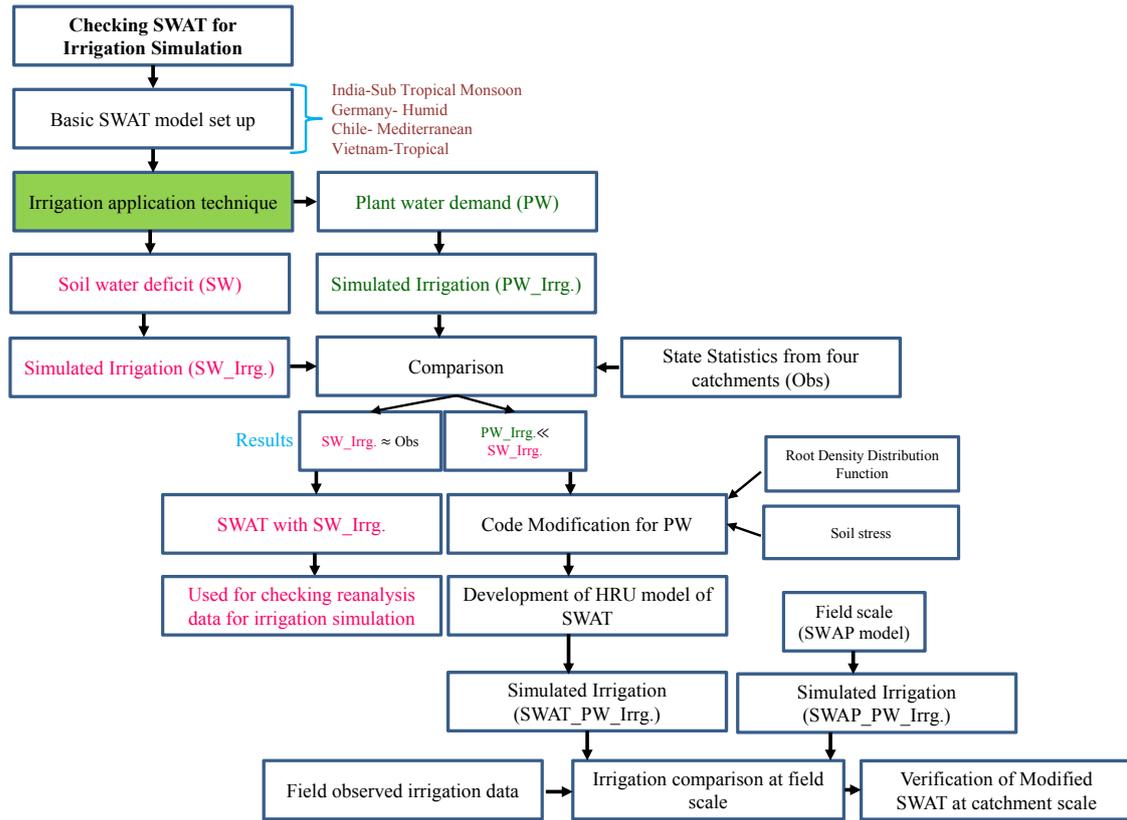
Figure 1.2: Work flow of irrigation simulation and model modification.

Chapter 2
State of the Art

2.1 State of the Art

The correct estimation of regional water demand using hydrological models has become a major concern for agriculturists for the effective water resource management. Water demand and water availability are the two most important parameters considered by the scientists for integrated water resources management. This chapter comprises of a number of reviews dealing with the measurement and simulation of water availability in the soil (soil moisture), water demand (irrigation amount) simulated by hydrological models at different scales and the errors or inconsistencies in the existing models in simulating water demand.

2.1.1 Soil Moisture: Measurement and Simulations

A good estimation of soil moisture is important in hydrology as it is the watershed's precondition that influences the surface runoff production and furthermore it would influence the amount of irrigation applied at the field as well as at the catchment level. Soil moisture is highly variable in space and time due to atmosphere forcing, heterogeneity in soils, topography, and vegetation, etc (Tromp-van Meerveld and McDonnell, 2006; Vereecken et al., 2007). In addition, the soil and vegetation together can either create or destroy the spatial variance in soil moisture (Teuling and Troch, 2005). At present, there are three ways to estimate soil water content: in-situ or point measurement using field instruments [(Meyles et al., 2003; Brocca et al., 2009); direct/indirect method], remote sensing (Schultz, 1988) and by simulation models (indirect methods) (Schmugge et al., 1980). In addition, according to spatial extent of soil moisture estimation, soil moisture is determined at three different spatial scales: point, field and watershed scales (Corradini, 2014).

(a) Point/Field Scale

Field scale estimations of soil moisture are expensive and time-consuming, whereas remote sensing soil moisture data is limited due to the errors from soil data, vegetation and surface roughness (Houser et al., 1998; Schultz, 1988). As soil moisture is spatially and temporally variable in nature, therefore, exhaustive representative sampling at point scale should be required for covering the overall variability at a field or catchment scale (Kalma et al., 1995). Satellite or drone based estimation of remote sensing will not only cover the whole area of interest but also these can be implemented for continuous applications.

The research on estimating soil moisture at field scale dates back to 1970s (Nielsen et al., 1973; Bell et al., 1980). The first intensive soil moisture research was conducted by the National Aeronautics and Space Administration (NASA) during 1974-1977 for different locations at United States (US). They conducted soil moisture study at 58 large field sites to determine the relationship between soil moisture variability and mean soil moisture value of the field. The statistical analysis confirmed that the soil moisture variability is inherent at large fields and

it is normally distributed about mean (Bell et al., 1980). Nielsen et al. (1973) also concluded the aforementioned results. Mohanty et al. (2000) conducted a field experiment where soil moisture content from 0-6 cm of soil profile was measured on consecutive time steps at 400 locations in Southern Great Plains of U.S during two sampling events. The results showed that field's mean soil moisture was nearly equal in both the sampling events however the spatial distribution was different. Since then huge progress has been made in devising new techniques for measuring soil moisture at field or point scale with the invention of instruments like electromagnetic soil moisture sensors [Time Domain Reflectometry: TDR, (Topp et al., 1980)], hydrogeophysical methods (Vereecken et al., 2014) (Ground Penetrating Radar: GPR, (Huisman et al., 2003), etc.), active and passive microwave remote sensing ((Jackson, 1993; Scott et al., 2003), and cosmic ray probe (Zreda et al., 2008), etc.

There has been an increase in the number of studies dealing with the combination of field study and validating hydrological models at field scale. Eitzinger et al.(2004) compared the soil water content simulated by using three crop models at field scale namely CERES, WOrld FOod STudies (WOFOST) and Soil Water Atmosphere Plant (SWAP) in Marchfeld, Austria. The results showed that complex models like SWAP and CERES did not perform significantly better than WOFOST in simulating soil moisture profile. Ma et al.(2011) used SWAP model to evaluate the water cycle at field scale in Beijing, China. SWAP was calibrated and validated using observed soil water contents at different soil depths. The developed model was then used to evaluate different optimal irrigation schedules under deficit irrigation scheduling. Jiang et al. (2011) used SWAP model to simulate the water and salt transport on an experimental site located in Gansu, Northeast China. They revealed that SWAP model is an effective tool to predict long-term variation in soil water and salt in the field under deficit irrigation with saline water.

Vereecken et al. (2014) reviewed the state of the art of characterizing and analysing spatial and temporal variability of soil moisture at field scale. Liang et al. (2016) compared the soil water, nitrogen and crop yield simulated by soil Water Heat Carbon Nitrogen Simulator (WHCNS) model with the 14 other models in North China. The comparison revealed that the WHCHNS model was among the top three models in simulating soil water, nitrate dynamics, crop dry matter and nitrogen uptake by crops. Shelia et al. (2018) coupled DSSAT and HYDUS-1D for simulating the soil water dynamics for an experimental field located in University of Florida during 1978-1990. The results revealed that the coupled model provides satisfactory simulations of change in the soil water content and crop growth. Furthermore, Wei (1995) suggested using remote sensing data in combination with the hydrological modelling to estimate soil moisture in a better way.

(b) Catchment Scale

Hydrological models are the powerful tools used to represent the complex physical interactions of water and atmosphere (including land surface and hydrological processes, etc.,) using the current available knowledge (Zuo et al., 2015). Water in the form of precipitation falls on the earth, excess water exits the catchment in the form of runoff whereas some portion infiltrates and later percolation takes place

according to the physical properties of the underlying soil strata. So a thorough knowledge of the governing process is required to have a better understanding of the movement of water occurring over, under and above the soil surface or between soil, plant and atmosphere continuum.

Several studies have been conducted in the past to explore the possibility of estimating the ground soil moisture from remote sensing products (Schmugge et al., 1974; Schmugge, 1978). Kalma et al. (1995) used Variable Infiltration Capacity model (VIC) to predict the relative wetness at 41 locations in a catchment located in Australia. The objective of this research was to find a connection between point and catchment scale soil moisture. Results showed that the VIC model is able to predict catchment soil moisture. Zappa and Gurtz (2003) used Precipitation-Runoff-Evapotranspiration-Hydrotope model (PREVAH) for three different meteorological datasets between the months of August and October, 1999 for an experimental site situated in Switzerland. In recent years many authors have used soil moisture data from different remote sensing products to improve the hydrological simulation of streamflow at catchment scale. Parajka et al. (2006) used the soil moisture data from European Remote Sensing (ERS) Scatterometer satellite to improve the hydrological simulation in gauged and ungauged catchments in Austria. The results showed improved soil moisture and streamflow simulation in gauged catchment whereas soil moisture simulation by the hydrological model was consistent with the soil moisture derived from scatterometer data in ungauged catchments. (Brocca et al., 2010) used the soil wetness index from Advanced SCATterometer (ASCAT) for improving the runoff prediction at Upper Tiber River basin, central Italy.

Different satellite products either provide soil moisture in terms of vegetative indices [Landsat: (Jackson et al., 2004)], MODIS: Wang et al. (2007), etc. or direct soil moisture data [Sentinel: (Paloscia et al., 2013)]. There has been a trend in the past that researchers perform assimilation of soil moisture data to improve streamflow (Pauwels et al., 2001), drought forecasting (Narasimhan et al., 2005), crop yield forecast (Vazifedoust et al., 2009), flood forecasting (Wanders et al., 2014), etc. Li et al.(2019) used Soil Moisture Active Passive (SMAP) soil moisture product and observed streamflow to calibrate the MIKE Système Hydrologique Européen (SHE) hydrological model for Beimiaoji watershed, China. They have used three different calibration approaches and the results show that multi-parameter calibration improves the model simulation of streamflow and root zone soil moisture.

Leroux et al.(2016) proposed a method to correct the real time satellite derived precipitation amount by assimilating Soil Moisture Ocean Salinity (SMOS) soil moisture. The results showed improvement in soil moisture, water table and streamflow simulated by the hydrological model using assimilated SMOS soil moisture product. The soil moisture is indirectly estimated from the remote sensing data in terms of soil moisture index. Many approaches have been applied in order to model the relationship between soil moisture and soil reflectivity mainly based on Normalized Difference Vegetation Index (NDVI) and the surface temperature (Ts) (Zhang and Zhou, 2016). The slope of the Ts/NDVI curve can

provide valuable information regarding soil moisture and vegetation conditions (Goetz, 1997). Sandholt et al. (2002) developed the Thermal Vegetation Dryness Index (TVDI). It is based on an empirical parameterization of the relationship between Ts and NDVI resulting from the triangular or trapezoidal shape of the Ts/NDVI scatter plots (Carlson et al., 1994; Moran et al., 1994; Xin et al., 2006). Such methodologies have been evaluated by many researchers for validating indirect methods of estimating soil moisture in large catchments (Carlson et al., 1995; Schultz, 1988; Muller and Décamps, 2001).

High variability of soil moisture can be quantified by performing the uncertainty assessment. This will help the decision-makers to make reliable and sustainable goals for effective water management. Uncertainty may arise from data, parameter, model and from operation (Tung, 2011). Knowledge of model uncertainty is important for making reliable predictions. Shafiei et al. (2014) used Generalized Likelihood Uncertainty Estimation (GLUE) framework to assess the parameter and model prediction uncertainty for SWAP model at two agricultural fields in Central Iran. Results revealed that different boundary conditions, crop characteristics and model simplification led to higher model uncertainty in soil moisture simulation.

2.1.2 Simulation of Irrigation Water Demand

Water has always been a restricting variable in crop production. As the irrigation water demand is sensitive to soil, landuse/land cover and climatic conditions (Wisser et al., 2008) therefore, irrigation water demand estimation using hydrological models play an important role in agricultural water management. Irrigation water demand is simulated mostly for operational purpose to optimize the water use at farm or catchment level. Its simulation will not only help in providing optimum amount and duration of irrigation water applied to the agricultural fields but also puts a check on the existing water availability. Under water scarcity conditions, the simulated irrigation water will help the agricultural community to grow crops according to the available water resources in any part of the world.

Droogers and Kite (2002) evaluated water use in terms of irrigation at field, irrigation scheme and basin scale using parametric basin-scale model and physically based crop-scale model. The results showed that crop-scale model better represented the amount and timing of irrigation water and therefore can be used to verify and calibrate the basin scale models. Researchers always simulate irrigation and crop yield together as both are directly linked to each other. Decisions makers are always interested in the response of different irrigation management scenarios on crop yield, nutrient balance and other water balance components (Sun et al., 2006; Geerts and Raes, 2009; Gheysari et al., 2009; Maier and Dietrich, 2016).

(a) Field Scale
Irrigation water requirement is mostly simulated at field and plot scale using field or point scale hydrological or crop models. The field models are mostly calibrated to simulate crop yield and once the model satisfactorily simulates the crop yield then

irrigation is simulated under different irrigation management scenarios. This section comprises of a short review of the commonly used crop models at field scale.

AquaCrop

It is a crop model developed by the Food and Agriculture Organization (FAO) to simulate attainable yield of major crops as a function of water consumption (Steduto et al., 2009). Heng et al. (2009) quantified the performance of AquaCrop by comparing the simulated leaf area index (LAI), biomass accumulation, crop yield, ET, and Water Use Efficiency (WUE) of maize against field measurements made under irrigated and rainfed conditions for maize at three field locations (Bushland and two in Spain). The results revealed that AquaCrop is valuable for quantifying crop productivity under different irrigation scenarios. In another study, it was combined with an economic model for optimizing irrigation water at farm-scale for cotton, maize, potato and sunflower in South-western Spain. This was done to help the pre-decision on cropping patterns and irrigation strategies. The results showed that the developed model was a good tool for analysing different scenarios which will help the irrigation managers and policy-makers to achieve sustainable irrigation management at farm level. It is also mentioned in the results that changing crop is the best sustainable strategy compared to changing water polices (García-Vila and Fereres, 2012). Additionally, there are several other studies around the globe which have used AquaCrop and verified the use of this model in any agro-climatic conditions (Iran: Wheat (Andarzian et al., 2011), Serbia: maize, sugar beet and sunflower (Stricevic et al., 2011), India: cabbage (Pawar et al., 2017)

CropWat

It is a decision support system developed by Land and Water Development Division of FAO (Smith, 1992). It is a tool used to quantify reference ET, crop water requirement and designing and management of irrigation scheduling. George et al. (2000) developed an irrigation scheduling model to perform irrigation scheduling at field scale. Later on, model simulations were compared against the field data and irrigation schedule given by CropWat model (Smith, 1992) for the experimental field located at the University of California during 1992. The results showed that the irrigation amount applied by the model was comparable to the actual depth applied in the field during first irrigation whereas it was not comparable in the second and third irrigation event. In 2014, crop water use was predicted under rainfed and irrigated field conditions for tomato in Nairobi, Kenya. Results pointed out that the crop yield is substantially affected by the stress during the senescence stage and supplemental irrigation during this stage could reduce the negative impact on crop yield (Karuku et al., 2014).

Daisy

Daisy is a dynamic model used for the simulating water, nitrogen and crop growth dynamics in agricultural fields (Abrahamsen and Hansen, 2000). Jensen et al. (2010) incorporated a xylem-Abscisic acid model with Daisy model to simulate the drought tolerance in potatoes and tomatoes in Italy. Amount of water applied was predicted using Abscisic Acid (ABA) root signal based on the in-situ measurement and monitoring of soil water content within the rooting zone under deficit

irrigation or partial root zone drying. The results showed an improved antioxidant content in the considered crops and size distribution of potato tubers were improved. Seidel et al. (2016) tested the three irrigation scheduling approaches (soil water balance calculations, real-time model application, automatic drip irrigation) on white cabbage crop grown in four experimental fields located in Dresden, Germany during 2013-2014 using a one-dimensional soil-plant-atmosphere system model Daisy (Abrahamsen and Hansen, 2000). The results revealed that irrigation strategy using automatic drip irrigation using soil tension thresholds yields good crop yield with low irrigation amounts compared to the other. The model was over-irrigating when irrigation was applied using soil water balance calculations whereas it was better when soil tension thresholds are used for irrigation application. In addition, the partially calibrated model led to the underestimation of the crop water requirements in conjunction with an incorrect timing of irrigation events and therefore resulted in the lowest yields. Seidel et al. (2017) evaluated the impact of irrigation on growth and development of white cabbage in an experimental field located in Dresden, Germany using the Daisy model. Results revealed that irrigation scheduling based on soil water balance calculations led to unproductive over-irrigation due to overestimated crop coefficients, which highlight the need for more accurate estimates of these coefficients.

DSSAT

DSSAT stands for Decision Support System for Agrotechnology Transfer is a software application comprised of over 42 crop simulation models as well as several other tools to facilitate its effective use (Jones et al., 2003). Crop Estimation through Resource and Environment Synthesis, [CERES,(Godwin, 1990)], CERES-Wheat is a crop model embedded in DSAAT was used to evaluate the different irrigation strategies for improving crop water use for spring wheat in International Maize and Wheat Improvement Center (CIMMYT) station in Mexico (Lobell and Ortiz-Monasterio, 2006). Fang et al. (2010) combined a root water quality model and DSSAT to investigate the impact of different irrigation strategies to improve the water use efficiency of winter wheat and summer maize double cropping system at Yucheng Ecological Station from 2001-2003 in North China. The study concluded that the effective irrigation will not only improve the WUE, but also mitigate the decline in groundwater and increase in nutrient leaching in the area.

EPIC

Erosion Productivity Impact Calculator (EPIC) is a mathematical model used for simulating the erosion, crop growth (Williams, 1990) and is capable of simulating the effects of management decisions on crop yield and other processes (Williams et al., 1989a). Bryant et al. (1992) used the EPIC model to simulate corn yield at Bushland, Texas. He found that the model can be used to analyse the impact of different irrigation strategies on the crop yield which is meaningful to the farmers . Cabelguenne et al. (1997) used EPIC-PHASE, a modified version of EPIC model to evaluate the real time irrigation management based on every 5 days model predictions. The study showed potential progress for dynamic irrigation scheduling based on the water stress intensities predicted by the model. However, the

reliability of this schedule depends more on the accuracy of weather forecasts. This was one of the first irrigation studies dealing with the real-time assessment of irrigation amount and time using the weather forecast. Rinaldi (2001) used a previously calibrated EPIC model to simulate sunflower yield against 66 different irrigation scenarios during 1953-1997 for an experimental farm in Southern Italy. The results showed that the bud flower is the crucial stage for irrigating sunflower to attain optimum yield. In addition, model provided a good benchmark at farm level decision making.

SWAP

Soil Water Atmosphere and Plant (SWAP) is a one dimensional model used for the simulation of water, solute and heat transport in the vadose zone along with vegetation development (Kroes et al., 2009). It is a commonly used hydrological model to schedule irrigation at a field scale. Ma et al. (2011) used SWAP model to explicitly address the water exchange between soil water and groundwater under deficit irrigation scheduling in China. Rallo et al. (2012) compared the irrigation scheduling simulated by the FAO model and SWAP for wine grape during 2005-2006 in Sicily, Italy. In addition, the number of crop water stress days were also evaluated for the two agro-hydrological models. The results showed that under different irrigation scenarios models gave similar outputs when the soil water content is low at the beginning of the growing season.

(b) Catchment Scale

The use of Satellite data and Geographic Information System (GIS) has helped the researchers to apply the field based models at a catchment or global scale and catchment scale models at global scale using extrapolation and regionalisation techniques. The catchment modelling studies are important as most of the water management decisions are either done on a regional or watershed scale.

CropWat

This model was used in conjunction with GIS to recommend the supplemental irrigation scheduling for the Beijing-Tianjin-Hebei region, China. The results revealed that there are serious water deficit conditions during the spring season for maize crop which results in lower yield per unit area in the studied region (Feng et al., 2007). Diaz et al. (2007) mapped the impact of climate change on irrigation water demand using CropWat model for Guadalquivir River basin, Spain. The results revealed that seasonal irrigation water requirement will increase between 15 and 20% by 2050 depending on location and cropping pattern as irrigation seasons are predicted to be longer. Additionally, it was also used for estimating irrigation water requirement and irrigation scheduling using the local meteorological data for the Gaza Strip. The results indicated that farmers irrigate 20-30% more than the required amount for the common crops (Al-Najar, 2011). CropWat was used to calculate the gross water needs of various crops in different agro-ecological units in Kollam district of Kerala, India. The future water balance scenario for the district showed water deficit condition which can be compensated by either decreasing the command area or by using water-saving technologies to achieve a sustainable future (Surendran et al., 2017).

DSSAT

He et al. (2013) used CERES-Wheat model to quantify the optimal irrigation scheduling and uncertainties associated with it due to climatic variations for spring wheat in Minquin County, China. It was seen from the results that applying irrigation four times during the total crop growing period is the best choice with higher long-term average yield under non-limited water availability condition. CERES-Wheat has also been used for predicting yield in irrigated plains of the Indian Punjab region (Hundal and Kaur, 1997) for spatial analysis on the agricultural impacts of climate change in the major wheat-growing regions of Spain (Iglesias et al., 2000). Jiang et al. (2016b) tested DSSAT-Maize (Jones et al., 2003) to analyse the effect of optimal irrigation strategies under different climatic conditions on maize yield in Heihe River watershed, China. The well calibrated model for crop yield, soil moisture, and phenological phases was used to simulate the effects of planting dates and different irrigation treatments on crop yield. The results revealed that there is a huge difference between the irrigation amounts applied by the model under different climatic conditions. The amount of irrigation water could be reduced to half compared to the current amount if simulated irrigation schedules are used.

EPIC

Jiang et al. (2015; 2016a) used SWAP-EPIC model for assessing irrigation performance and optimizing regional irrigation water use for Heihe River basin, China. Results revealed that improved water conveyance and irrigation scheduling could reduce 30% deep percolation and 15% irrigation water with minimal effect of crop yield. In addition, for water optimization, they have used a two level process based economic optimization model with SWAP-EPIC. It was seen from the results that on an average 23% of irrigation water could be reduced without reducing the annual current benefit.

Crop yield and irrigation water requirement are also calculated at global level by many researchers in recent years. Liu et al. (2007) simulated wheat yield and crop water productivity using Global EPIC model. The results showed a linear relation between crop water productivity and crop yield. In addition, crop water productivity and yield could increase with efficient water and fertilizer management. Wisser et al. (2008) quantified the variability and uncertainty due to land-use and climate data in simulating irrigation water demand at the global level using a water balance model. The results revealed that there is huge variability in simulating irrigation water demand at the regional scale (nearly 70%) compared to the national scale (less than or nearly equal to 10%). Shen et al. (2013) used Penman–Monteith method and observed crop data to assess and analyze the temporal and spatial variations in irrigation water demand for main crops grown in central Eurasia during 1989-2010. The results revealed an increasing irrigation demand due to the increase in the irrigated agricultural areas. Zaussinger et al. (2019) proposed a new method of estimating the actual irrigation water use from a combination of three different remotely sensed data and a modeled reanalysis soil moisture data for in US during 2013-2016. It was observed from the results that in intensively irrigated areas, the temporal dynamics of irrigation water use estimated in this research was close to ancillary data on local irrigation practices.

It was seen from the extensive review of literature from the aforementioned sections dealing with soil moisture and irrigation water demand that the scientists have used a variety of field scale, catchment scale and global scale hydrological models to estimate different water balance components around the world. From the last two decades, researchers around the world have been actively using Soil and Water Assessment Tool (SWAT) model for simulating different components of hydrologic cycle and the effect of different management scenarios on water balance components in agricultural catchments (Griensven et al., 2012). SWAT has become a popular agro-hydrological model amongst researchers and planners dealing with the simulation of hydrology, agricultural water management and nutrient loads of agricultural watersheds around the world (Neitsch et al., 2011). In addition, it is an open-source software which allows its users to read, edit/modify the code as per different scientific questions to be solved by the users. Therefore, considering the model flexibility, its strong scientific community, SWAT was chosen for this study.

2.1.3 SWAT

In this section, a small glimpse of the studies using SWAT model dealing with soil moisture simulation, irrigation water demand assessment/impact of best management practices on catchment's water balance has been provided. The available literature describing and discussing the use of SWAT on agricultural catchment is vast. Fig. 2.1 gives an idea about the number of studies performed using SWAT under the three aforementioned broad topics around the world in the English language using a database developed by Philip Gassmann `https://www.card.iastate.edu/swat_articles/index.aspx`. It can be seen from Fig. 2.1 that the number of studies dealing with the three topics namely soil moisture estimation, irrigation/best management practices assessment and model development to improve irrigation water simulation at catchment scale has increased more in the last 10 years. However, the number of studies dealing with simulating and improving irrigation water management at a catchment scale is still gaining momentum.

Soil Moisture Studies
Narasimhan et al. (2005) used a SWAT model to develop a long-term spatio-temporal (4×4 km spatial and weekly temporal) soil moisture data for drought monitoring and crop yield predictions in different watersheds across Texas. The SWAT simulated soil moisture was verified against the normalized difference vegetation index (NDVI) derived from National Oceanic and Atmospheric Administration (NOAA-AVHRR: Advanced Very High Resolution Radiometer) satellite data. The results showed that there was a lag of atleast one week in the soil moisture simulated by SWAT compared to the NDVI which was attributed to the delayed response of plants against water stress in the root zone. In addition, the results indicated that NDVI can be considered as a good indicator for evaluating crop stress and for determining the onset of agricultural drought in semi-arid areas. In Cobb Creek watershed, Oklahoma (Chen et al., 2011) calculated the root zone soil moisture, ET, runoff, and streamflow using SWAT. Ensemble Kalman filter (EnKF) was used to assimilate the surface soil moisture data. The results showed that EnKF had effectively updated the soil moisture
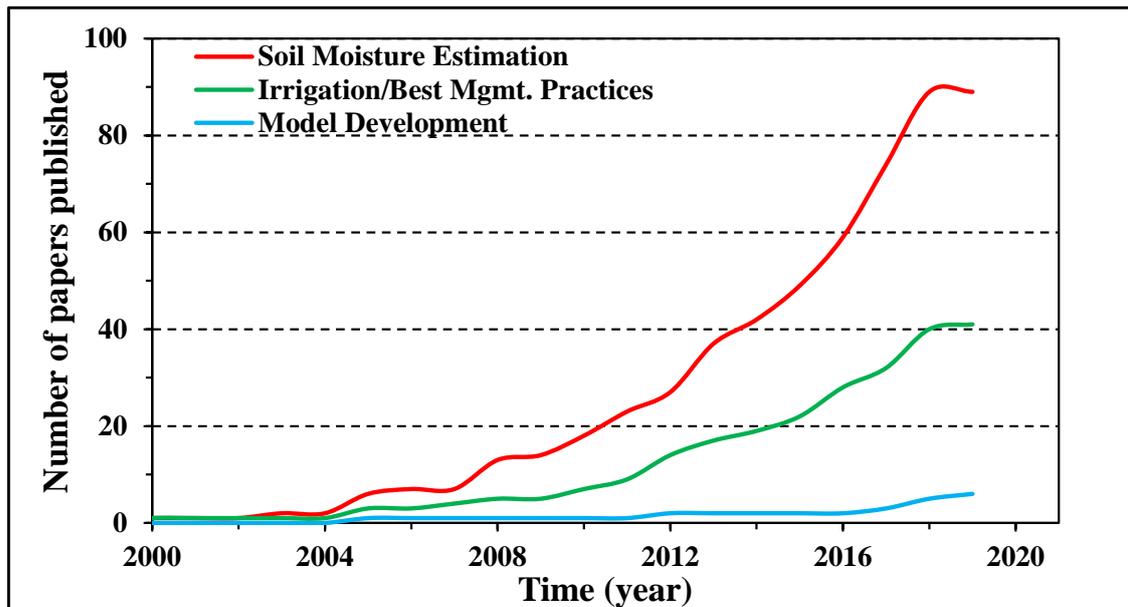
Figure 2.1: Number of SWAT studies performed during 2000-2019.

simulated by SWAT for the upper layer and also provide moderate improvement in soil moisture simulation at lower layers and ET . Jha (2012) used SWAT to quantify and evaluate the distribution of soil moisture on Raccoon watershed, US under cover crop conservation practice. The results showed that the cover crop conservation practice was effective in improving the soil and water quality but it has an adverse impact on the amount of soil moisture present in the soil profile.

Joh et al. (2011) assessed the impact of climate change on hydrological components of a forest watershed located in Korea. In addition to streamflow, SWAT model was calibrated using ET and soil moisture (TDR). An upward trend was seen in annual temperature, precipitation, and streamflow, whereas soil moisture showed a downward trend.

Li et al. (2010) used SWAT to simulate soil moisture variability in Shaanxi Province, China. The comparison of observed and SWAT simulated soil moisture showed that the model reasonably simulated the long-term soil moisture trend and spatio-temporal variability in soil moisture. Muttiah and Wurbs (2002) investigated the change in the water balance components, specifically ET, soil water storage and water yield corresponding to two soil maps with different spatial resolution. It has been revealed from the results that the aforementioned change in water balance components are more sensitive to watersheds under wet climate and heterogeneous soils. DeLiberty and Legates (2003) and Mapfumo et al. (2004) studied the spatial and temporal variability of soil moisture in the US and Canada. No seasonal variation in the temporal autocorrelation was found in the first study whereas, the simulated soil moisture in the second study was under and over predicted by the model in dry and wet conditions, respectively.

Milzow et al. (2011) combined three datasets namely, surface soil moisture from

radar, radar altimetry by Envisat and the temporal change in total water storage recorded by Gravity Recovery and Climate Experiment (GRACE) for calibrating a data-scarce catchment (Okavango River) using rainfall input from three different sources (European Centre for Medium-Range Weather Forecasts - ECMWF ERA-Interim, Tropical Rainfall Measuring Mission - TRMM 3B42, FFamine Early Warning Systems Network-EWS-Net). The results revealed that the error in simulated model outflow can be reduced by reducing error in the precipitation. Park et al. (2014) evaluated the soil moisture simulated by SWAT using MODIS NDVI and land surface temperature (LST) for a forest in Spain. The results revealed that except in frequent rainy years SWAT simulated soil moisture showed a higher correlation with MODIS LST and NDVI during forest leaf growing and falling periods, respectively. Li et al. (2016) assessed the spatio-temporal variation in soil moisture and other water balance variables under different precipitation gradients in the Yellow River basin, China. Results showed that soil moisture has a non-linear relationship to precipitation and ET, however, all the variables exhibited an annual decreasing trend. Rajib et al. (2016) evaluated the spatially distributed surface and root zone soil moisture in two watersheds of Indiana, US for improving the hydrologic predictability of SWAT. It was indicated from the results that the root zone soil moisture may play an important role in model calibration.

Irrigation Studies
Applicability of SWAT has also extended to irrigation studies to help the researchers/policy-makers for simulating irrigation scheduling under different climate, soil and cropping patterns. Santhi et al. (2005) improved the capabilities of SWAT by introducing a canal irrigation component into the model for the effective regional planning of an irrigated agricultural catchment in the Rio Grande, U.S. Xie and Cui (2011) developed SWAT for simulating paddy fields in the Zhanghe Irrigation District located in China. Dechmi et al. (2012) used SWAT to simulate the intensive agricultural irrigated catchment of the Del Reguero watershed in Spain. Panagopoulos et al. (2014) evaluated the economic effectiveness of different best management practices for reducing the irrigation water abstraction in Pinios, Greece. In addition to this, SWAT was also used to find out the best management practices for irrigation considering crop water requirement, productivity, management strategies costs and crop market prices in Crete, Greece (Udias et al., 2018). Woznicki et al. (2015) used a SWAT model for Kalamazoo River watershed, Michigan is to understand how climate change would affect the water balance, future irrigation demand for corn and soybean. In addition, a spatial variability map for irrigation demand was created along with the possible adaptation strategies primarily based on shifting planting dates. The results indicated that uncertainty in irrigation demand for corn and soybean has increased from 1980-1999 to 2060-2079, with higher uncertainty in the months having the highest irrigation demand. Late planting will help to reduce irrigation water demand with compromising reduction in corn yield. Maier and Dietrich (2016) compared different irrigation strategies, where different methods of auto-irrigation implemented into SWAT showed considerably different results for a humid catchment in Germany.

Marek et al. (2016) investigated the simulation of the LAI and ET in SWAT and found deficiencies, which may have an impact on the accuracy of simulated plant water uptake. Chen et al. (2018) proposed an improved auto-irrigation function for SWAT based on previous field studies in Texas (Chen et al., 2017) carried out a year earlier. Fu et al. (2019) used SWAT to simulate the irrigation schedules of corn and soybean in the downstream of the Songhua River basin, China. Additionally, the study used the Analytic Hierarchy Process (AHP) to define optimal irrigation schedules. The results reveal that deficit irrigation treatments were valuable in improving water use efficiency and crop yield.

SWAT Modification
Santhi et al. (2005) developed a canal irrigation component in SWAT and validated it for regional planning of an agricultural catchment in Lower Rio Grande Valley, Texas. Dechmi et al. (2012) modified SWAT to correctly simulate the hydrological process in an intensively irrigated catchment located in Spain. Panagopoulos et al. (2014) assessed the cost-effectiveness of different irrigation water management practices in a water-scarce agricultural catchment in Pinios, Greece. Githui et al. (2016) tested different irrigation inputs in SWAT and evaluated them against the observed and simulated flow and ET in an irrigated catchment in Australia. Wei et al. (2018) modified seepage simulation from earthen irrigation systems to improve the simulation of management practices and hydrological processes mainly instream flows in an intensively managed agricultural watershed in Colorado, US. McInerney et al. (2018) evaluated the response of 120 different spatio-temporal irrigation inputs in simulating streamflow, ET and potential recharge. Marek et al. (2017) used SWAT for simulating the crop yields, crop water use as well as the irrigation required by a semi-arid watershed located in the Texas High Plains, US. The overall results concluded that SWAT's plant growth algorithm is not suitable for simulating the representative cotton yield of the catchment, which could be due to the limitation of auto-irrigation function. Chen et al. (2018) also found that although the SWAT default auto-irrigation triggered by soil water content method provided a reasonable simulation of actual ET, the irrigation amount varied greatly from actual irrigation amount observed in the field. They developed a new management allowable depletion based auto-irrigation algorithm in SWAT based on scheduled date and accumulated heat units. The updated SWAT+ model will improve the control of auto-irrigation by decision tables (Arnold et al., 2018).

Chapter 3
Evaluation of SWAT simulated soil moisture at catchment scale by field measurements and Landsat derived indices

Abstract

The quantification of soil moisture under different soils and crops at the regional scale is a challenging task. Hence, such studies are limited by the availability of ground-based measurements. The current study evaluates the spatial and temporal patterns of daily soil moisture simulated by the Soil and Water Assessment Tool (SWAT) for the upper 30 cm of the soil profile with indirect soil moisture estimates from Landsat for 2016. The Thermal Vegetation Difference Index (TVDI), was calculated based on the Normalized Difference Vegetation Index (NDVI) and the brightness temperature (BT) using Landsat images, from which regression models were trained by using field measurements from Time Domain Reflectometer (TDR) to calculate soil moisture. Two agricultural catchments namely, Gerdau and Wipperau in Germany were satisfactorily calibrated using SWAT for daily streamflow (1975-2000) with NSE (Nash Sutcliffe Efficiency) >0.55 and PBIAS (Percent bias) < 5.5 %. The parameter uncertainty assessment during the irrigation season(Mar-Sept, 2016) for soil moisture revealed that the uncertainty band is narrow (*p-facto*r = 0.57-0.83; *r-factor* = 0.52-1.3). Spatial and temporal patterns of soil moisture from Landsat and SWAT were evaluated by using boxplots and absolute soil moisture difference maps. Results revealed that the overall spatial and temporal patterns of boxplots matched better for the dry period (correlation, r ≥ 0.90) compared to the wet period (r ≥ 0.57). The mean absolute difference between soil moisture from Landsat and SWAT ranged between 0.9-10% for most soils. In addition to it, the soil map was refined to match soil moisture patterns shown in Landsat images for one sandy soil, which further improved the mean absolute difference (1.06-6%). The current study provides an approach to use remotely sensed soil moisture for verifying hydrological modeling results and for optimizing the parameterization of soils, which may bridge the gap between global, regional and field studies in agricultural water management.

Keywords*: Soil Moisture; Landsat; TVDI; NDVI; TDR; Parameter uncertainty*

3.1   Introduction

Soil water availability plays a vital role in crop productivity. Agricultural and hydrological models often use the depletion of soil water as the trigger for

irrigation operations. Thus, soil moisture is a key hydrological state variable, which is of great interest amongst agriculturists, meteorologist and hydrologists (Brocca et al., 2010; Schmugge et al., 1980; Walker et al., 2001; Zucco et al., 2014). The amount and vertical distribution of soil water depends non-linearly on soil physical properties (Timm et al., 2006) , topography (Western et al., 1999), type and stage of crop (Liding et al., 2007), and previous and current weather conditions (Seneviratne et al., 2010). The soil moisture present in the upper soil layer shows maximum spatio-temporal variation compared to the lower soil layers (Chen et al., 2010; Li et al., 2016). It also plays a major role in checking the water use intensity in agricultural catchments. Therefore, a good insight of soil moisture variability will bring researchers a step closer in understanding the catchment's hydrology, crop processes, irrigation control and the management of green water in a better way.

Soil moisture estimation can be performed by direct and indirect methods. One of the direct methods is the gravimetric technique (oven-drying technique), which is widely used because of its simplicity, reliability, and accuracy (Schmugge et al., 1980). Most of the direct methods are labor-intensive, time-consuming and prohibitive on monetary basis for continuous application in large catchments. On the other hand, indirect methods are simple and can be implemented for continuous applications. These include neutron scattering (Gardner and Kirkham, 1952), gamma-ray attenuation (Gurr, 1962), electromagnetic techniques Topp et al. (1980), tensiometric techniques (Richards and Gardner, 1936), hygrometric techniques, soil water and hydrological models (Tavakoli and De Smedt, 2013) and remote sensing techniques (including ground-based drones, Vivoni et al., 2014).

Satellite-based estimations of surface soil moisture have received considerable attention in hydrology and water resources management because antecedent soil moisture is a critical variable in rainfall-runoff modeling (Han et al., 2012) and model-based irrigation studies (Phogat et al., 2012). The European SpaceAgency's (ESA) Soil Moisture and Ocean Salinity (SMOS) mission (2009); Sentinel-2A (2015) (`http://apps.sentinel-hub.com/sentinel-playground`) and National Aeronautics and Space Administration's (NASA) latest Soil Moisture Active/Passive (SMAP) mission (2014) are designed to better monitor the soil moisture on a global extent with increasing spatial resolution (Gruhier et al., 2009; Entekhabi et al., 2010; O'Neill et al., 2010). The technique of indirect soil moisture estimation in terms of soil moisture index from remote sensing data on a catchment scale dates back to the 1980 (Schultz, 1988). The evaluation of remotely sensed soil moisture using eco-hydrological catchment models is the subject of current research (Narasimhan et al., 2005; Li et al., 2010; Rajib et al., 2016). Many approaches have been applied in order to model the relationship between soil moisture and soil reflectivity mainly based on Normalized Difference Vegetation Index (NDVI) and the surface temperature (Ts) (Zhang and Zhou, 2016). The slope of the Ts/NDVI curve can provide valuable information regarding soil moisture and vegetation conditions (Goetz, 1997). Sandholt et al. (2002) developed the Thermal Vegetation Dryness Index (TVDI). It is based on an empirical parameterization of the relationship between Ts and NDVI resulting from the triangular or trapezoidal shape of the Ts/NDVI scatter plots (Carlson

et al., 1994; Moran et al., 1994; Xin et al., 2006). Such methodologies have been evaluated by many researchers for validating indirect methods of estimating soil moisture in large catchments (Carlson et al., 1994; Schultz, 1988; Muller and Décamps, 2001).

The Soil Water Assessment Tool (SWAT) has been used by many researchers for evaluating soil moisture on the catchment scale. Muttiah and Wurbs (2002) investigated the change in the water balance components, specifically evapotranspiration (ET), soil water storage and water yield corresponding to two soil maps with different spatial resolution. It has been revealed from the results that the aforementioned change in water balance components are more sensitive to watersheds under wet climate and heterogeneous soils. DeLiberty and Legates (2003) and Mapfumo et al. (2004) studied the spatial and temporal variability of soil moisture in the US and Canada. No seasonal variation in the temporal autocorrelation was found in the first study, whereas the simulated soil moisture in the second study was under and over predicted by the model in dry and wet conditions, respectively. Narasimhan et al. (2005) used SWAT to produce a long-term soil moisture dataset for drought monitoring and crop yield prediction in the US. The results indicated that NDVI can be considered as a good indicator for evaluating crop stress and for determining the onset of agricultural drought in semi-arid areas. Milzow et al. (2011) combined three datasets namely, surface soil moisture from radar, radar altimetry by Envisat and the temporal change in total water storage recorded by GRACE for calibrating a data-scarce catchment (Okavango river) using rainfall input from three different sources (ECMWF ERA-Interim, TRMM 3B42, FEWS-Net RFE). The results revealed that the error in simulated model outflow can be reduced by reducing error in the precipitation. Park et al. (2014) evaluated the soil moisture simulated by SWAT using MODIS NDVI and land surface temperature (LST) for a forest in Spain. The results revealed that except in frequent rainy years SWAT simulated soil moisture moisture showed a higher correlation with MODIS LST and NDVI during forest leaf growing and falling periods, respectively. Li et al. (2016) assessed the spatio-temporal variation in soil moisture and other water balance variables under different precipitation gradients in the Yellow river basin, China. Results revealed that soil moisture showed a non-linear relationship to precipitation and ET, however all variables exhibited an annual decreasing trend. Rajib et al. (2016) evaluated the spatially distributed surface and root zone soil moisture in two watersheds of Indiana, US for improving the hydrologic predictability of SWAT. It was indicated from the results that root zone soil moisture may play an important role in the model calibration.

The outcome of most of the soil moisture estimation methods is at point or field scale, whereas hydrological simulation and remote sensing techniques can be used to quantify soil moisture not only at point/field but also in catchment or global scale. Soil moisture can also be estimated for previous years with models and remotely sensed data, which is impossible to derive in case of experimental measurements. Therefore, the availability of model simulated results and remotely sensed data can fill temporal and spatial data gaps and improve long-term catchment studies of soil moisture and related agricultural water management problems. The spatio-temporal

evaluation of soil moisture at the catchment scale was done in a few studies only. Therefore, an attempt has been made through this study to check the applicability of Landsat data to be used for monitoring the soil moisture at a catchment scale. The basic objective of the current study is to evaluate the spatial and temporal behavior of SWAT simulated soil moisture with direct and indirect estimates of soil moisture obtained from field and remotely sensed data. It also includes examining the effect of parameter uncertainty on the simulated soil moisture under different soil and land-use conditions. The following main innovations were done in this study:

• Evaluation of SWAT simulated soil moisture at Hydrologic Response Unit (HRU) scale using high-resolution indirect estimation from Landsat data (30 m) and field measurements.
• Creation of soil moisture parameter uncertainty bands for specific combinations of soils and crops.
• Development of absolute soil moisture difference maps using soil moisture from Landsat and SWAT.
• Adjustment of SWAT soil parameters to match soil moisture patterns in SWAT using Landsat image.

3.2 Materials and methods

3.2.1 Model description

The Soil and Water Assessment Tool (SWAT) is a semi-distributed catchment scale hydrological and water quality model (Arnold et al., 1998, 2012). It is often used in simulating hydrology, chemicals, sediments, crop growing, agriculture management, etc. within agricultural watersheds. The water balance equation used by the model is well explained in the SWAT manual (Neitsch et al., 2011; Arnold et al., 1998). The soil water movement in different soil layers present in the root zone follows a cascade model. Based on this, the model provides net water to the first layer, after canopy interception and evaporation loss. Then according to its field capacity and hydraulic conductivity, storage, runoff excess and infiltration takes place. Excess water further seeps into the next layers. In this process, if the last layer is saturated and still there is excess water then the model assigns it to the first layer. The soil moisture in each subsurface layer is updated by using the following equation in the model:

$$sol_{st_i} = sol_{st} - sepday_i - latlyr_i - lyrtile_i \qquad (3.1)$$

where sol_{st_i}(mm) is the amount of water stored in the soil layer onthe ithday; $sepday_i$(mm) is the percolation from the soil layer onthe i^{th} day; $latlyr_i$ is the lateral subsurface flow in the layer on the ith day; and $lyrtile_i$(mm) is tile drainage in the soil layer on the ith day. In addition to this, the lateral flow in each subsurface soil layer is calculated with Sloan's kinetic storage model (Sloan and Moore, 1984; Sun et al., 2016).

3.2.2 Study area and data

This study is conducted in two sub-catchments of the Ilmenau River basin in Northern Germany (52-54°N, 10-11°E), namely Gerdau (Hansen gauging station,

308 km^2 catchment area) and Wipperau (Oetzmühle, 201 km^2) (Fig. 3.1). The average annual precipitation from 1975 to Sept 2016 was 793 mm and 721 mm in Gerdau and Wipperau, respectively. Both catchments are dominated by agricultural land use with more than 50% of its total area under agriculture.
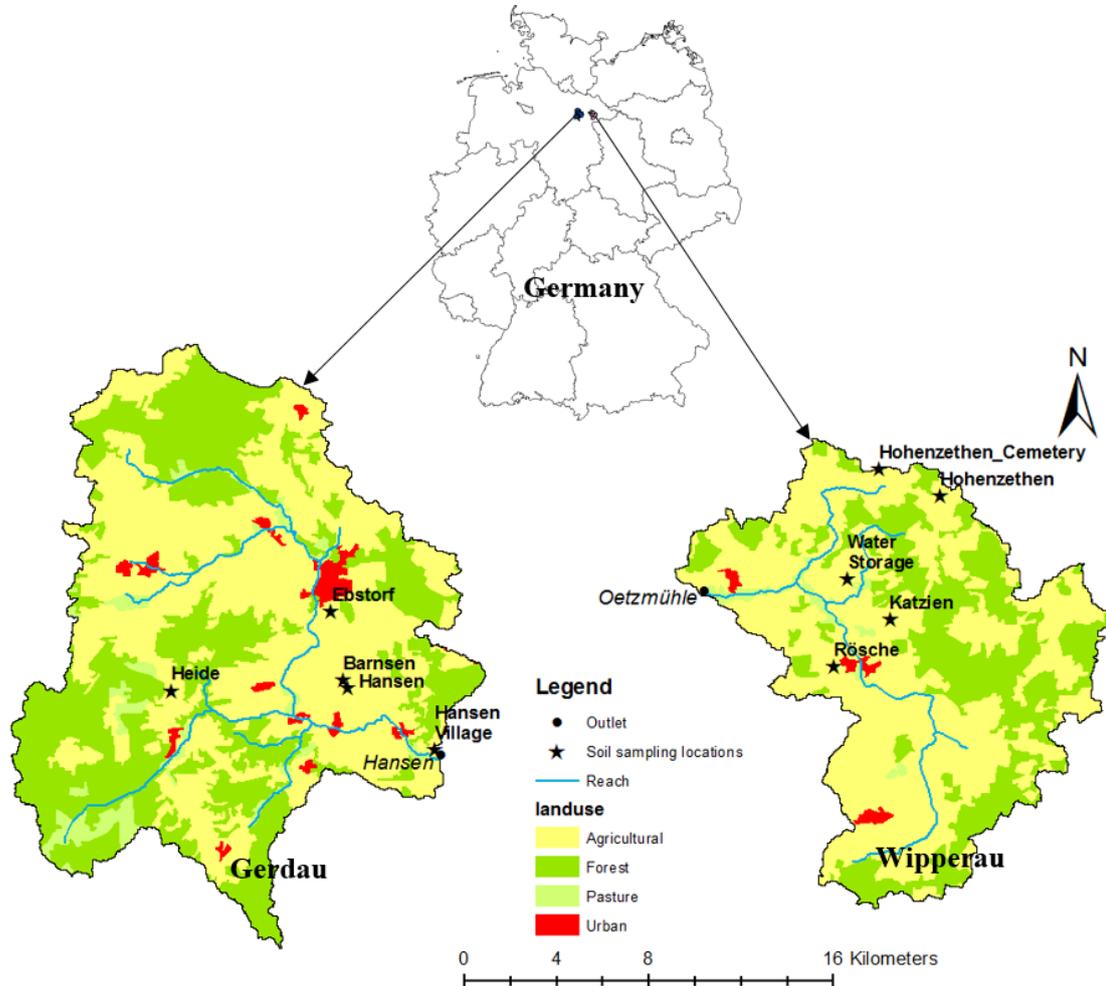
Figure 3.1: Location of the catchments along with the soil sampling locations.

Most of the soils in the catchments can be categorized as medium to fine sand with more than 80% of sand material and more than 90% sand in the lower layers, resulting in low water holding capacity and fast drainage (Tables 3.1 and 3.2). As a result, irrigation is highly required for carrying out agriculture even under humid climatic conditions (Maier and Dietrich, 2016). Sources for irrigation water are the shallow quaternary aquifer (Wittenberg, 2003), a navigation canal and reuse of processed water from the sugar industry. Crops grown in this area are wheat, potatoes, corn silage and sugar beets (Agrarstrukturerhebung, tables Z6070421,K6070411, K6070412 and K6080014 with data from 1977 to 2007 reported every four years, Niedersächsisches Landesamt für Statistik). These crops are irrigated mostly by sprinklers but few fields in this region are nowadays using pivots.

The watershed was delineated from a 20 m resolution Digital Elevation Model

(DEM), which was aggregated from the original 5 m resolution DEM of NLWKN (Niedersächsischer Landesbetrieb für Wasserwirtschaft, Küsten- und Naturschutz). Soils were represented by BÜK200 (Bundesanstalt für Geowissenschaften und Rohstoffe, 2016 (`https://www.bgr.bund.de/DE/Themen/Boden/Produkte/Karten/Downloads/FlyerBUEK200.pdf?blob=publicationFile&v=`) using soil hydraulic parameters from Wessolek (2009).

Table 3.1: Specifications of the soil moisture measuring sites in Gerdau

| Sl. No. | Name & Crop grown | Location | Soil Name | Soil Physical Properties | |
				Texture (%) (sand/silt/clay)	Bulk density (g/cm3)
1.	Hansen (Onion)	10.48° E 52.95° N	128	73/20/7	1.365
2.	Hansen Village* (Winter Wheat)	10.48° E 52.95° N	449	73/20/7	1.365
3.	Barnsen (Corn)	10.42° E 52.98° N	129	73/20/7	1.365
4.	Ebstorf * (Sugar beet)	10.41° E 53.01° N	161	93/5/2	1.045
5.	Heide (Corn)	10.31° E 52.98° N	165	94/5/1	1.41

soil sampling locations used for further analysis.

Table 3.2: Specifications of the soil moisture measuring sites in Wipperau

| Sl. No. | Name & Crop grown | Location | Soil Name | Soil Physical Properties | |
				Texture (%) (sand/silt/clay)	Bulk density (g/cm3)
1.	Rösche (Herb)	10.74° E 52.98° N	161	93/5/2	1.41
2.	Katzien (Corn)	10.77° E 53.00° N	165	94/5/1	1.05
3.	Water Storage* (Corn)	10.75° E 53.02° N	165	93/5/2	1.41
4.	HZ* (Potato)	10.81° E 53.05° N	129	73/20/7	1.36
5.	HZ_Cemetery (Fodder)	10.77° E 53.06° N	165	93/5/2	1.41

soil sampling locations used for further analysis.

The Land cover map was generated by combining CORINE (CORINE Land Cover

CLC2006, Federal Environment Agency, DLR-DFD 2009) with crop distribution statistics of Lower Saxony for the year 2007 (Niedersächsisches Landesamt für Statistik, 2010). Based on these data, crops reported at the community level were distributed in each sub-basin. SWAT hydrological response units (HRUs) were generated by an overlay of soil land use and slope, then the agricultural land use was split by using the crop fractions within each sub-basin. In this process, the net area of crops within a sub-basin is secured but the actual spatial locations of the HRUs are not retained. Apart from the spatial data, temporal weather data for Gerdau and Wipperau catchments were available from 1/1/1975 to 30/09/2016. Daily precipitation data from 6 rain gauge stations in Gerdau and 12 stations in Wipperau were used. Precipitation data were corrected for measurement errors using Richter (1995) depending on temperature. Daily data on temperature, relative humidity, and wind velocity were interpolated from four weather stations. These aforementioned weather parameters were interpolated for all sub-basins using inverse distance interpolation. Solar radiation data was used from the lysimeter station at Hohenzethen (Landesamt für Bergbau, Energie und Geologie, LBEG) for 2001–2013. This time series was extended until Sept 2016 by using solar radiation values from Deutscher Wetterdienst (DWD) Braunschweig station. The solar radiation values of Braunschweig were multiplied by a factor representing the bias in the past data between both stations, which differ in location and hence exhibit a systematic difference in radiation. Daily streamflow data were procured from NLWKN for the respective catchment outlet marked in the map (Fig. 3.1).

3.2.3 Soil moisture estimation from field experiment

The soil moisture field measurements coincided with the Landsat satellite crossing date over the region. The field measured soil moisture was used for calibrating the indirect soil moisture estimation from Landsat images. Out of the total field measurement days, only 7 days in case of Gerdau and 6 in case of Wipperau could be used for the irrigation season of 2016 (Mar-Sep). This was due to unclear sky at 10:15 am (Universal Time Coordinated: UTC) over the catchments for the rest of the days. The clear sky at image recording time was a prerequisite for interpreting Landsat images. Soil moisture was estimated by using Time Domain Reflectometer (TDR) at 10 sites (Fig. 3.1), which were spatially distributed in the two catchments. Gravimetric measurements were conducted on seven days for assessing the quality of soil moisture measured from TDR. TDR provides a representative measure of the volume of soil moisture present in the entire length of the rod (16 cm) placed in the soil profile. The instrument is specially designed for field use and calibrated for universal soils (`https://imko.de/en/products/soilmoisture/soil-moisture-sensors/trimepico64`). Tables 3.1 and 3.2 show the type of crops grown (in the year 2016) and soil physical characteristics of the specific field locations present in Gerdau and Wipperau, respectively. Grain size analysis of all the ten sites was performed according to DIN EN 933-1 for the upper layer of the soil. This has helped to cross-check the soil database and get a better understanding of the spatial variability of soil physical properties.

3.2.4 Soil moisture estimation from Landsat

The satellite images from Landsat 7 and 8 were acquired from the United States Geological Survey (`https://espa.cr.usgs.gov/index/`). The Landsat surface reflectance high-level data products i.e., NDVI based on the surface reflectance and the brightness temperature BT, at top of atmosphere) were used in order to calculate the TVDI (Masek et al., 2006; Vermote et al., 2016). The cloud mask product was used for masking anything else except clear land. The scatter plot of Ts and Ts/NDVI space usually follows the trapezoidal form shown in Fig. 3.2. This distribution is defined by the upper edge which is the dry edge and the lower wet edge. The TVDI is based on the empirical parametrization of the dry edge (T_{smax}) and the wet edge (T_{smin}) given by (Sandholt et al., 2002):

$$T_{smax} = (a_1 * NDVI) + b_1 \qquad (3.2)$$

$$T_{smin} = (a_2 * NDVI) + b_2 \qquad (3.3)$$

Then, TVDI is calculated by using the formula:

$$TDVI = \frac{T_{smax} - T_s}{T_{smax} - T_{smin}} \qquad (3.4)$$

where, T_{smax} and T_{smin} are the dry and the wet edge, respectively; $NDVI$ is the observed normalized difference vegetation index and T_s is the observed surface temperature. For small intervals of NDVI, the maximum and minimum temperatures are observed in order to estimate a_1, b_1, a_2 and b_2 coefficients of T_{smax} and T_{smin} through linear regression. Most approaches are based on the estimation of T_{smax} and T_{smin} for each image that is being studied. However, this approach may result in incomparable results between different dates since the TVDI relies on the maximum and minimum temperatures for each image per day. Furthermore, the cloud fraction influences the pixels that are masked i.e., pixels that are not plotted.
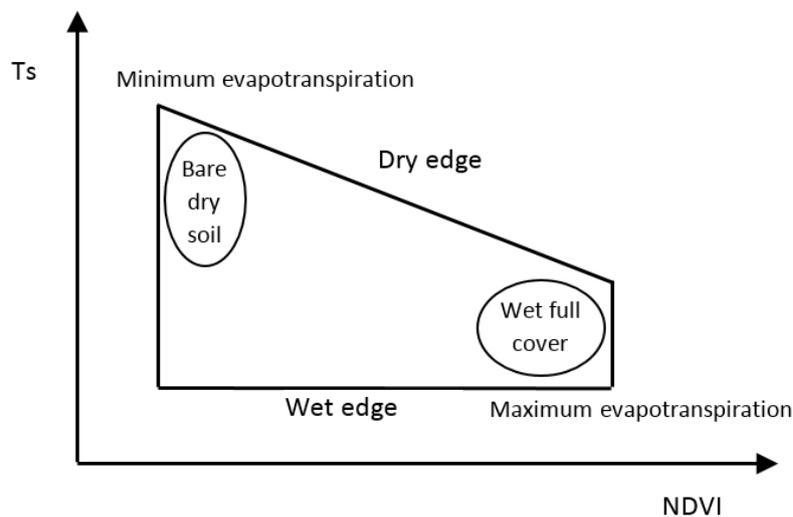
Figure 3.2: Scatter plot of Ts/NDVI space.

In order to cope with this drawback in the current research, dryand wet edges were estimated using universal scatter plot where the Ts/NDVI values for all images were plotted at the same time. Hence, the TVDI for all images are based on common dry and wet edges. Next step was the calculation of correlation between the soil moisture values from field experiments and the TVDI, NDVI and BT values of the corresponding pixels. In order to explore this correlation, linear regression and curve estimation methods were applied to get the best fit.

3.2.5 Model set up, calibration and soil moisture extraction

For this study, Gerdau was divided into 18 sub-basins and 1382 HRUs, whereas, Wipperau was divided into 8 sub-basins and 567 HRUs. This is considered as a satisfactory representation of the basin heterogeneity. Surface runoff was estimated by using the SCS Curve Number method, flow in the catchments was routed by using Muskingum's routing equation. The Penman-Monteith equation was used for estimating the evapotranspiration of the study area. Auto-irrigation was activated in the catchments based on plant water demand. Crops were scheduled according to the planting and harvesting dates provided by the agricultural chamber of Lower Saxony. The eco-hydrological model SWAT was calibrated for streamflow from 1975 to 2000 at the respective outlets of the Gerdau and Wipperau catchments with a five-year warm-up period. Semi-automatic calibration was performed for Gerdau and Wipperau using both manual and automatic calibration by SWAT-CUP (Abbaspour, 2011). A base flow filter program was also used to have an initial estimation of the groundwater flow parameters as well as the percentage of base flow occurring in the catchments (Arnold et al., 1995).

The ranges of the sensitive parameters were chosen from previous studies performed in German catchments (Lam et al., 2011) as well as from the SWAT database (Neitsch et al., 2011). The sensitive parameters used for calibration are shown in Table 3.3. Model performance was evaluated by matching observed and simulated hydrographs visually as well as by using statistical indicators. In addition to this, the parameter uncertainty evaluation was also provided by SWAT Calibration and Uncertainty Procedures (SWAT-CUP) in terms of 95% parameter uncertainty (95PPU) band, *r-factor* and *p-factor* for evaluating the model performance. The *p-factor* denotes the percentage of measured data bracketed by the 95% prediction uncertainty (95PPU), whereas the *r-factor* denotes the average thickness of the 95PPU band divided by the standard deviation of the measured data (Abbaspour, 2011). After attaining an acceptable model performance during the calibration period (1980-2000), model validation was performed (2001-2014). Soil moisture at HRU level was extracted from the final model output. In the current study, the first layer of the soil was evaluated, which corresponds to the top 30 cm of the soil profile. The model simulated soil water content (in mm) was first converted into relative soil moisture (percentage) and then into total moisture present in the respective soil layer.The moisture content at wilting point (WP) corresponding to different soil texture and bulk density was extracted from (Wessolek, 2009). The aforementioned source was used for converting the SWAT output i.e., plant available water content (SW) to total moisture present (SW + WP) in the selected soil layer.

3.2.6   Soil moisture data analysis

The spatial and temporal analysis of the soil moisture derived from three different sources i.e., Landsat, SWAT, and TDR were conducted. There is a scale gap between soil moisture extracted from remote sensing (Landsat resolution 30 m) and soil moisture data from SWAT (Average HRU area: 22.32 ha for Gerdau and 35.35 ha for Wipperau) due to their different resolutions. Landsat provides precise spatial estimates of soil moisture under varying soil and crop present in the catchment on a given day. However, in SWAT crops were not explicitly incorporated in terms of spatial extent, they were distributed only on the basis of actual land use statistics. Therefore, boxplots were drawn to represent the overall distribution of soil moisture when a clear image from the Landsat was available. Apart from this, the seasonal dynamics of soil moisture during the entire irrigation season extracted from different sources (TDR, SWAT, and Landsat) was also evaluated separately using the boxplots for Gerdau and Wipperau. In addition to the graphical measures, one-on-one comparison of the soil moisture extracted from different sources was performed for the entire irrigation period of 2016. In addition to the overall soil moisture distribution using boxplots, soil and land use (agricultural land use) specific soil moisture maps were also developed. The absolute soil moisture difference maps for four days in the entire irrigation period (7 March, 12 May, 24 Aug, and 9 Sept) were created for agricultural soils in the two catchments. The aforementioned soil moisture difference maps were developed by creating the soil moisture raster maps from SWAT and Landsat, respectively. Furthermore, the soil specific maps were extracted from SWAT and Landsat soil moisture raster maps corresponding to the agricultural land use and analysis was performed using these maps. For space constraints, soil moisture difference maps and spatial statistics for the Wipperau catchment are shown in the results section.

3.2.7   Quantification of SWAT soil parameter uncertainty

Parameter uncertainty is one of the key uncertainties present in modeling studies. There is a huge concern in hydrological modeling about equifinality, which means that different combinations of parameters can lead to the same model result (Beven and Binley, 1992). Therefore, to keep a check on the possible non-uniqueness of model results corresponding to the model parameters, parameter uncertainty is usually quantified in hydrological modelling for streamflow. In this study, a parameter uncertainty band for simulated soil moisture was created for specific combinations of crops and soils on HRU basis to represent the soil moisture dynamics in the catchment. The selections of the HRUs were based on two soils (sandy and sandy loam) covering the major portion of the two catchments along with the major grown crops in the area, corn, potato, sugar beet, and winter wheat. First, SWAT was run with different combinations of parameters by using the SWAT-CUP software. Then, the parameter sets from SWAT-CUP yielding good model efficiency (Nash-Sutcliffe Efficiency greater than 0.5) were selected. SWAT was run for these parameter sets and the corresponding simulated soil moisture data for each parameter set were extracted. After that the soil moisture parameter uncertainty band for different combinations of soil type and crop was created from the maximum and minimum values of soil moisture for each time step. The overall spatio-temporal variation (1980-2014) in soil moisture was

evaluated by using boxplots for Gerdau and Wipperau, respectively. In addition to this, soil moisture parameter uncertainty bands during the irrigation period 2016 were shown for the four experimental locations along with the observed soil moisture values in Wipperau and Gerdau, respectively (marked * in Table 3.1 and 3.2). Both statistical, as well as graphical indicators were used to evaluate the parameter uncertainty band for the chosen locations in the two catchments.

3.3 Results and discussion

3.3.1 Hydrological model performance

Model calibration is performed using both surface and groundwater parameters for calibrating the developed models for streamflow. Table 3.3 shows the sensitivity ranking of the different parameters and their final values for the two catchments.

Table 3.3: Sensitive parameters along with the final uncertainty range

Sl. No.	Parameters	Gerdau		Wipperau	
		Sensitivity Ranking	Parameter range & Best calibrated parameter value	Sensitivity Ranking	Parameter range & Best calibrated parameter value
1.	r__CN2.mgt (SCS curve number)	*8*	(−0.20, −0.15), -0.17	*3*	(−0.20, −0.15), -0.17
2.	v__ALPHA_BF.gw (Base flow recession constant, days)	*4*	(0.0, 0.42), 0.37	*7*	(0.43, 0.84), 0.8
3.	v__GW_DELAY.gw (Groundwater delay, days)	*5*	(372.64, 704.98), 586.33	*4*	(117.16, 213.97), 185.17
4.	v__RCHRG_DP.gw (Recharge to deep aquifer)	*1*	(0.12, 0.5), 0.4	*1*	(0.60, 0.81), 0.67
5.	r__SOL_AWC().sol (Available soil water capacity, mm H20/mm of soil)	*3*	(-0.18, -0.02), -0.17	*2*	(-0.18, -0.02), -0.17
6.	r__SOL_K().sol (Soil hydraulic conductivity, mm/h)	*6*	(-0.016, -0.11), -0.17	*6*	(-0.016, -0.11), -0.17
7.	v__ESCO.hru (Soil evaporation compensation factor)	*2*	(0.5, 1.0), 0.97	*5*	(0.04, 0.4), 0.14
8.	v__GW_REVAP.gw (Groundwater re-evaporation coefficient)	*7*	(0.009, 0.046), 0.024	-	-

v means replace and r means relative change.

As shown in this table, the sensitivity ranking of a particular parameter is different in different catchments. Groundwater recharge to the deep aquifer was found to be most sensitive in both catchments, which is in accordance with the study performed by Wittenberg (2015). The relatively high value of recharge to the deep aquifer (RCHRG_DP) in Wipperau (0.7) can be justified by high infiltration rates, low density of surface water bodies and groundwater streams to the north (Elbe basin) makes it a losing catchment.

The graphical results are shown for calibration (Figs. 3.3-3.6), whereas the statistical model evaluation is provided for both calibration and validation periods for the two catchments (Table 3.4). Apart from the streamflow hydrographs (Figs. 3.3 and 3.5), flow duration curves (Figs. 3.4 and 3.6) of observed and simulated streamflow are drawn on a logarithmic axis for the better representation of the low flow.
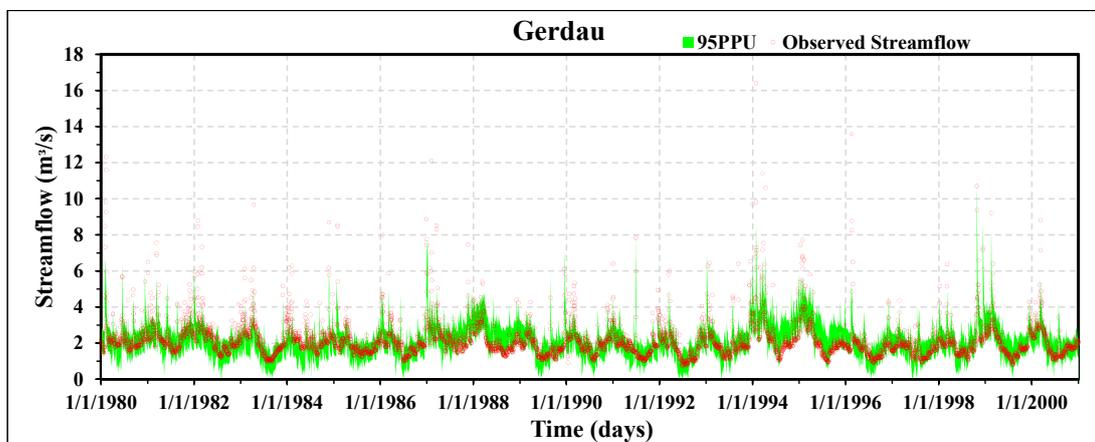
Figure 3.3: Comparison of daily streamflow hydrographs for calibration period (1980–2000) for the Gerdau catchment.
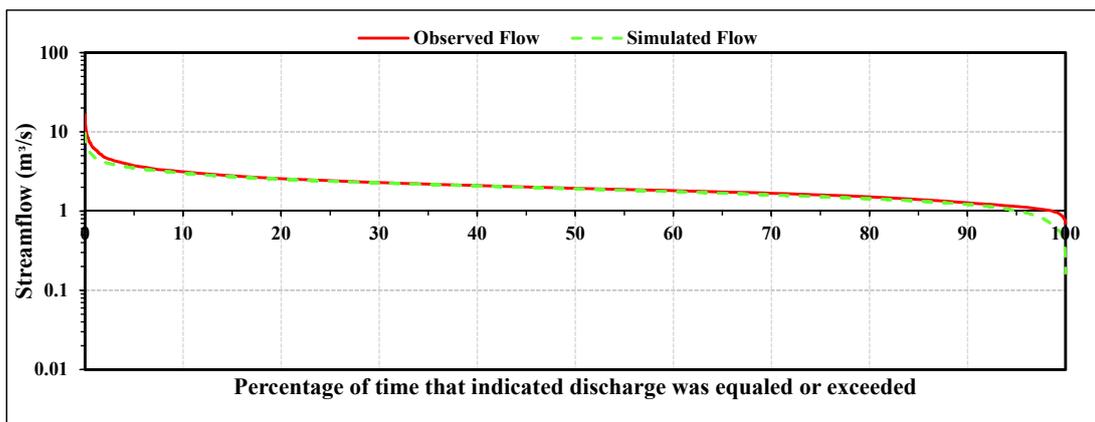
Figure 3.4: Flow duration curve for the Gerdau during calibration period.
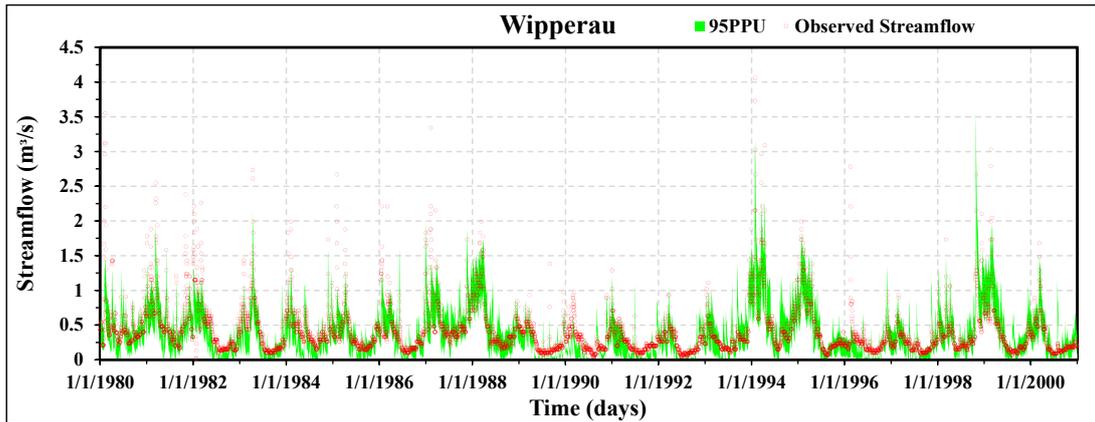
Figure 3.5: Comparison of daily streamflow hydrographs during calibration period (1980–2000) for the Wipperau catchment.
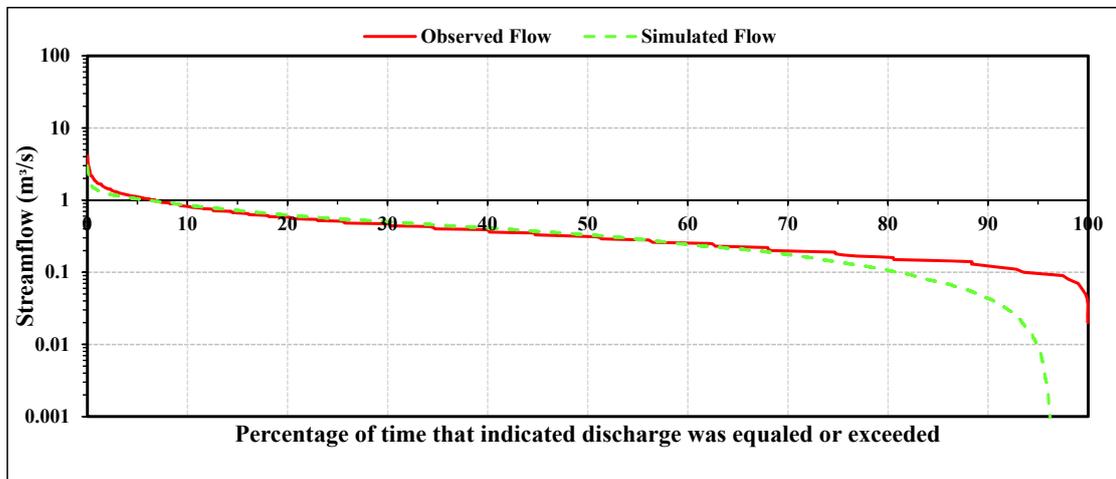
Figure 3.6: Flow duration curve for the Wipperau during calibration period.

The low and mean flows are predicted relatively well in both the cases (Figs. 3.4 and 3.5), whereas few peaks are underestimated. Both models under predict the very low flow (<0.05 m^3/s in case of Wipperau & <1 m^3/s in case of Gerdau) (Figs. 3.4 and 3.6) [NSE (Gerdau) = 0.57 & NSE (Wipperau) = 0.67; PBIAS (Gerdau & Wipperau) = 5.2%]. This might be due to the high groundwater loss and disconnection of the deep aquifer in SWAT. However, according to the statistical model evaluation (Table 3.4), the performance of both of the models ranged between good to satisfactory for different statistical indicators (Moriasi et al., 2007). It can be seen from the aforementioned table that there is more uncertainty in case of Gerdau (*r-factor* = 1.41) as compared to that of Wipperau (*r-factor* = 0.87), as the width of 95PPU band (*r-factor*) is more. This justifies the higher *p-factor* in case of Gerdau (*p-factor* = 0.76) as compared to the Wipperau catchment (*p-factor* = 0.72) during the calibration period.

Table 3.4: Model evaluation statistics

Statistical Indicator	Gerdau		Wipperau	
	Calibration (1980-2000)	Validation (2001-2014)	Calibration (1980-2000)	Validation (2001-2014)
p-factor	0.76	0.87	0.72	0.61
r-factor	1.41	1.39	0.87	0.65
R^2 (Coefficient of Determination)	0.59	0.52	0.68	0.67
NSE (Nash-Sutcliffe Efficiency)	0.57	0.45	0.67	0.65
PBIAS(%, Percent Bias)	5.2	5.3,	5.2	1.4
KGE (Kling-Gupta Efficiency) (Gupta et al., 2009)	0.71	0.71	0.81	0.81

3.3.2 Uncertainty in SWAT soil moisture simulation

For analyzing the parameter uncertainty of SWAT simulated soil moisture, a combination of four relevant crops and two characteristic soil types were investigated. Corn silage (CSIL), potato (POTA), sugar beet (SGBT) and winter wheat (WWHT) are the main crops grown in both of the catchments. Soil 128 is sandy loam, whereas soil 165 is medium sand (Tables 3.1 and 3.2). SGBT and WWHT were analyzed for Gerdau, whereas CSIL and POTA were used in case of Wipperau to show the overall dynamics of soil moisture under two different selected soils. Figs. 3.7 and 3.8 show the spatial and temporal distribution of SWAT simulated soil moisture during the model simulation period (1980–2014) for the whole Wipperau and Gerdau, respectively.

It can be seen from Fig. 3.7 that there is a clear difference between the median soil moisture values in 165 (sandy) and 128 (sandy loam) soils. It can also be concluded from the results that the soil texture plays a more important role in soil moisture storage than the crops (Fig. 3.7, SGBT & WWHT; Fig. 3.8 CSIL & POTA). In addition to this, one can also see a clear difference in overall variability of soil moisture in the same soils with different crops. Even though the median is nearly the same for the same soil with different crops in all the four cases, the overall spread is different (including upper quantile, lower quantile, and outliers).
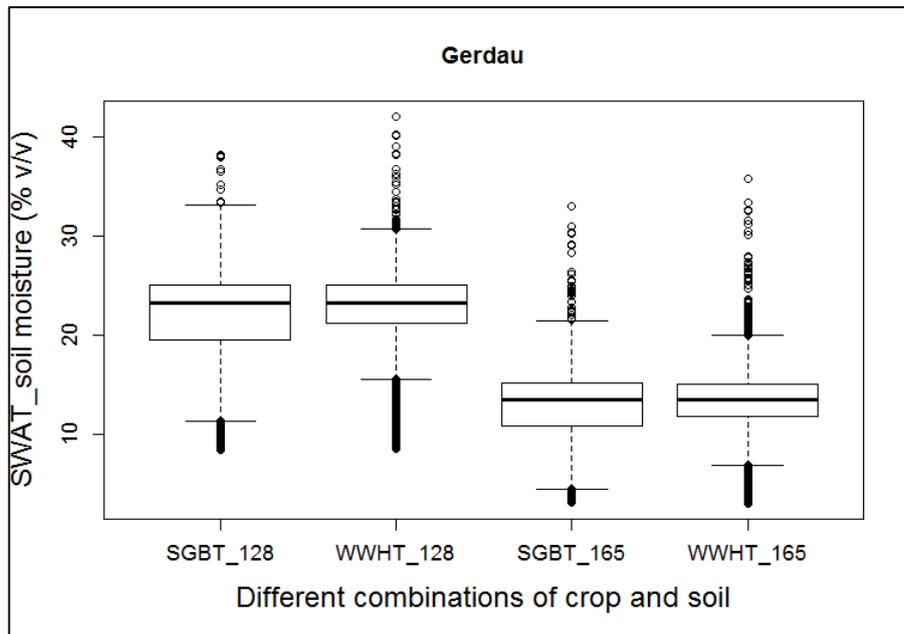
*128 and 165 denotes the sandy loam and sandy soil.

Figure 3.7: Overall variation in SWAT simulated soil moisture of the top layer (30 cm) for 128 and 165 soils with sugar beet (SGBT) and winter wheat (WWHT) for the Gerdau catchment.
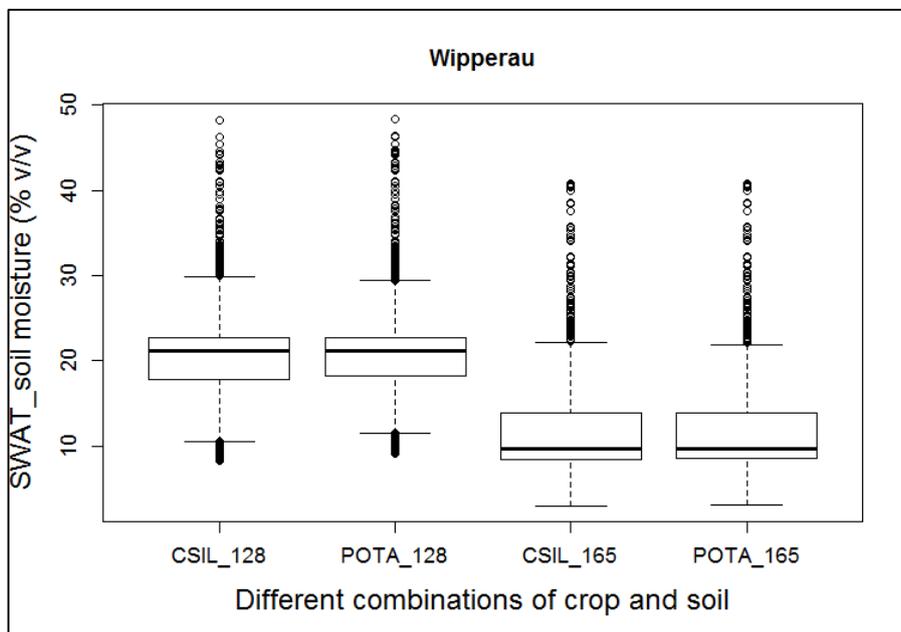
*128 and 165 denotes the sandy loam and sandy soil.

Figure 3.8: Overall variation in SWAT simulated soil moisture of the top layer (30 cm) for 128 and 165 soils with corn silage (CSIL) and potato (POTA) for the Wipperau catchment.

This deviation in the soil moisture band corresponding to different crops growing (SGBT & WWHT) in same soil (Fig. 3.7) can be explained by the different rate of evapotranspiration of root and grain crops and also different planting and maturing periods. At some time-steps, the simulated soil moisture exceeds the field capacity. This can be justified by the over-saturation of soil after intensive rainfall and frost periods during the winter season. When the soil surface temperature increases, the melting of frozen water starts in the upper layers. If the lower soil layer is still frozen, then the water accumulates in the top layer resulting in over saturation of the upper soil layer.
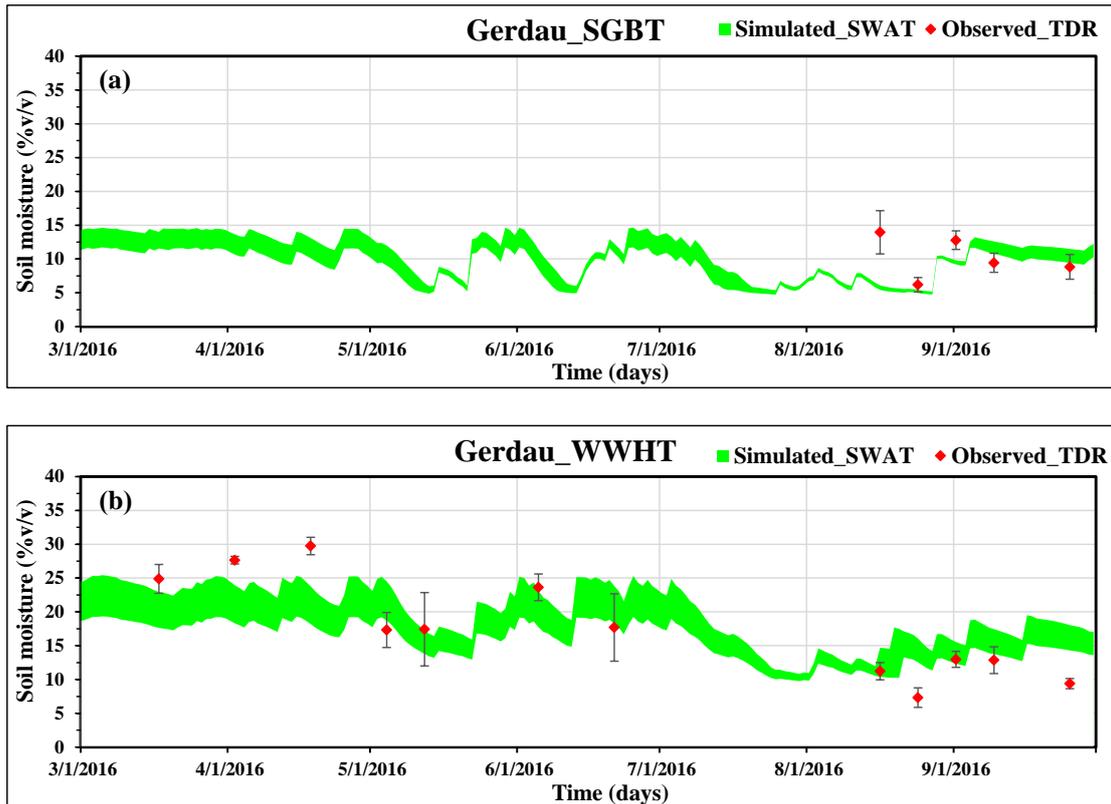
Figure 3.9: (a,b) Soil moisture parameter uncertainty band for SGBT and WWHT with the respective range of observed soil moisture at different soil sampling locations (*marked) in the Gerdau catchment.

Apart from the boxplots, soil moisture uncertainty bands were created specifically for 2016 along with the observed range of soil moisture values from field measurements for Gerdau and Wipperau [Figs. 3.9(a,b) and 3.10(a,b)]. In this case, one specific HRU corresponding to the sampling site is considered (Marked * in Table 3.1 and 3.2), unlike in the previous case where all the HRUs comprising of a particular crop and soil in the catchment were considered for creating the boxplots.

It can be seen from Figs. 3.9(a,b) and 3.10(a,b) that most of the observed range of soil moisture measurements are within or close to the soil moisture parameter uncertainty band simulated by SWAT. The range represented as bar depicts the spatial variability of soil moisture at the sampling location obtained from 10 samplings within one field. It can also be seen from the observed TDR soil

moisture values that the overall seasonal variability is met relatively well by SWAT except during the harvesting period. This may be explained by the activation of auto-irrigation based on plant water demand. The model provides irrigation water, whenever the soil moisture falls below the threshold value of soil moisture for triggering irrigation, whereas in actual practice farmers stop irrigating their crops a few weeks before the harvest. Another aspect to note would be, the field measurements might not be well representative for the HRU as the area of measurement is relatively low as compared to the area of the HRU.
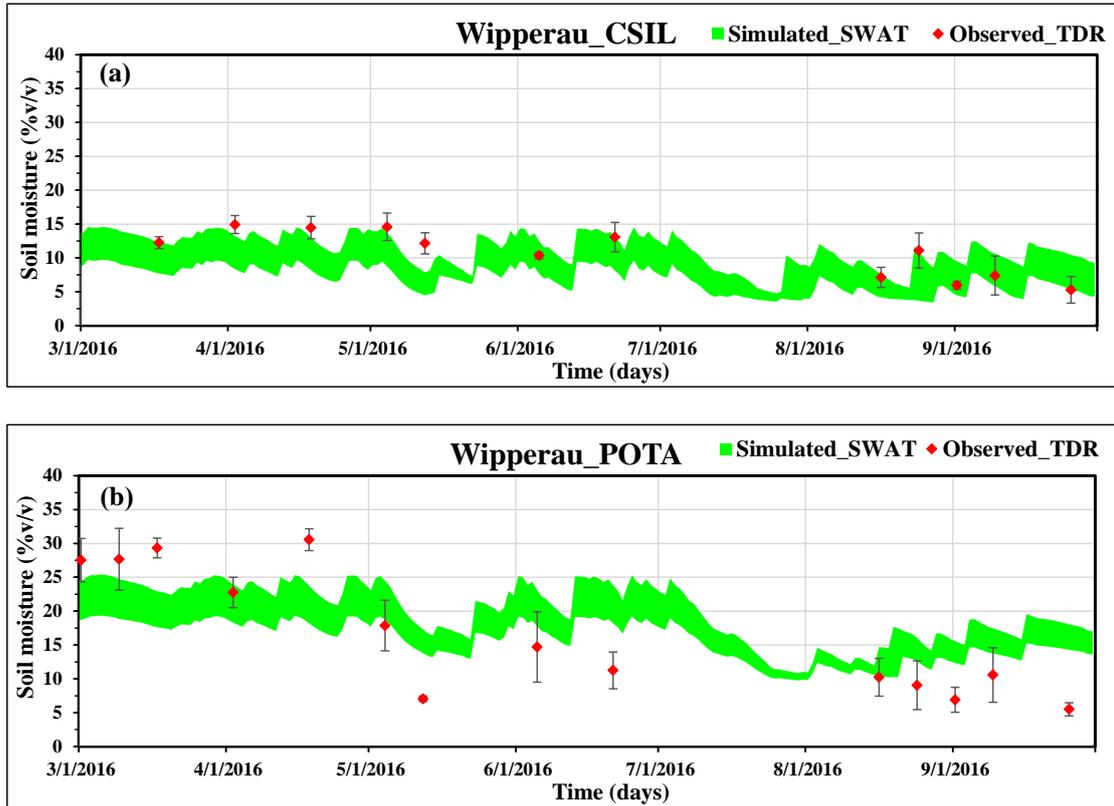
Figure 3.10: (a,b) Soil moisture parameter uncertainty band for CSIL and POTA with the respective range of observed soil moisture at different soil sampling locations (*marked) in the Wipperau catchment.

Table 3.5: Parameter uncertainty estimators

	Gerdau		Wipperau	
Statistical Indicator	SGBT	WWHT	CSIL	POTA
p-factor	0.60	0.66	0.83	0.57
r-factor	0.72	0.65	1.31	0.52

* SGBT: Sugar beet; WWHT: Winter wheat; CSIL: Corn silage; POTA: Potato

Additionally, Table 3.5 shows the parameter uncertainty estimators for the soil

moisture uncertainty band at the selected sampling locations. The *p-factor*, which is nearly or more than 0.6 in all the cases, suggests that an acceptable number of observed data lies within the uncertainty band. An *r-factor* (uncertainty width) close to one is usually acceptable which is in accordance with the current case. However, it should be noted that the uncertainty band in the current research only includes parameter uncertainty.

3.3.3   Remote sensing moisture modelling

The scatter plot of the temperature and NDVI for all images is presented in Fig. 3.11. The dry and wet edges are defined by the following equations:

$$T\_smax = (-0.0101 * NDVI) + 3100.4 \tag{3.5}$$

$$T\_smin = (-0.0018 * NDVI) + 2765.6 \tag{3.6}$$

Then, the TVDI value for each sampling pixel was calculated based on its corresponding NDVI and BT values retrieved from satellite images. The whole dataset was randomly divided into 70 % training and 30% validation. Six different models were used to train the TVDI and NDVI values for calculating the respective soil moisture using Landsat imagery. The models and the performance results in training (R^2 and RMSE) as well as in validation (RMSE) sets are shown in Table 3.6.
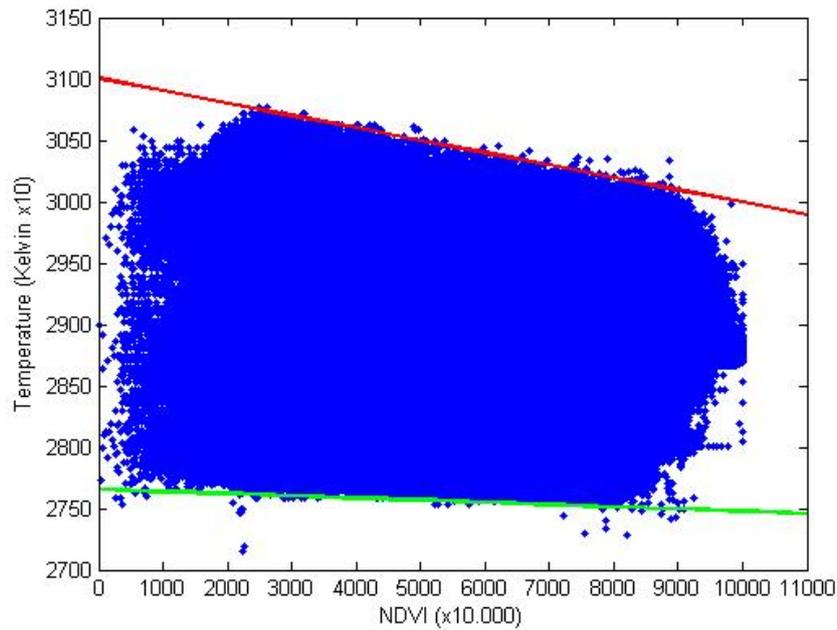
Figure 3.11: Ts/NDVI scatter plot of all satellite images and the wet (shown as green line) and dry (shown as red line) edges.

The overall spatial variation of soil moisture on 24 August 2016 is evaluated corresponding to the observed values from TDR. Fig. 3.12 represents the spatial

comparison of soil moisture from 6 different models (M1-M6) for 24 August 2016 explained in Table 3.6. The aforementioned day is selected because soil is assumed to be dry during this period and also from the review that the overall error in remotely sensed data is relatively less in dry periods as compared to the wet days. It can be easily accessed from the figure that in spite of having comparable model performance in training and testing (Table 3.6), the overall model spread is quite different in all the models. Therefore, out of all the selected models, M5 is selected for further analysis as its spread and median is closer to the observed soil moisture data.

Table 3.6: TDR modelling results of linear regression and curvature estimation

Model	Goodness of fit		Goodness of validation
	R^2	RMSE	RMSE
(M1) TDR = 22.68*TVDI + 4.203 TDR	0.64	4.1	4.1
(M2) TDR = 35.83 * TVDI^2– 14.03 * TVDI + 11.3	0.69	3.9	3.9
(M3) TDR = 23.29 * TVDI$^{2.327}$ + 9.065	0.69	3.9	4
(M4) TDR = 6.722 * exp(1.528 * TVDI)	0.68	3.9	4.1
(M5) TDR = 225.4 – 0.0008178 * NDVI – 0.07095 *T	0.64	4.3	4.1
(M6) TDR= 25.46 + 0.04966 * NDVI – 0.005673*T – 3.531e –0.7 NDVI^2 –1.591e–(0.5*NDVI*T)	0.67	3.9	4.9
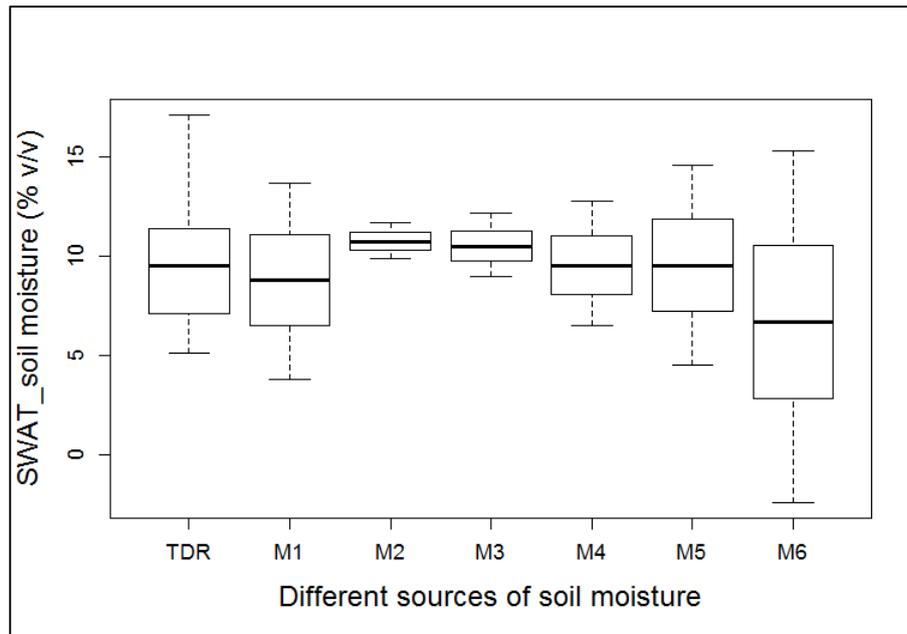
Figure 3.12: Comparison of observed soil moisture (TDR) with soil moisture calculated from different regression models (M1-M6) using NDVI/Ts/TVDI on August 24th, 2016.

3.3.4   Soil moisture comparison

In this section, soil moisture values from three different sources (TDR, SWAT, Landsat) are compared for two dates close to the beginning and end of the irrigation season, i.e., 17 March and 24 August 2016. Practically the irrigation ended in September but there is no clear Landsat image available after 24 August 2016. It can be seen from the boxplots (Figs. 3.13 and 3.14) that the median values of soil moisture from Landsat (RS), SWAT simulated soil moisture for the top 30 cm (SM_30) and soil moisture measured by using TDR (TDR) are not in the same range for Gerdau and Wipperau on 17 March 2016. However, median and spread of soil moisture extracted from all the sources match relatively well for August. In addition to it, the overall boxplots comparison is worse for March in both the models.

Although the comparison of boxplots between the two catchments [Gerdau, Fig. 3.13 & Wipperau Fig. 3.14] revealed that the soil moisture distribution is better in case of Wipperau as compared to Gerdau. It can also be seen that there are outliers in the soil moisture simulated by SWAT for the upper 30 cm of the soil profile. Few unexplainable values of soil moisture from SWAT($\geq$40% v/v) may be explained by the complete filling of pore space in the first layer. Table 3.7 shows the correlation between the soil moisture from TDR, RS and the SM_30. Soil moisture correlation varies from 0.68 to 0.88, except at one point in Wipperau where the correlation between TDR and SM_ 30 is only 0.54. As mentioned earlier, there is a scale gap between the methods, so this single point evaluation is not expected to give very high correlations, but results in Table 3.7 show a good overall correlation of the three methods.
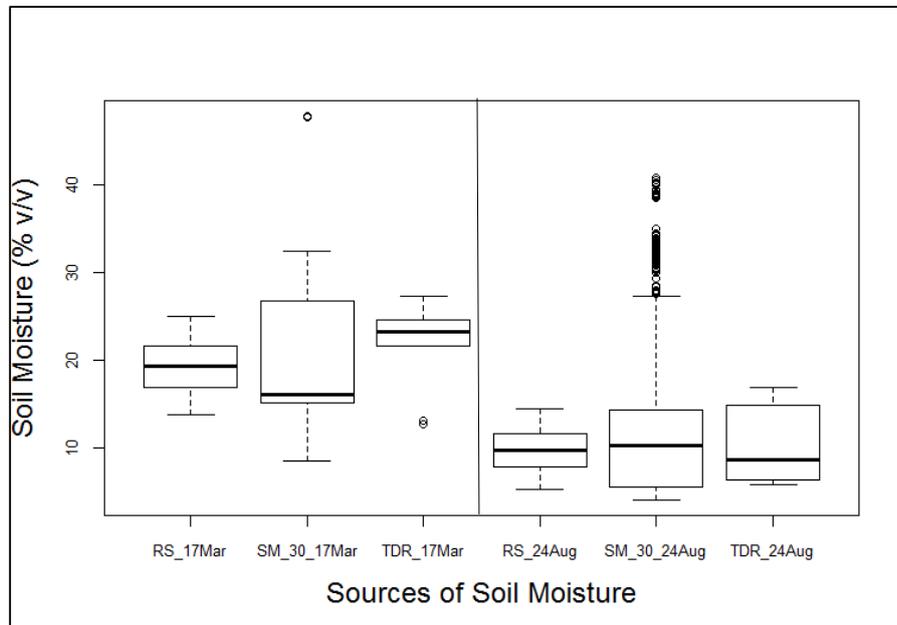
Figure 3.13: Comparison of remotely sensed (RS), SWAT simulated (SM_30) and observed (TDR) soil moisture on March, 17 and August, 24 in the Gerdau catchment.
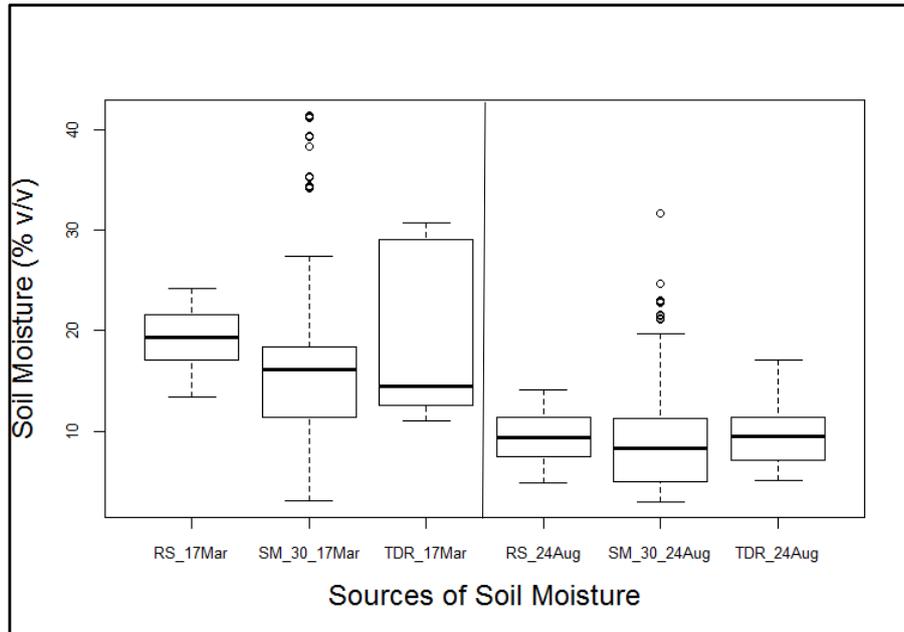
Figure 3.14: Comparison of remotely sensed (RS), SWAT simulated (SM_30) and observed (TDR) soil moisture on March, 17 and August, 24 in the Wipperau catchment.

Table 3.7: Soil moisture correlation matrix.

Gerdau				**Wipperau**			
Sources of soil moisture	TDR	RS	SM _30	Sources of soil moisture	TDR	RS	SM _30
TDR	1.00			TDR	1.00		
RS	0.87	1.00		RS	0.88	1.00	
SM_30	0.78	0.82	1.00	SM_30	0.54	0.68	1.00

In addition to this, the temporal dynamics of soil moisture for Gerdau and Wipperau is also evaluated. The boxplots in case of Wipperau [Fig. 3.15(a–c)] for the six days of the irrigation season 2016, where clear Landsat images are available, show that although edian and spread of the data from all the sources do not match well with each other (on a particular day), still the overall temporal dynamics of soil moisture is relatively consistent during the irrigation season. Soil moisture difference maps are used to provide a better visual representation of the overall spatial and temporal dynamics of soil moisture for specific combinations of soils under agricultural landuse. Fig. 3.16 shows the major soils in the Wipperau catchment which are considered for creating the absolute soil moisture difference maps from Landsat and SWAT.
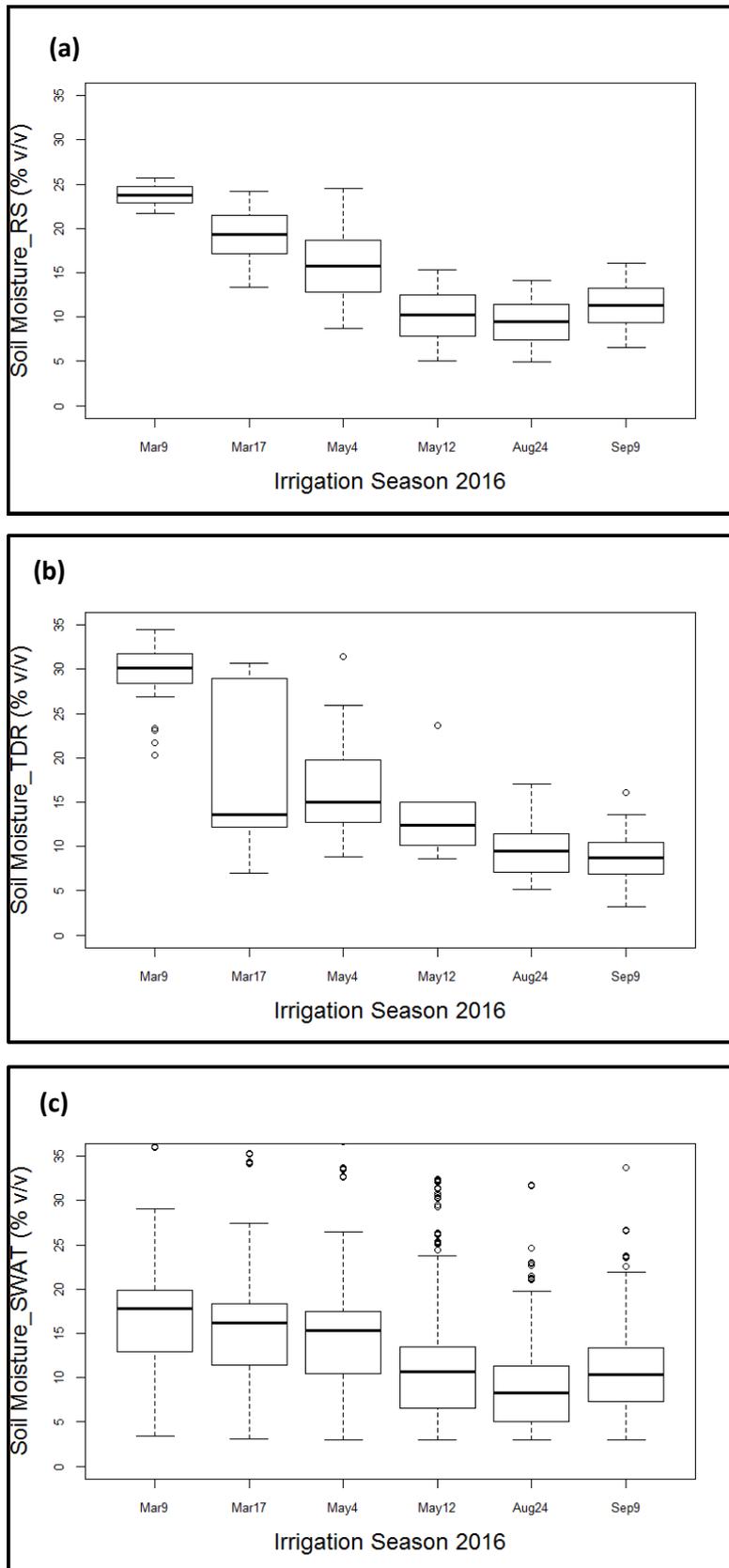
Figure 3.15: (a–c) Temporal dynamics of soil moisture in the Wipperau catchment for the field sampling dated during the irrigation season 2016.
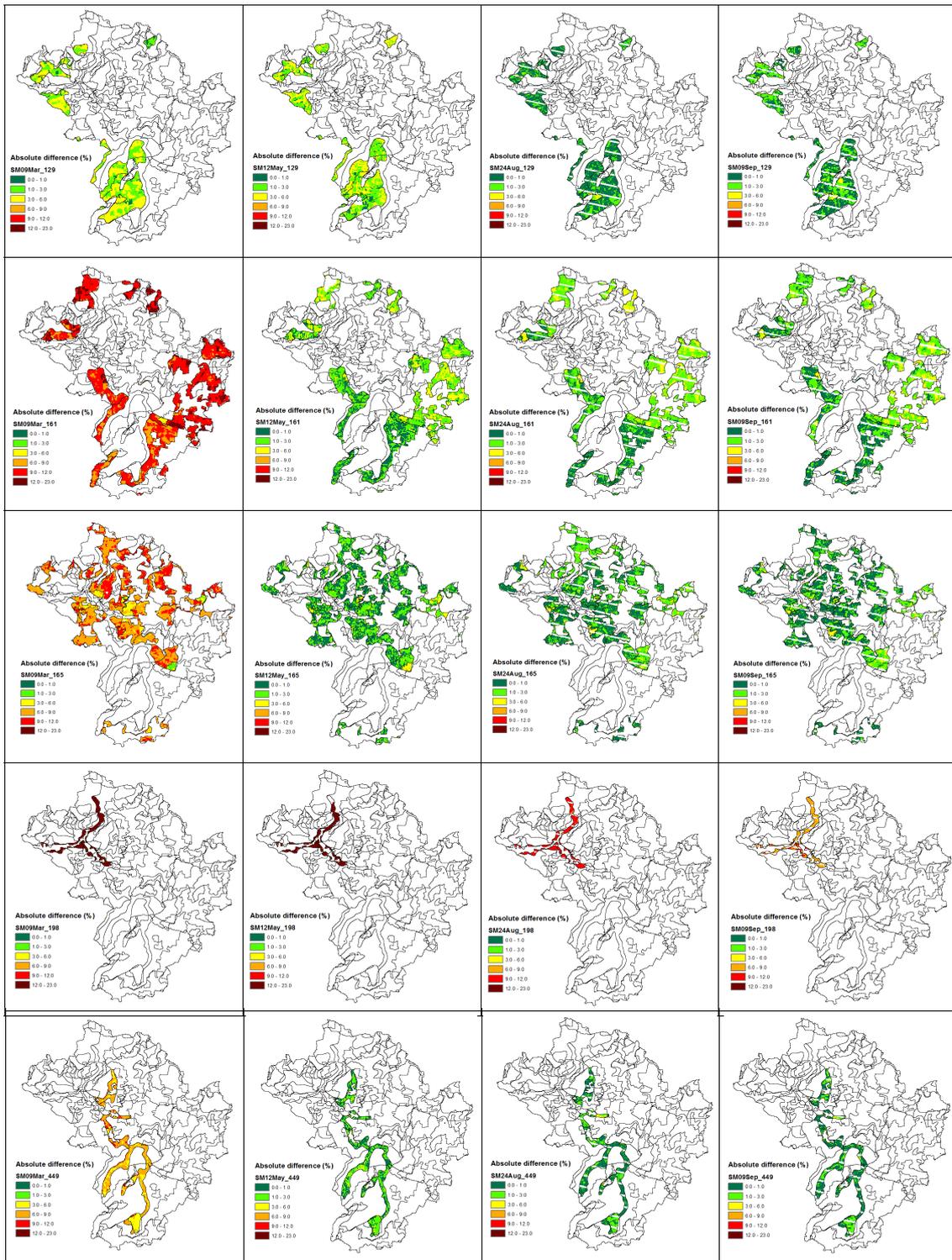
Figure 3.16: Soil moisture absolute error maps for Wipperau under major agricultural soils in the area.

It can be assessed that the absolute difference in most of the spatial maps is low (less than 10%, shown in green color). In addition to this, the range of absolute difference in case of soil 198 for all the considered days (09 March, 2016, 12 May, 24 Aug, and 09 Sept 2016) is usually higher in all the cases (6–23%). Landsat

fails to represent soil 198, which has higher field capacity equal to 0.40 mm/mm (Wessolek, 2009), which was also confirmed by field investigations. However, soil 198 was not included into the calibration of regression models. The absolute soil moisture difference map show very low difference (<3%) in the most of the maps (SM24Aug_129) with relatively high difference in SM09Mar_161 and SM09Mar_165 maps. The soil moisture difference maps are also backed by the average spatial statistics using Table 3.8. It can be evaluated from the table that the overall mean absolute difference (4-15.69%) and standard deviation (1.74-4.06)is high in the 198 soil type. The mean absolute difference of sandy soils (161 and 165) are more than that of sandy loam soil (128). In addition, it can also be seen that the mean absolute difference is reducing from March to Sept, which confirms that the Landsat extracted soil moisture can be better used as an indicator for irrigation planning and management during dry periods.

Table 3.8: Spatial statistics for the Wipperau catchment

Sl. No.	Date	Soil_type	Mean absolute difference	Standard deviation
1.	9-Mar-16	165	8.17	1.79
2.	9-Mar-16	449	6.87	1.76
3.	9-Mar-16	198	15.69	2.66
4.	9-Mar-16	129	3.33	1.64
5.	9-Mar-16	161	10.15	1.58
1.	12-May-16	165	1.38	1.47
2.	12-May-16	449	1.45	1.45
3.	12-May-16	198	18.79	4.06
4.	12-May-16	129	2.86	1.59
5.	12-May-16	161	2.08	1.40
1.	24-Aug-16	165	1.28	1.09
2.	24-Aug-16	449	0.91	0.78
3.	24-Aug-16	198	10.04	1.74
4.	24-Aug-16	129	0.81	0.72
5.	24-Aug-16	161	1.97	1.20
1.	9-Sep-16	165	1.17	1.11
2.	9-Sep-16	449	0.89	0.86
3.	9-Sep-16	198	7.45	1.86
4.	9-Sep-16	129	1.10	0.94
5.	9-Sep-16	161	1.77	1.23

3.3.5 Adjustment of SWAT soil parameters

Based on the absolute soil moisture difference maps shown in Fig. 3.16, it can be concluded that the soil 161 shows a typical behavior, which can be explained by using image SM24Aug_161. It can be seen from the figure that the absolute difference is less in the lower section (south-western) as compared to the upper section (north-eastern). The aforementioned pattern is common in all the cases with soil type 161, which prompted for refinement of the soil parameters. The original database of

profiles of the soil map BÜK 200 provides alternative profiles for a single soil type, along with the frequency of occurrence. Backed by field/lab investigations of the grain size distribution on several locations, a sub-type of soil 161 (161_1; Table 3.9) with new parameters from a less frequent profile is created. After re-simulating the SWAT model, new spatial maps are drawn for all the four days considered for this analysis. Fig. 3.17 shows the soil moisture absolute difference maps after adjusting the model parameters. It can be seen from the modified difference maps that the soil moisture absolute difference range is reduced in all the four days, which are considered for creating difference maps.

Table 3.9: Physical properties of the sub-type (161_1) of 161 soil

Soil depth (mm)	Soil texture (%) sand/silt/clay	Hydraulic conductivity (mm/h)	USLE_K	Available soil water capacity ($mm\,of\,soil/mm\ of\,water$)	Bulk density (kg/m^3)
$0-300$	85/13/2	65.42	0.24	0.18	1.397
300-530	85/13/2	36.67	0.23	0.16	1.397
530-2000	94/5/1	75	0.20	0.10	1.640
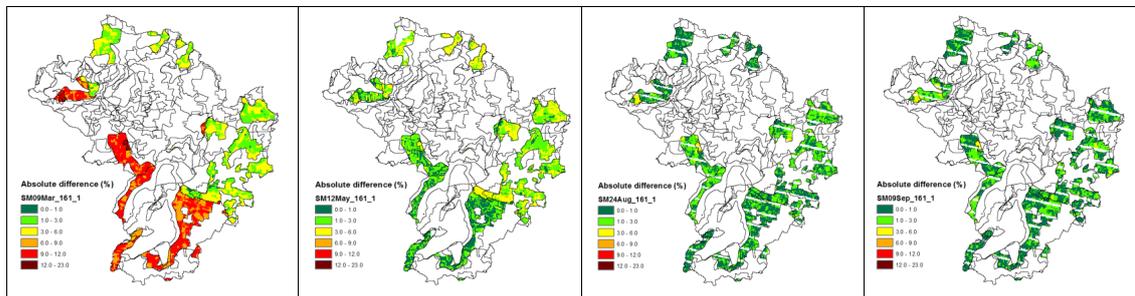
Figure 3.17: Absolute soil moisture error maps for Wipperau under new soil sub-type for 161 (161_1) soil.

In addition to this, the overall absolute difference statistics have also reduced in all the cases (Table 3.10). It is concluded from this analysis that Landsat plays a significant role in improving the overall distribution and also reducing the mean absolute soil moisture difference. Therefore, this may be noted as a considerable advantage of Landsat data in hydrological modeling as it not only provides the indirect soil moisture estimations but has an upper hand in improving the overall spatial soil moisture patterns.

Table 3.10: Spatial statistics for adjusted 161 soil in the Wipperau Catchment

Sl. No.	Date	Soil_type	Mean absolute difference	tandard Deviation
1.	9-Mar-16	161_1	6.00 (10.15)	3.41 (1.58)
2.	12-May-16	161_1	2.24 (2.08)	1.3 (1.4)
3.	24-Aug-16	161_1	1.09 (1.97)	0.87 (1.2)
4.	9-Sep-16	161_1	1.06 (1.77)	0.88 (1.23)

*Values in italics are the previous mean absolute error and standard deviation before the soil adjustment.

3.4 Conclusions

The present study demonstrates the application of remote sensing and field data in evaluating SWAT simulated soil moisture at the regional scale for two catchments in Northern Germany. The calibrated and validated model was used to derive soil moisture uncertainty bands under different soils and crops of the irrigation season 2016 by considering the uncertainty of soil related model parameters. The results reveal that parameter uncertainty varies with different soils and different crops. The results showed that parameter uncertainty almost frames the observed soil moisture values. However, there is considerable uncertainty of the model structure, which can be related to the simplified soil water equations of SWAT, using a cascade of tipping buckets approach. In addition to this, there is also substantial variability in the observed soil moisture data. Temperature, NDVI, and TVDI were calculated from Landsat images, which were converted into soil moisture by using several regression models. Regression models were trained by using the TDR measurements and the one, whose median and overall data spread matched relatively well with the TDR, was used for further analysis. The current study reveals that soil moisture extracted from Landsat could be used as a good indicator to evaluate the spatial and temporal dynamics of soil moisture extracted from the hydrological model when field-based soil moisture data is not enough. The field based soil moisture data is necessarily required to calibrate the spatial maps obtained from the Landsat. For both aspects, only a few data are available due to the lack of soil moisture monitoring stations and due to the need for a clear sky for the remote sensing method. The spatial and temporal resolution of soil moisture procured from three sources is not exactly comparable. In addition to this, the soil moisture extracted from SWAT provides the average value of soil moisture of the upper 30 cm of the soil profile, whereas TDR gives the average soil moisture values from the upper $\sim$ 16 cm of the soil profile. However, Landsat provides soil moisture of the top few centimeters of the soil profile only, without knowing the precise depth, from which the image is influenced. Therefore, further research could be done to improve the level of precision. This would involve extended studies at the field scale, which is beyond the focus of the current study. In the current research, the SWAT soil parameters were modified by investigating a consistent behavior of spatial soil moisture patterns from Landsat images. The modification was confirmed by a higher resolution soil map and by field investigations. However, using the results of this analysis, the hydrological model

can be rectified and applied with higher confidence in simulating soil moisture. SWAT provides daily estimates of soil moisture at a finer resolution, which can be used for continuous simulation and forecasting of soil moisture. Possible fields of application are studies in planning and design of large scale irrigation systems and irrigation control schemes, and investigations about the impact of climate change on soil moisture and irrigation scheduling. However, further research is required to study the behavior of SWAT in simulating crop processes. This research helped to improve knowledge about large scale spatio-temporal dynamics of soil moisture at finer resolution in a humid country. Arid or semi-arid countries have an advantage of the clear sky throughout the year, and irrigation demand is there during the entire growing season. As the spread and behavior of soil moisture is better matching during the dry season from all the sources in this study from a humid region, we expect that this method can be even better applied under semi-arid and arid conditions. Additionally, the Landsat extracted soil moisture can also be used for recalibrating the hydrological model with the aim of reducing the uncertainty of simulated soil moisture. The findings of this study and the follow-up studies can also be used for predicting and monitoring agricultural droughts in the catchments around the globe. Future research will be done in comparing multiple hydrological models and in simulating the effect of the quality of soil moisture simulation on irrigation control. The latter brings uncertainty to water balance and water management studies in agricultural catchments, which is much less investigated compared to hydrological model parameter uncertainty.

Acknowledgements

Chapter 4
Simulation of regional irrigation requirement with SWAT in different agro-climatic zones driven by observed climate and two reanalysis datasets

Abstract

Irrigation water is one of the most substantial water uses worldwide. Thus, global simulation studies about water availability and demand typically include irrigation. Nowadays, the regional scale is of major interest for water resources management but irrigation lacks attention in many catchment modelling studies. This study evaluated the performance of the agro-hydrological model SWAT (Soil and Water Assessment Tool) for simulating streamflow, evapotranspiration, and irrigation in four catchments of different agro-climatic zones at meso-scale (Baitarani/India: Subtropical monsoon; Ilmenau/Germany: Humid; Itata/Chile: Mediterranean; Thubon/Vietnam: Tropical). The models were calibrated well with Kling-Gupta Efficiency (KGE) varying from 0.74-0.89 and percentage bias (PBIAS) from 5.66-6.43%. The simulated irrigation is higher when irrigation is triggered by soil water deficit compared to plant water stress. The simulated irrigation scheduling scenarios showed that a significant amount of water can be saved by applying deficit irrigation (25-48%) with a small reduction in annual average crop yield (0-3.3%) in all climatic zones. Many catchments with a high share of irrigated agriculture are located in developing countries with low availability of input data. For that reason, the application of uncorrected and bias-corrected National Centers for Environmental Prediction (NCEP) and ERA-interim (ERA) reanalysis data were evaluated for all model scenarios. The simulated streamflow under bias-corrected climate variables is close to the observed streamflow with ERA performing better than NCEP. However, the deviation in simulated irrigation between observed and reanalysis climate varies from -25.5-45.3%, whereas the relative irrigation water savings by deficit irrigation could be shown by all climate input data. The overall variability in simulated irrigation requirement depends mainly on the climate input data. Studies about irrigation requirement in data-scarce areas must address this in particular when using reanalysis data.

Keywords: *Irrigation water requirement; SWAT; Auto-irrigation; Agro-climates; MODIS; Reanalysis data*

4.1   Introduction

The major proportion (about 70%) of the world's water resources is consumed by agriculture although the share of total water use varies drastically under different

continents from around 10% in Europe to nearly 90% in South Asia (`http://www.fao.org/nr/water/aquastat`). However, fast population growth will increase the demand for food, resulting in increased future demand for agricultural irrigation. Rabiee et al. (2013) postulated in a global study that 52 countries will face a water deficit crisis by 2025. Irrigated agriculture has expanded by 480% (47.3 to 276.3 Mha) since the last century. Nowadays, 18% of cropland is irrigated and the rest accounts for rainfed agriculture. The increase in irrigated agriculture is majorly concentrated to developing countries as they are more affected by population growth (Rockström and Falkenmark, 2000; Siebert et al., 2000; Scanlon et al., 2007; Bruinsma, 2017).

Water demand and water availability are two main parameters for effective water resources management and water scarcity is the main driver for water resources planning and optimization. In order to overcome the probable future water stress and to ensure food security, the irrigation water use efficiency must be optimized. Crop water requirement is the fundamental input for regional planning and policy-making for irrigated agriculture (Santhi et al., 2005). Besides meteorological variables, crop water requirement also depends on soil physical properties and crop parameters like leaf area index, crop stage, rooting depth, etc. (Doorenbos and Pruitt, 1977; Allen et al., 1998).

Hydrological models are tools that can simulate dynamic hydrological processes taking into consideration the spatio-temporal distribution of water in different compartments (Zuo et al., 2015). Irrigation requirement is mostly simulated at field scale for operational purpose to optimize the water use at farm scale by using one dimensional soil hydraulic models like SWAP [Soil-Water-Atmosphere-Plant System, (Van Dam et al., 1997; Droogers and Kite, 2002; Singh et al., 2006; Ma et al., 2011)] and Daisy (Abrahamsen and Hansen, 2000). However, there has been an increase in the number of studies on optimizing the resource allocation at aggregated scales like command area, catchment or watershed scale (Bastiaanssen et al., 2000). Early models for quantifying the irrigation water requirement at aggregated scale are CADSM [Command Area Decision Support Model, (Walker et al., 1995)] and EPIC (Erosion Productivity Impact Calculator, (Williams et al., 1989b; Meinardus et al., 2001). With the advanced application of remote sensing techniques, SEBAL [Surface Energy Balance Algorithm for Land, (Bastiaanssen et al., 1998; Zwart and Bastiaanssen, 2007; Teixeira et al., 2009; Allen et al., 2011)] was developed. Conceptual hydrological models allow the simulation of larger catchments including horizontal flows of water. Examples with application in irrigated catchments are SLURP (Semi-distributed, Land-Use-based, Runoff Processes, (Barr et al., 1997; Kite, 1998; Kite and Droogers, 2000), SWAT (Soil and Water Assessment Tool, (Arnold et al., 1998; Neitsch et al., 2011), WaSIM (Water flow and Balance Simulation Model, (Niehoff et al., 2002; Schulla and Jasper, 2007) and WEAP (Water Evaluation and Planning System, (Danner et al., 2006; Mehta et al., 2013; Esteve et al., 2015). Moreover, several studies have also been carried out by upscaling field scale models and by nesting the best components of different models (hydrology + plant growth; Groundwater + plant growth). Jiang et al. 2015 used SWAP-EPIC for assessing the performance of irrigation and water productivity in the irrigated areas of middle Heihe River,

China. Whereas, the irrigation performance was also estimated by using SEBAL and SWAP in Gediz Basin, western Turkey by Droogers and Bastiaanssen (2002).

Nowadays, the interpretation algorithms of satellite imagery from the terra moderate resolution imaging spectroradiometer (MODIS) have been approved (Mu et al., 2013) and used by many researchers in assessing the spatio-temporal hydrologic behavior of agricultural catchments (Stehr et al., 2009; Tang et al., 2009; Zhang et al., 2009; Rafiei Emam et al., 2017). Remote sensing can provide satisfactory estimates of irrigated areas and also crop water indicators by capturing the phenological development of crops through multi-temporal image classification (Van Niel and McVicar, 2004; Thenkabail et al., 2009; Ozdogan et al., 2010; Pervez and Brown, 2010; Conrad et al., 2011; Romaguera et al., 2012; Peña-Arancibia et al., 2016; Zhang et al., 2018). Errors in the remotely sensed actual evapotranspiration (ET) are generally in the order of 10-20% in Australia (Glenn et al., 2011), whereas the specific MODIS ET product was reported to have an error of 24.1% relative to the flux towers (Mu et al., 2013; Vervoort et al., 2014). In this paper, we always refer to the actual evapotranspiration as ET.

Reanalysis data from different spatial and temporal resolution [e.g., National Centers for Environmental Prediction (NCEP), (Saha et al., 2010); ERA-interim, (Dee et al., 2011); etc.] have been used in simulating the global as well as regional hydrological response of different agricultural catchments. Essou et al. (2017) compared different climate datasets to perform lumped hydrological modelling over 42 catchments in the United States and later on, evaluated the impacts of combining reanalysis and weather data to check the accuracy in discharge simulation over 460 Canadian watersheds (Essou et al., 2017). Wisser et al. (2008) used NECP data to simulate the global irrigation water demand and confirmed that the weather-driven variability in global irrigation was less than 10% but it could be much higher at the national scale (±70%). Since some reanalysis data provide time series of more than 30 years, therefore they have been increasingly used in studying climate trends (Poveda et al., 2006; Wang et al., 2006; Stammerjohn et al., 2008).

The application of SWAT has gained momentum during last the 10-15 years for modelling agricultural catchments (Griensven et al., 2012). Santhi et al. (2005) improved the capabilities of SWAT by introducing a canal irrigation component into the model for the effective regional planning of an irrigated agricultural catchment in the Rio Grande, U.S. Xie and Cui (2011) developed SWAT for simulating paddy fields in the Zhanghe Irrigation District located in China. Dechmi et al. (2012) used SWAT to simulate the intensive agricultural irrigated catchment of the Del Reguero watershed in Spain. Panagopoulos et al. (2014) evaluated the economic effectiveness of different best management practices for reducing the irrigation water abstraction in the Pinios, Greece. Maier and Dietrich (2016) compared different irrigation strategies, where different methods of auto-irrigation implemented into SWAT showed considerably different results for a humid catchment in Germany. Marek et al. (2016) investigated the simulation of the leaf area index (LAI) and ET in SWAT and found deficiencies,which may have an impact on the accuracy of simulated plant water uptake. Chen et al. (2018) proposed an improved auto-

irrigation function for SWAT based on field studies in Texas (Chen et al., 2017). In addition to this, SWAT was used to find out the best management practices for irrigation considering crop water requirement, productivity, management strategies costs, and crop market prices in Crete, Greece (Udias et al., 2018). The updated SWAT+ model will improve the control of auto-irrigation by decision tables (Arnold et al., 2018).

Irrigation water availability is a key driver to determine cropping patterns. Climate change will potentially affect natural hydrological and plant growth processes around the world. Therefore, cropping patterns/amounts should be adjusted/evaluated for this challenge (Wang et al., 2011; Dubey and Sharma, 2018). Consequently, agro-hydrological models should be evaluated regarding their ability and performance to simulate plant growth and hydrology under climate and management constraints.

The objectives of this study are: (i) to investigate the application of SWAT models in different agro-climatic zones of the world (Chile-Mediterranean; Germany-Humid; India-Sub tropical and Vietnam-Tropical) for simulating irrigation water requirement; (ii) to compare plant water requirement using MODIS generated ET and SWAT simulated ET; (iii) to simulate the irrigation water requirement under different irrigation control scenarios; and (iv) to investigate the use of climate reanalysis datasets like NCEP (National Centers for Environmental Prediction) and ERA-Interim for agro-hydrological studies in data-scarce catchments.

4.2   Study Area and Data

The study area consists of four different agricultural catchments located in different agro-climatic conditions (Fig. 4.1). The selection of the four catchments was based on different climatic conditions, spatial location, type of crop grown, size and type of catchment area (mainly agricultural catchments of meso-scale) and data availability. The salient information about these catchments, the data used, irrigation techniques used and the sources of irrigation water are summarized in Table 4.1. A brief description of the four catchments is provided below.

(1) The Upper Baitarani River basin (1776.6 km^2) lies between 21-22.5°N latitude and 85-86°E longitude and is located in Eastern India, Odisha (Fig. 4.1). The Baitarani River originates from Guptaganga hills (900 m above MSL) in the Keonjhar district of Odisha. The climate of the study area is characterized as a subtropical climate with defined winter, summer and monsoon seasons. More than 80% of the annual rainfall (1165 mm) occurs during June to October. The mean monthly maximum temperature is 34 °C experienced in May, whereas the minimum temperature is 11 °C in January. The dominant type of soil in this basin is 'sandy clay loam', which consists of 22% clay, 13% silt and 65% sand and occupies 50% of the river basin. A majority of soils in the basin are light textured red soils, which have low water-holding capacity, low fertility and high erodibility (Verma and Jha, 2015). Forest comprises the major portion of the land cover (∼50% of the area) followed by agriculture (42%) and 10% fallow. Surface water conveyed through canals is used for flood irrigation.

(2) The second studied catchment is a sub-catchment of the Ilmenau River, located in the Federal state of Lower Saxony, Northern Germany. It lies between 52-54°N and 9-11°E (Fig. 4.1). The average annual rainfall is around 720 mm, which is temporally distributed throughout the year. The soils are mostly sandy-loam (75% sand) and medium sand (95% sand), resulting in low water holding capacity and fast infiltration (Uniyal et al., 2017). Agricultural land cover is the dominant land use (54%) followed by forest cover (31.5%). Consequently, many fields are irrigated. The irrigation water is mostly extracted from the shallow porous aquifer present in this region and applied via sprinkler systems (Wittenberg, 2003).
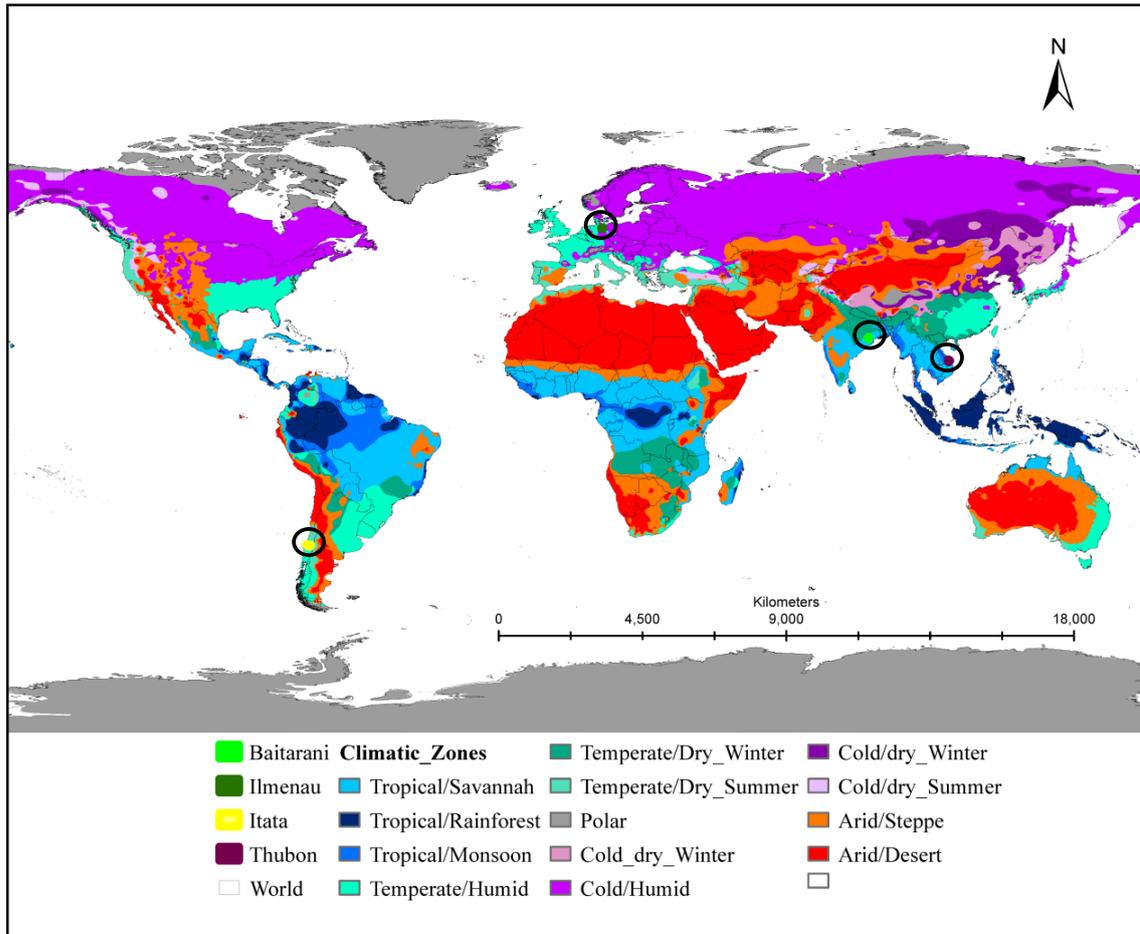
Figure 4.1: Location of different catchments around the world with major Köppen-Geiger climatic classification (modified from Peel et al. 2007).

(3) The Itata catchment in the Nuble province in Chile is chosen from the Southern Hemisphere for the current research. The Itata catchment is located between 72.4°-71.2° W longitude and 36.4°-37.2 °S latitude (Fig. 4.1). Average annual rainfall of the study area is around 1420 mm, of which more than 80% occurs in May to October. The mean maximum temperature is 19.4 °C, whereas the mean minimum temperature is 6.9 °C (Muñoz et al., 2016). The major soils in this catchment comprise of mountain alluvium (16.7%) and volcanic soils (11%) with poor soil quality. The major portion of the catchment is comprised of agricultural land use with nearly 48% of the total area followed by the forest land cover (36%). The most popular irrigation techniques followed around this

catchment are surface, canal and pressurized irrigation systems and a few center pivots.

(4) The Thubon River originates from the Truong Son mountain range, which is at an altitude of greater than 2000 m above MSL (Mean Sea Level). The catchment is located between the longitudes 107.84° E and 108.47° E, and latitudes 14.95° N and 15.75° N (Fig. 4.1). The catchment has an average annual rainfall of more than 2000 mm/year. The average maximum temperature is around 26-27 °C in June and July, while the average minimum temperature is within 20.5-21.5 °C in December and January. The soils are mostly sandy clay loam covering nearly 83% of the catchment with 26% clay and silt and 48% sand, respectively (Nam et al., 2013). The major land use of the Upper Thubon River catchment (3124 km^2) selected for the study is comprised of 85.38% forest cover followed by 8% agricultural land cover, which is mostly rice grown under rainfed agriculture (Nay-Htoon et al., 2013).

Table 4.1: General information of the catchments

Sl. No.	Study area and Köppen-Geiger climatic zones	Area (km^2)	Mean avg. rainfall	Investigation period	% Agri.	Source of irrigation water	Mode/ irrigation technique	Dominati-ng crops
1.	Baitarani-India (Aw-Tropical dry summer) Subtropical-monsoon	1776	1340	1998-2010	42	Canals	Canals Surface irrigation	Rice, pulses, oil, seeds
2.	Ilmenau-Germany (Dfb-Cold warm summer) Humid	1478	720	1979-2010	55	Ground-water	Sprinkler Pressurized irrigation	Wheat, potato, corn, sugarbeet
3.	Itata-Chile (Cfa-Temperate hot summer) Mediterranean	4529	1420	1979-2010	66	Canals	Canals drip, sprinkler, Pressurized, surface irrigation	Fruit, plantation, alfalfa, oats
4.	Thubon-Vietnam (Am-Tropical monsoon) Tropical	3124	3828	1979-2010	8	Canals	Canals Surface irrigation	Rice,

The selected catchments show huge variability in terms of temporal rainfall distribution ranging from Germany, in which rainfall is distributed throughout the

year, to India, which has a clear monsoon season, along with the variation in annual average rainfall amount ranging from 760 mm (Germany) to more than 2000 mm (Vietnam). Therefore, it is worth to explore the performance of the agro-hydrological model (SWAT) for simulating streamflow, evapotranspiration, and irrigation water demand under the aforementioned diverse agro-climatic conditions (Table 4.1).

Reanalysis Data

To assess and manage the water resources available within a river basin, good estimates of hydro-meteorological data, such as precipitation, temperature, and streamflow, are required (López et al., 2017). However, many river basins around the world still have a limited number of in-situ observations, being either ungauged (Sivapalan et al., 2003) or poorly gauged (Loukas and Vasiliades, 2014). Several studies have utilized the dynamically downscaled datasets for simulating the hydrology of a watershed (Bastola and Misra, 2014; Polanco et al., 2017). In this study, two datasets from dynamically downscaled climate reanalysis datasets called National Center for Environmental Prediction (0.5°; `https://globalweather.tamu.edu/`) and ERA-interim (0.125°; `http://apps.ecmwf.int/datasets/data/interim-full-daily/levtype=sfc/`) were used. Climate Forecast System Reanalysis is a product developed by NCEP, whereas ERA-interim (ERA) daily is a product from the European Centre for Medium-Range Weather Forecast. The global models provide daily climate data from 1/1/1979 to 7/31/2014 and 7/31/2017 for NCEP and ERA, respectively.

Evapotranspiration Data

Evapotranspiration acts as a vital link between climate, hydrology, and ecology (Gharbia et al., 2018). Long-term direct ground measurements of ET are typically not available and therefore, it is mostly calculated from meteorological variables. Nowadays, remote sensing techniques can be used to calculate spatio-temporal ET indirectly on a larger scale. The precision and accuracy of satellite ET algorithms, which incorporate land surface temperature data are sufficiently high. Therefore, they can be used for enhancing the water management at the catchment scale (Cuenca et al., 2013; Steele et al., 2015; Tang et al., 2009). Moderate Resolution Imaging Spectroradiometer (MODIS) provides valuable spatio-temporal evapotranspiration data which helps to check the evapotranspiration simulated by hydrological models. Spatio-temporal maps of ET were downloaded from 2000 to 2010 using Moderate Resolution Imaging Spectroradiometer (MODIS, Mu et al., 2013, NASA MODIS16A2/A3). It has a spatial resolution of 1 km. MODIS provides cumulative ET for every 8 days interval.

4.3 Methodology

4.3.1 Hydrological Model Setup and Calibration

The physically-based continuous time scale model, Soil and Water Assessment Tool (SWAT) can simulate water fluxes, plant growth and agricultural land management operations at catchment scale (Arnold et al., 1998). The agro-hydrological SWAT models in this study were developed by using the same

model equations and comparable input weather data, crops, etc., for each of the four catchments. This was done to bring the models into a comparable level so that the model's application in simulating hydrological processes under different agro-climatic conditions can be evaluated. Runoff was simulated by using the SCS curve number method, evapotranspiration was calculated by the Penman-Monteith equation. Furthermore, Muskingum routing was used for routing the flow through the catchment (Neitsch et al., 2011). Vertical processes are performed at the hydrological response unit (HRU) level. An HRU is the unique combination of soil, land use and slope within a sub-basin.

4.3.2 Crop Model Setup

SWAT uses a simplified version of the crop growth model used in EPIC (Neitsch et al., 2011). It uses the same crop growth equations for all the crops but each crop has unique values for the model parameters. In this way, the crop growth model differentiates between different crops. Plant growth is calculated by simulating leaf area development, interception of light and its conversion into biomass. Crop yield is a function of biomass above ground and harvest index on the day of harvesting. In addition, biomass on a day depends on the total intercepted solar radiation and also on leaf area index, whereas the harvest index depends on the accumulated heat units. Heat units are climate-based mechanism to grow crops according to thermal input and to initiate irrigation and fertilizer application in the model. Crops grow if the accumulated temperature above a threshold value reaches to a user-defined value. SWAT categorizes plants into seven different types based on the season (cold or warm), type (legumes/others), growing period (seasonal, annual or perennial) and trees (Neitsch et al., 2011).

Latest available crop statistics at the district or regional level was incorporated into the models. Different crop types were randomly distributed in the agricultural areas of the respective basins using their respective percentage of the total agricultural area determined by GIS overlay analysis. However, in the case of Baitarani River basin the state crop statistics were taken to distribute crops in the agricultural area. Through this, all the catchments show average crop spatial statistics according to the recent census. As fixed operations under local conditions were not available, therefore the developed models mostly depend on climate input data. The crops in all the catchments were grown using heat units. Auto-fertilization was activated, so there was no nutrient stress. Harvesting is done by using 'harvest and kill' function or by using 'harvest only' function. The 'harvest and kill' function harvests the plant biomass and kills the crop upon harvest. Whereas the other function only harvests the crop, but allows the plant to continue growing. One crop is grown in the model in a year. However, in the case of Thubon rice is grown twice a year. The possible intermediate crops are neglected because they are mostly not irrigated if grown. Forest and rangeland are modelled as perennial plants in the catchment.

4.3.3 Implementation of Irrigation Schemes

SWAT does not regard the method of irrigation directly. Only the losses associated with the different methods of irrigation can be given via parameters called surface

runoff ratio (IRR_ASQ) and irrigation efficiency (IRR_EFF: the amount of water which is completely lost from the system). Therefore, the user can assign the overall water loss from the system (e.g. leaching, evapotranspiration) by the parameter IRR_EFF, whereas IRR_ASQ is used to implement the return flow occurring from the surface runoff to the system. Values for the irrigation system efficiency for different irrigation techniques were taken from the Food and Agricultural Organization database (`http://www.fao.org/docrep/t7202e/t7202e08.htm`).

Nearly 85% of the irrigation demand is satisfied with surface water in the Baitarani River basin. According to FAO, only 3.2% of the agricultural area in Chile is irrigated by using groundwater (http://www.fao.org/nr/water/aquastat/irrigationmap/CHL/ index.stm). In Vietnam, total groundwater withdrawal is only 1.7%, which is mainly used for supplying municipal water to the urban areas (`http://www.fao.org/nr/water/aquastat/countriesregions/VNM/`). This justifies the use of surface water for irrigation in Baitarani, Itata and Thubon catchments. For Ilmenau River basin, only groundwater was used as the source of irrigation water.

4.3.4 Irrigation Scheduling

Irrigation operations can be initiated in SWAT either by the pre-defined schedules or automatically based on climate and plant growth using heat units. Automatic irrigation can be triggered by defining plant water stress or soil water deficit threshold in the model (AUTO_WSTR: water stress threshold). If irrigation is triggered by plant water stress, then the water stress threshold is a fraction of potential plant growth. Plant water stress is simulated in SWAT by a comparison of actual and potential plant transpiration:

$$wstr = 1 - \frac{E_{t,act}}{E_t} = 1 - \frac{w_{actualup}}{E_t} \qquad (4.1)$$

Where $wstr$ is the water stress, E_t is the maximum plant transpiration, $E_{t,act}$ is the actual amount of transpiration and $w_actualup$ is the total plant water uptake. The irrigation source has to be defined on a sub-basin level like reach, reservoir, shallow and deep aquifer, etc. Automatic irrigation adds water until the field capacity of the soil profile (root zone) is reached and the excess water returns to the source.

When water stress is based on the soil water deficit, the water stress threshold is the soil water deficit below field capacity (mm H_2O). Whenever the water content of the soil profile falls below FC (field capacity) – AUTO_WSTR [the acceptable amount of water depletion (mm H_2O) in the total soil column], the model will automatically apply water to the HRU. If enough water is available from the irrigation source, the model will add water to the soil until it is at FC (Neitsch et al., 2011). Considering the vertical and horizontal heterogeneity of FC, the individual soil water depletion (AUTO_WSTR) values for different soil and crop types have to be quantified. In all the calibrated SWAT models, automatic irrigation was scheduled by using plant water stress.

All the developed models were calibrated using streamflow observed at the catchment's outlet. For the Ilmenau and Itata catchments, streamflow data from intermediate stream gauging stations were used to improve the calibration. All of the developed models were iteratively calibrated by using the manual as well as automatic techniques along with local expert knowledge about the four catchments. Nash Sutcliffe Efficiency (NSE > 0.5) and percentage bias (PBIAS < 10%) were used as objective functions to calibrate the developed models.

In addition, the SWAT simulated ET was compared with ET extracted from MODIS for all the four catchments on monthly basis and for all agricultural HRUs during 2000 - 2010. In order to compare the overall spatial and temporal variation in SWAT simulated ET with MODIS, ET bands were created from the minimum, maximum and average values of ET for a particular month from the agricultural HRUs.

4.3.5   Irrigation Scheduling Scenarios

For the scenario simulations, two different irrigation scenarios (optimal and deficit irrigation) were used for scheduling irrigation for both plant water stress and soil water deficit with different thresholds. For soil water deficit scheduling, the optimal scenario irrigates when the moisture content in the soil falls below FC – 0.5*FC in mm (scenario 1 - S1) and the deficit scenario irrigates when soil moisture falls below FC – 0.65*FC in mm (scenario 2 - S2). For the plant water stress scenarios, threshold values of 0.9 (scenario 3 - S3) and 0.8 (scenario 4 - S4) were chosen for scheduling irrigation in all the catchments.

4.3.6   Application of Climate Reanalysis Data in Simulating Streamflow and Irrigation

Climate reanalysis simulations aim at providing climate data for unobserved or insufficiently monitored regions of the world. However, these data can be biased against climate observations (Hwang et al., 2014). Therefore, after comparing the reanalysis datasets (NCEP and ERA) with observed values used in this study, daily precipitation, temperature (minimum and maximum) and solar radiation were bias-corrected by using quantile mapping (Piani et al., 2010a,b; Thrasher et al., 2012). The bias correction is performed to reduce the effect of local over or underestimation of climate variables by the global models (Varis et al., 2004; Christensen et al., 2008; Teutschbein and Seibert, 2010). Quantile mapping was conducted using the R statistical tool package 'qmap'. This program first estimates the empirical cumulative distribution function of the observed and reanalysis data for 10 quantiles and derives a transformation function for each quantile. Later on, the quantiles of the original reanalysis dataset are transformed into the quantiles of the bias-corrected dataset. For the values that are outside of the fitted distribution function, their transformation is estimated by using spline interpolation (`ftp://ftp.gr.vim.org/mirrors/CRAN/web/packages/qmap/qmap.pdf`). For this study, month specific bias correction for daily weather variables was selected due to the significant difference in the seasonal rainfall patterns. The observed data were replaced with the reanalysis dataset in the developed models to evaluate their performance, assuming that the model calibration with observed data is valid

i.e., representing the hydrological system response to climatic forces. The accuracy of simulations with bias-corrected and uncorrected reanalysis climate data was tested against simulations with observed climate data for the four catchments.

4.4 Results and Discussion

4.4.1 Calibration and Validation of SWAT

All the selected catchments were calibrated using the daily streamflow at their respective outlets. The streamflow hydrographs of the selected catchments are shown in Figs. 4.2(a-d) for the respective calibration periods. It can be seen that the calibrated models replicate the range of values of streamflow hydrographs during the calibration period in all the catchments with different performance. Overall, it can be assessed from the hydrographs that SWAT consistently underestimates the peak flows as compared to the low flows and recession limbs, which are well replicated. This can also be seen from the flow duration curves, which are shown in section 4.4.5.
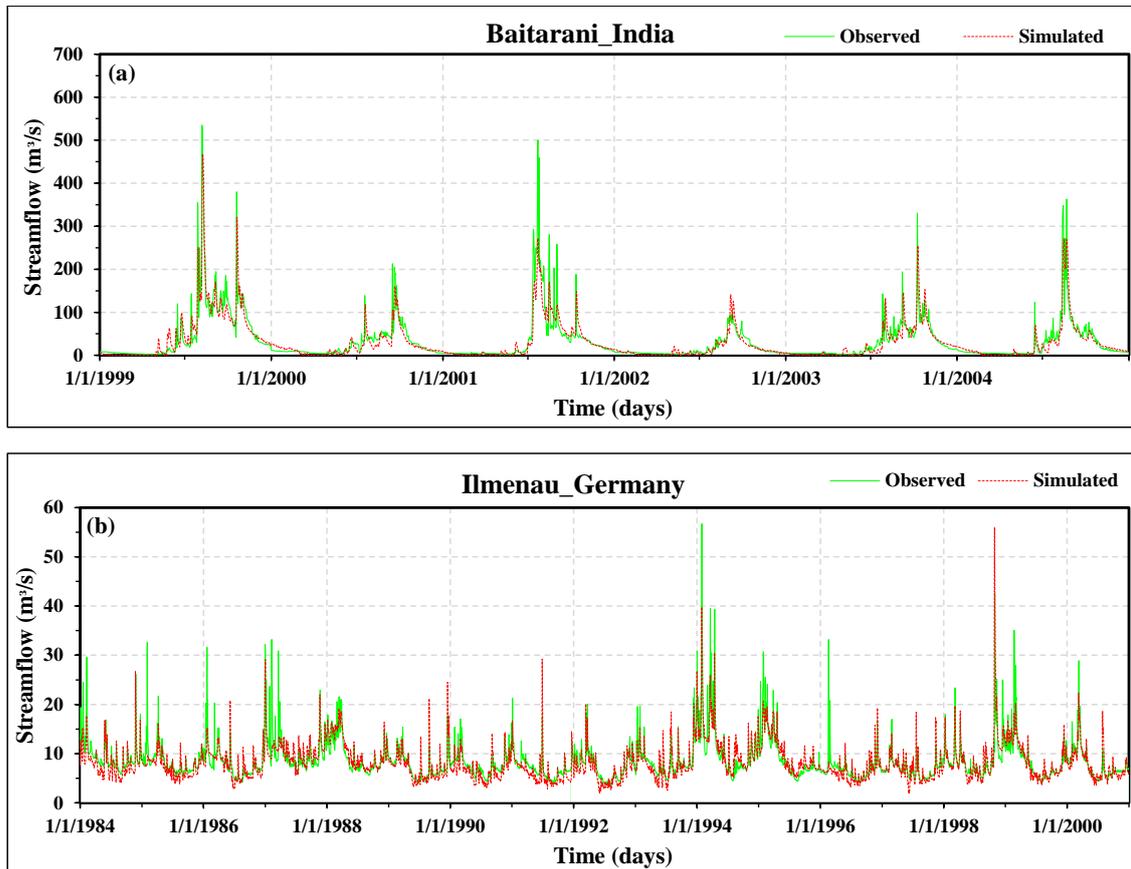
Figure 4.2: (a,b) Streamflow hydrographs for the (a) Baitarani and (b) Ilmenau catchments during their respective calibration periods.

The daily hydrograph simulated by SWAT can underestimate the peak if the travel time is less than one day as this is a limitation of the Muskingum's routing equation used in the model (Kim and Lee, 2010). Furthermore, the available weather stations

might not be enough to represent the overall spatial variability of local events in the catchments. The Kling-Gupta Efficiency (KGE, Gupta et al., 2009) varies from 0.74 to 0.89 and the percentage bias (PBIAS) from -7.02 to 6.9% (Table 4.2), which indicates a good to very good model performance according to (Moriasi et al., 2007).
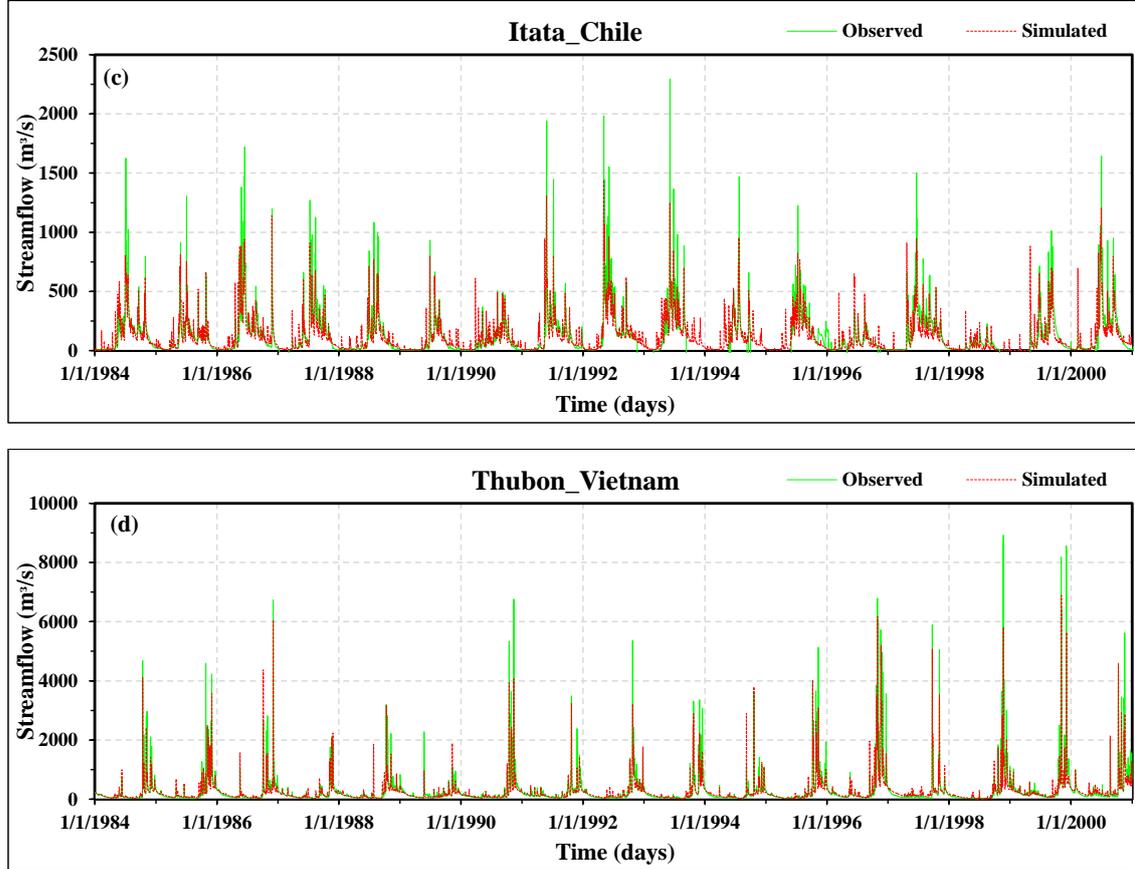
Figure 4.2: (c,d) Streamflow hydrographs for the (c) Itata and (b) Vietnam catchments during their respective calibration periods.

Table 4.2: Model evaluation statistics

| Catchment | Period | Statistical Indicator | | | |
		R^2	NSE	PBIAS	KGE
Baitarani	Calibration (1999-2004)	0.81	0.81	6.90	0.89
	Validation (2005-2010)	0.60	0.60	-3.23	0.76
Ilmenau	Calibration (1981-2000)	0.67	0.64	2.08	0.81
	Validation (2001-2010)	0.61	0.51	3.46	0.76
Itata	Calibration (1984-2000)	0.68	0.68	3.39	0.74
	Validation (2001-2010)	0.70	0.70	-7.02	0.80
Thubon	Calibration (1984-2000)	0.85	0.84	4.98	0.81
	Validation (2001-2010)	0.88	0.87	1.39	0.87

In addition to it, Table 4.2 also shows the performance of SWAT models for other criteria of fit as well as the performance of the model during the validation period. It shows a comparable level of performance as shown in the calibration period except in case of Baitarani River basin. This is due to the poor rainfall data during the validation period (2007).

Fig. 4.3 shows the boxplots for monthly rainfall (mm), average monthly simulated streamflow (mm) and areal average actual evapotranspiration (mm) in the four studied catchments. It can be inferred from the figure that even though the overall variability in rain, ET and streamflow is huge, the average values of precipitation and streamflow are relatively close for Baitarani, Ilmenau, and Itata, whereas the tropical catchment of Thubon shows a different characteristic. A direct relation can be seen between rainfall and streamflow in all the catchments. A nonlinear relation between rainfall and streamflow is seen in the tropical mountainous catchment of Thubon. The overall water yield is high in this catchment as compared to the others. Monthly streamflow also shows a clear difference between a wet tropical catchment (Thubon) and a subtropical catchment (Baitarani), even the low flows in the Thubon catchment are more than the high flows in the Baitarani catchment.

The overall behavior of monthly average ET can provide information about the climate of a respective catchment. It can be seen from the ET boxplots that overall spreads of the Baitarani and Ilmenau catchments are more than that of the Itata and Thubon catchments. The widespread of ET in the Baitarani catchment support its subtropical climatic characteristic with defined winter, summer and monsoon season and in case of the Ilmenau catchment, it shows its distinct summer and winter season. In addition, the ET boxplots show an increasing gradient towards the equator from Ilmenau to Thubon with a bigger step in Baitarani catchment. However, the overall spread and monthly average ET for Thubon is expected to be higher but SWAT has been reported to underestimate ET of tropical evergreen forests systematically (Plesca et al., 2012; Alemayehu et al., 2017).

4.4.2 Evaluation of Simulated Evapotranspiration and Yield for Agricultural Land Use

The spatio-temporal comparison of monthly ET from MODIS and SWAT was performed for the four catchments during 2000 to 2010. The overall spread from MODIS data was plotted with the simulated ET band from SWAT. It can be seen from Figs. 4.4(a-d) that even though the overall spread of monthly ET from MODIS and SWAT is not exactly matching, the overall dynamics is similar in both datasets for all the four catchments. In addition to it, the mean ET from MODIS mostly falls inside the simulated ET band from SWAT. However, SWAT simulates higher ET as compared to MODIS by 3 to 20% in the Baitarani, Ilmenau and Itata catchments, whereas lower ET in case of Thubon ($\sim$25%). It can be seen that during the growing period, the spread is wide in both cases and narrows down during non-growing periods. Statistical results showed that the percentage deviation in mean monthly ET estimated for SWAT and MODIS has different behavior for different catchments. This might be due to the difference in topography and climatic conditions of the respective catchments. It can be seen

BAI: Baitarani, ILM: Ilmenau, ITA: Itata and THU: Thubon
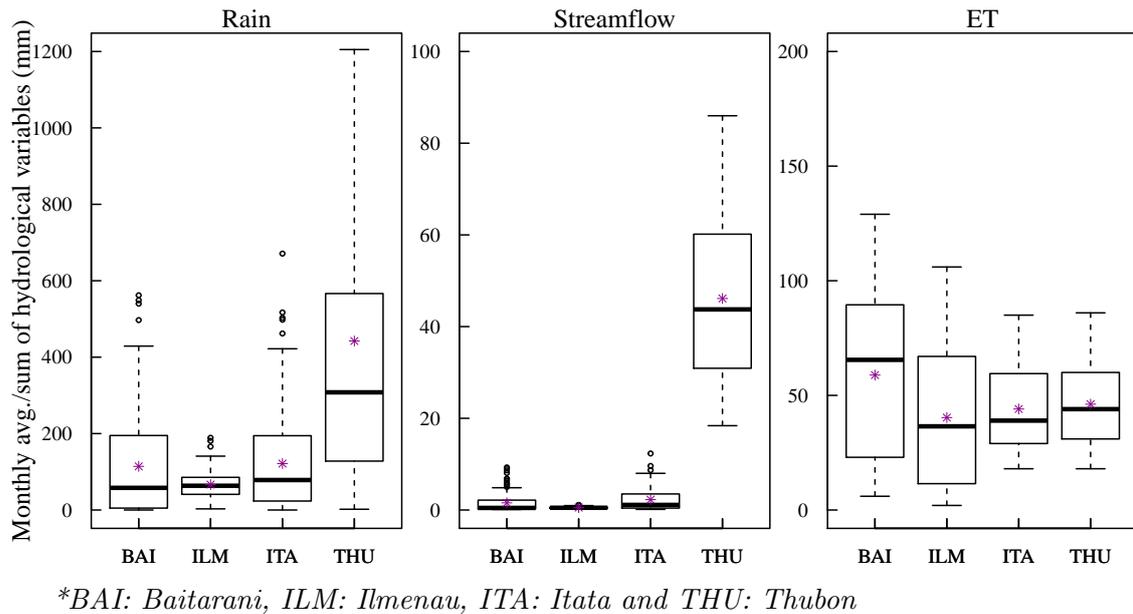
Figure 4.3: Main water balance components of all the catchments.

from Fig. 4.4(b) that for the Ilmenau catchment, the overall spread of the estimated and simulated ET matched well as compared to the other catchments. This can be attributed to the good water balance simulated by SWAT in this basin because it was calibrated by using three more intermediate stations apart from the outlet. The data quality and quantity play a crucial role in this context.

Fig. 4.4 (a) shows that the ET estimated from MODIS data for the Baitarani River basin during March-May is lower than the simulated ET from SWAT. It is also apparent that the period of plant growth and the receipt of rainfall for this catchment is in the same period. Therefore, with the available justification and local knowledge about the area, it can be concluded that MODIS is underestimating ET for this catchment.

It can be seen from Fig. 4.4 (c) that the overall variation in ET simulated by SWAT and MODIS is high in the Itata catchment during April-October. This is explained by the inclusion of agro-forest under agricultural land. This is confirmed by evaluating the Google earth imagery with the agricultural area of the Itata catchment. In addition to this, during this period Chile experiences winter and growing crops are not generally favored in this tenure.

In Thubon catchment [Fig. 4.4(d)], the overall spread and mean values of estimated ET from MODIS are larger than that of the simulated ET in SWAT. Two plausible reasons for this result are: a) SWAT underestimates actual ET from the highly saturated agricultural surface by limiting ET to potential ET (Neitsch et al., 2011), whereas in the case of rice production actual ET can be more than potential ET as described for ponds by (Xie and Cui, 2011) the parameters for the crop varieties could not be calibrated for the local conditions. Hai (2003) confirmed that Vietnam uses hybrid rice varieties (high yielding varieties), which consume more water and
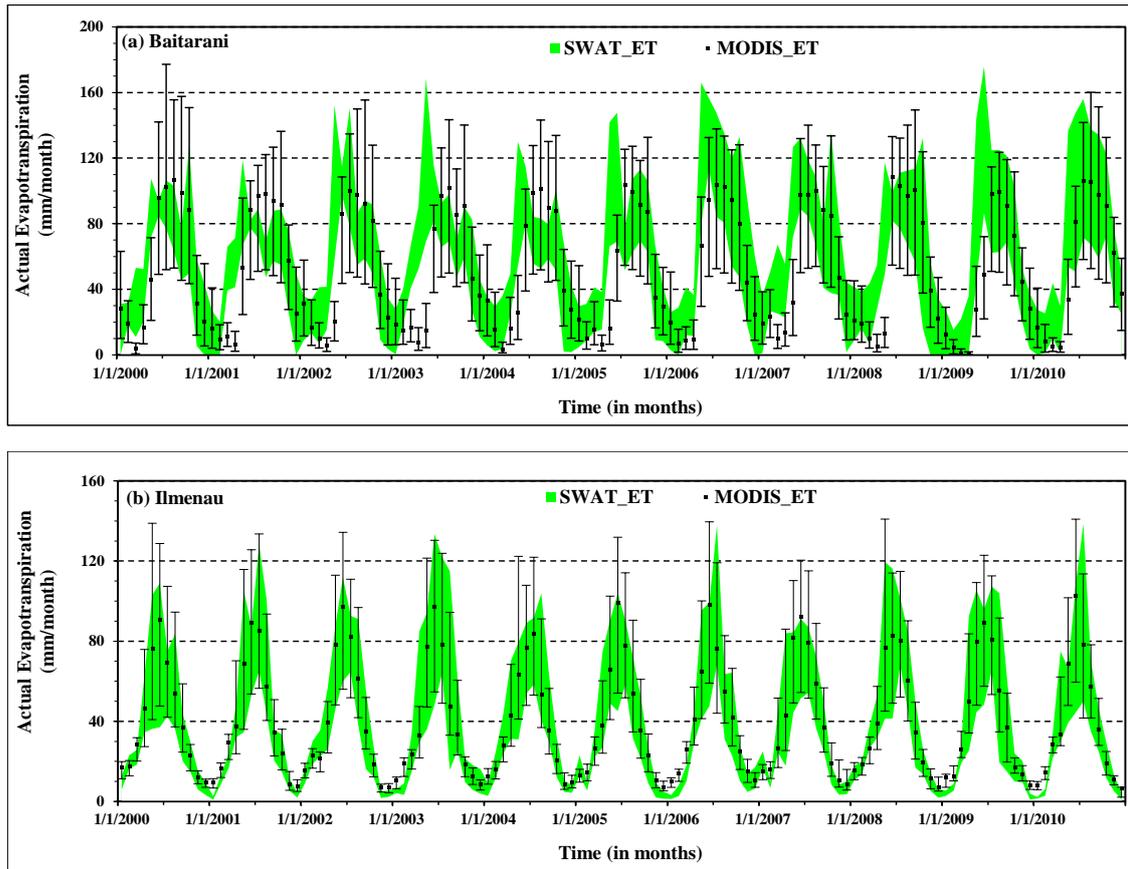
Figure 4.4: (a,b) Spatio-temporal variation of actual evapotranspiration in (a) Baitarani; (b) Ilmenau from 2000 to 2010 at monthly time step.

in turn might have more ET than the standard varieties as included in the SWAT database.

The ET estimated by MODIS also has some uncertainty as the meteorological data used in the estimation of MODIS ET is non-linearly interpolated as it was too coarse for one MODIS pixel (Mu et al., 2013). The aforementioned interpolation is assumed to improve the ET calculations, however, there is also some uncertainty at the local scale.

The crop yield was not used to calibrate the models in this study, because local data were not available. For evaluating the plausibility of the obtained yield, Table 4.3 shows the overall range of the annual yield as simulated by SWAT for main crops compared to publicly accessible crop statistics from census data. It can be seen from this table that even though the range is matching for most of the catchments, still there is huge uncertainty in simulated yield as well as the statistics used for comparison. In general, it is a difficult task to calibrate yield due to input data limitations in terms of planting and harvesting dates, fertilizer and water inputs (quantity and frequency of application), losses due to pests, floods and droughts etc. The reported model uncertainty can be due to input data, model parameters as well as the climatic variation during the simulation period. Authors accept this uncertainty as they are in similar ranges as other studies have shown, e.g. Abbaspour
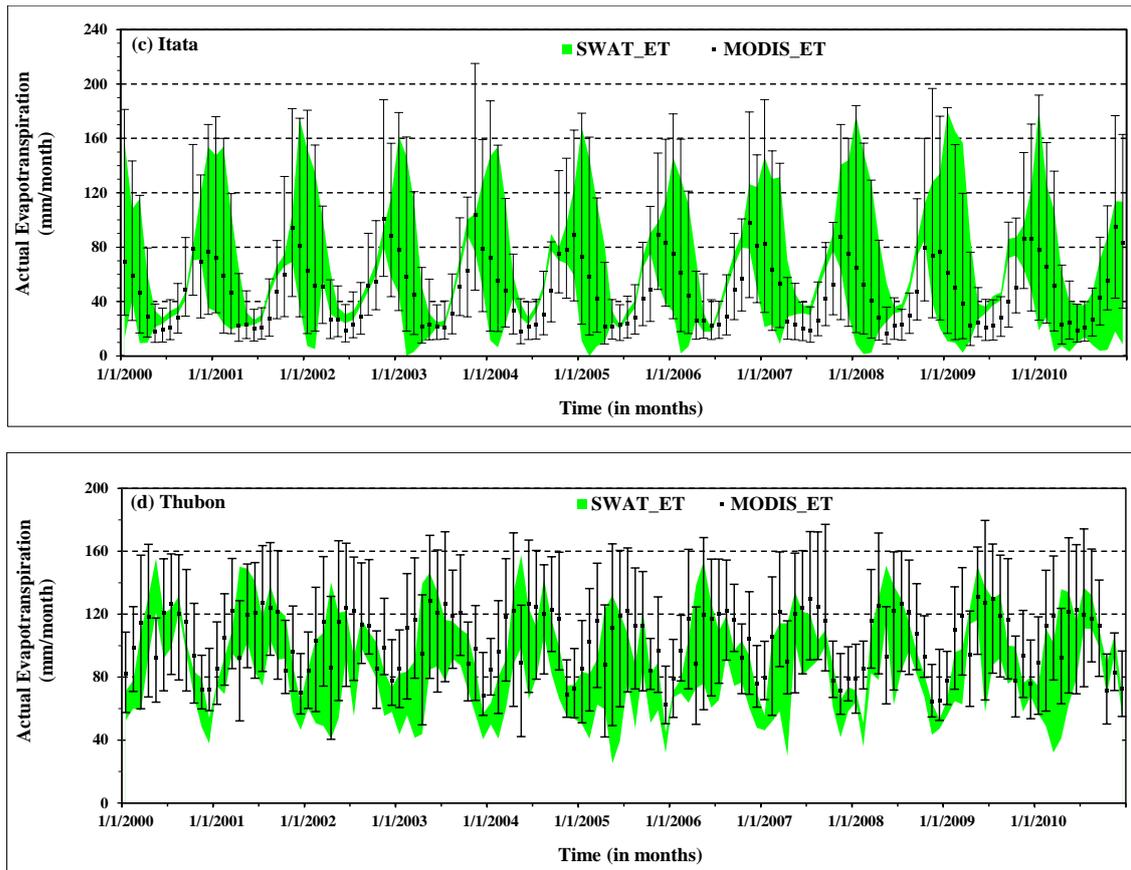
Figure 4.4: (c,d) Spatio-temporal variation of actual evapotranspiration in (c) Itata and (d) Thubon from 2000 to 2010 at monthly time step.

et al. (2015).

4.4.3   Comparison of different irrigation control scenarios

This section explains the results corresponding to different irrigation control scenarios used in the current study for simulating annual irrigation water requirement for major crops grown in the different catchments. Fig. 4.5 shows the average annual irrigation demand of cotton, sunflower and rice in the Baitarani River basin for the 2000-2010 period. It can be seen that the average annual irrigation water provided by the model is approximately two times more in the case of soil water deficit scenarios (S1 and S2) compared to the plant water stress scenarios (S3 and S4).

Table 4.3: Comparison of crop yield

Catchment	Type of crop	Crop yield (dry, t/ha)	
		Simulated	Statistics
1. Baitarni	Rice	2-2.4	1.1-2.5[1]
2. Ilmenau	Potato	6.4-7.3	7.7-8.5[2]
	Sugarbeet	8.1-11.1	9.8-11.2[2]
	Winter Wheat	3.1-3.2	5.7-6.9[2]
3. Itata	Oats	4.1-4.3	2.7-5.3[*]
	Winter Wheat	2.5-6.6	2.1-6.9[*]
4. Thubon	Potato	2-2.4	1.1-2.5[1]
	Rice	1.6-5.4	5[3]

Average crop statistics of the whole country, Chile (FAO) 1980-2010; 1: Technical rice report of Odisha 1980-2010 and Keonjhar 2005; 2: Niedersächsisches Landesamt für Statistik 1990-2000, 3:Firoz et al. 2018.
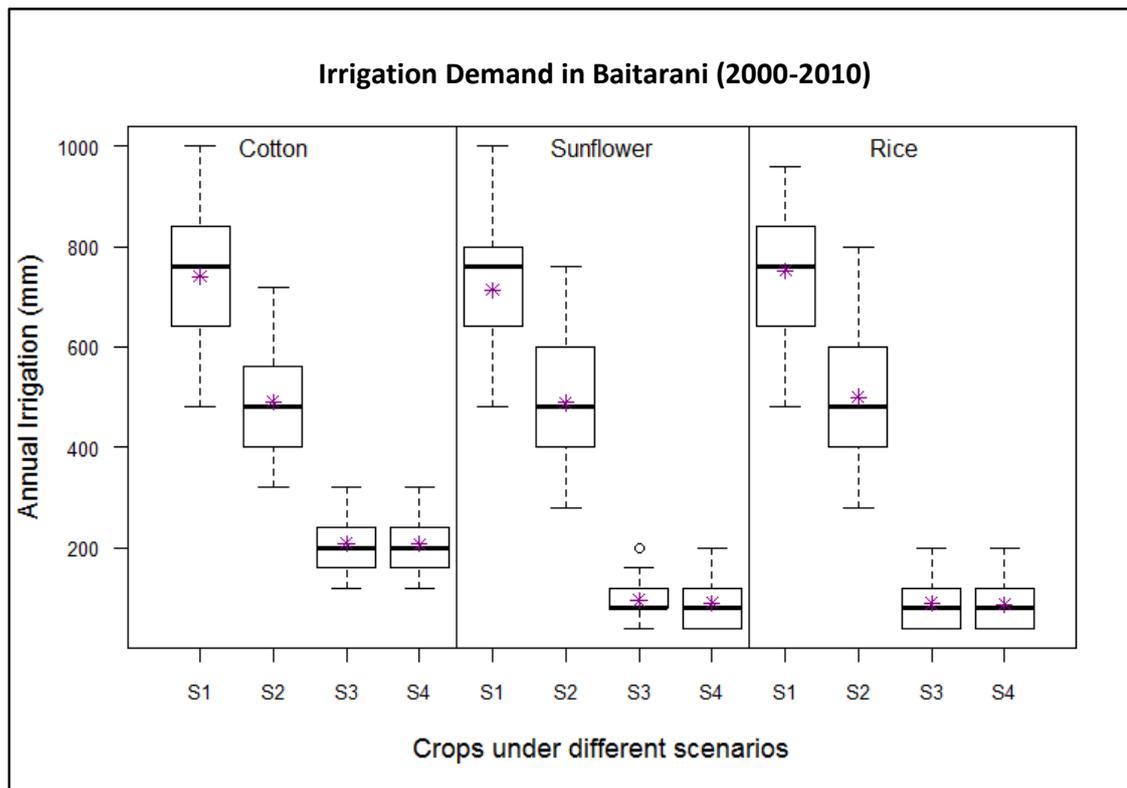
S1: model irrigates when moisture content in the soil falls below FC – 0.5 × FC in mm, S2: model irrigates when soil moisture falls below FC – 0.65 × FC in mm, S3: model irrigates when plant water stress threshold values is 0.9, and S4: model irrigates when plant water stress threshold values is 0.8.

Figure 4.5: Spatio-temporal variation of simulated annual Irrigation in Baitarani under different irrigation scenarios from 2000 to 2010.

The annual average water requirements under soil-water deficit scenarios are in

accordance with the annual irrigation water applied in the field during conventional planting of rice (Nayak, 2006). Due to the scarcity of literature in this catchment for the actual amount of water applied to cotton and sunflower production, the simulated results cannot be validated against observed data or previous modelling studies. Sunflower is grown in Kharif season (during July-December) as well as in Rabi season (summer). It requires no irrigation during winter season. However, if it is grown in non-rainy seasons then around 500-1000 mm irrigation water is required depending on the soil type. The crop (sunflower) is growing in summer season in the developed model. Therefore, the irrigation water simulated by SWAT is justified (100-700 mm). The change in overall yield has also been analyzed under the four irrigation scenarios, which was found to be less than 10% in plant water stress irrigation control scenarios as compared to the soil water deficit scenarios. However, water-saving is nearly equal to 50% if the soil water deficit scenario (S2) is used with minimal change in the annual average yield.

S1: model irrigates when moisture content in the soil falls below $FC - 0.5 \times FC$ in mm, S2: model irrigates when soil moisture falls below $FC - 0.65 \times FC$ in mm, S3: model irrigates when plant water stress threshold values is 0.9, and S4: model irrigates when plant water stress threshold values is 0.8.

Figure 4.6: Spatio-temporal variation of simulated annual Irrigation in Ilmenau under different irrigation scenarios from 1980 to 2010.

The irrigation water depth for the Ilmenau region is limited to 70 mm per summer over a seven-year average, i.e., higher abstractions in dry years can be compensated by lower ones in wet summers (Wittenberg, 2015). It can be assessed from Fig. 4.6 that the annual average irrigation water requirement simulated by the model under-considered management scenarios is less than 100 mm. In addition to it,

under different water application scenarios, the amount of irrigation simulated by the model under optimal scenario is 2 to 1.5 times more than the deficit scenario in case of corn, sugar beet and winter wheat. Under S3 and S4 scenarios, the net reduction in the crop yield (corn, potato, sugar beet and winter wheat) varies from 0.23% (sugar beet) to 10% (potato). It can be seen that the water demanding crops have more variation in their yield than the low water demanding crops under different water scheduling scenarios.

Fig. 4.7 shows the annual average irrigation applied in the Itata catchment for alfalfa, oats and winter wheat during 1980 to 2010. There is very few literature available to validate the amount of irrigation simulated by the model. In addition to this, there are several HRUs in which the crop yield is relatively low or zero as compared to the mean yield (4.5 t/ha). It might be due to the very small HRU size and due to the small depth of soil profile in some soils. The amount of irrigation water applied by the model in case of winter wheat is in accordance with the experiment conducted by (Vidal et al., 1999), in which they applied 225-880 mm of irrigation in four steps. Due to the scarcity of literature for the actual amount of water applied in oats and alfalfa crops, we cannot exactly validate the results against observed data or previous modelling studies.
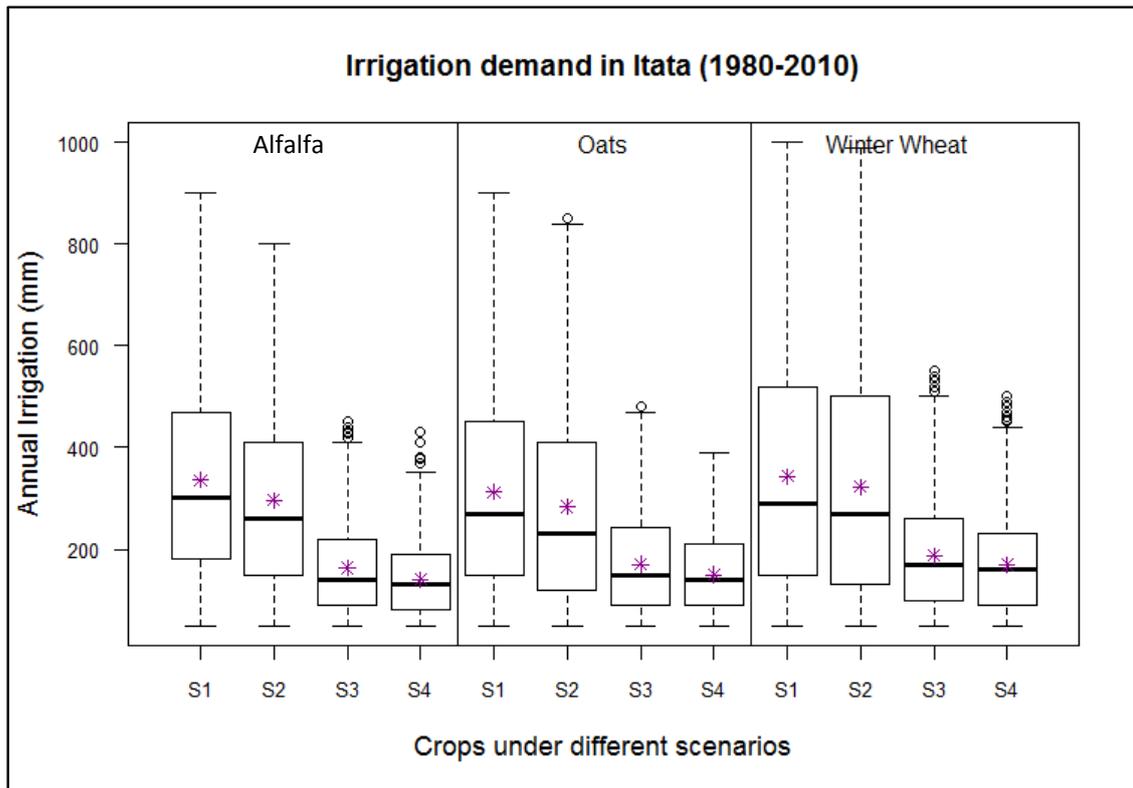
*S1: model irrigates when moisture content in the soil falls below FC − 0.5 × FC in mm, S2: model irrigates when soil moisture falls below FC − 0.65 × FC in mm, S3: model irrigates when plant water stress threshold values is 0.9, and S4: model irrigates when plant water stress threshold values is 0.8.

Figure 4.7: Spatio-temporal variation of simulated annual Irrigation in Itata under different irrigation scenarios from 1980 to 2010.

The average annual irrigation in Vietnam is around 400 mm but supplemental irrigation can vary from 80-400 mm (Shrestha et al., 2016), which is within the annual irrigation range simulated by SWAT during 1981-2010 (Fig. 4.8). The difference in the annual average crop yield is less than 5% under soil water deficit and plant water scenarios. The average simulated irrigation water demand is lower than the country's average water demand. This might be due the reason that the rice yield (Avg. yield = 4.0 t/ha, range: 1.6-5.4 t/ha) simulated by the SWAT model is relatively low in some HRU's as compared to the country's average rice yield [∼5 t/ha, (Firoz et al., 2018)].

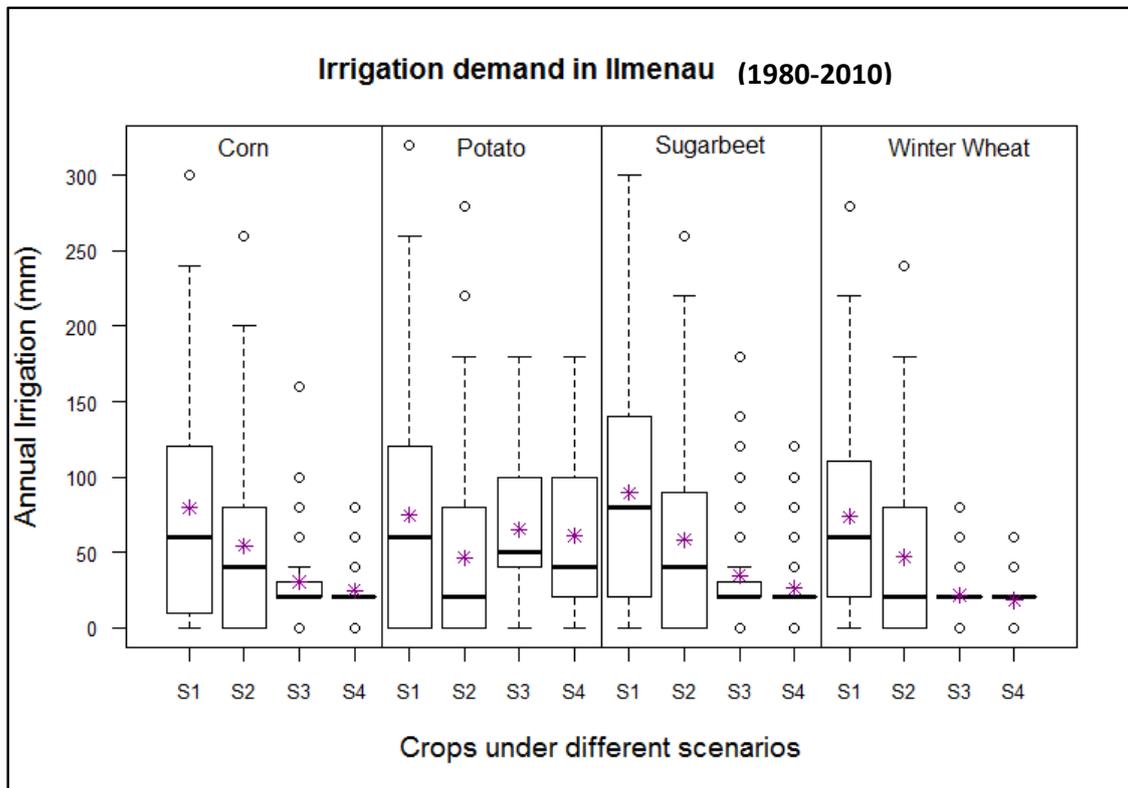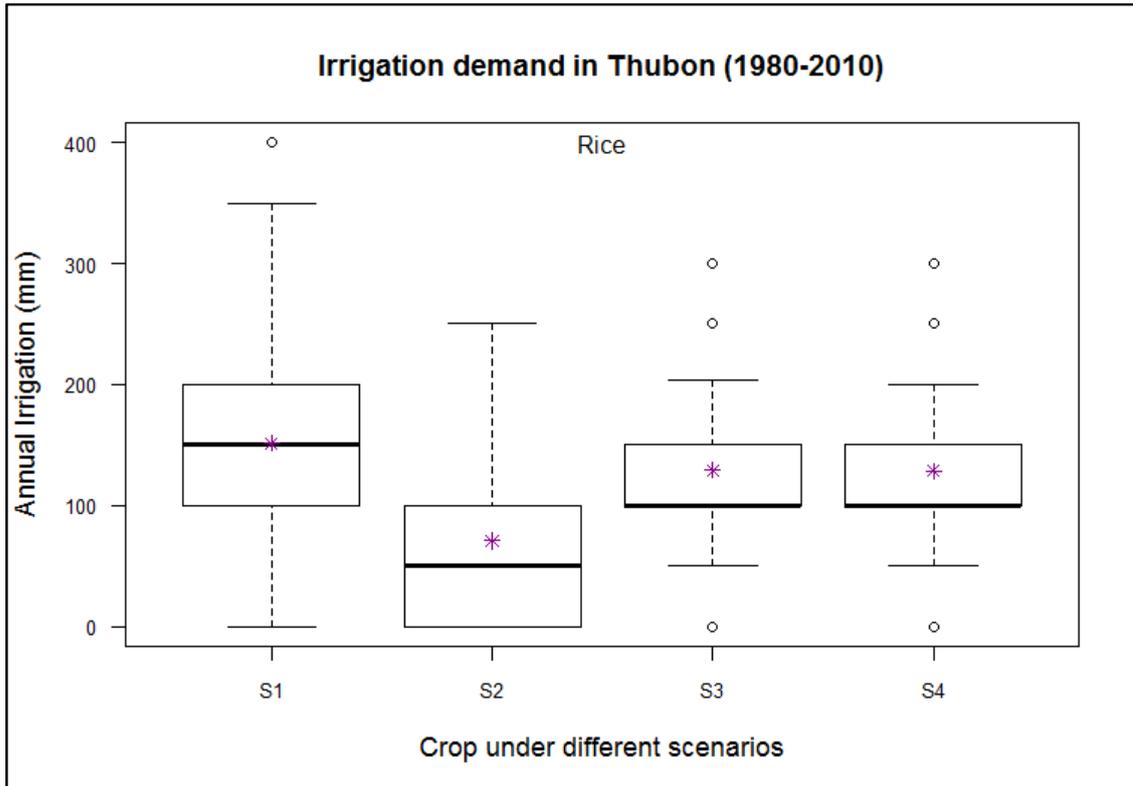**S1: model irrigates when moisture content in the soil falls below FC – 0.5 × FC in mm, S2: model irrigates when soil moisture falls below FC – 0.65 × FC in mm, S3: model irrigates when plant water stress threshold values is 0.9, and S4: model irrigates when plant water stress threshold values is 0.8.*

Figure 4.8: Spatio-temporal variation of simulated annual Irrigation in Thubon under different irrigation scenarios from 1980 to 2010.

This low rice yield could be attributed to some really small HRU's which are not well simulated by the model or different high yielding rice varieties currently used in the country whose plant parameters are entirely different from the one (generic rice) used in SWAT (Hai, 2003; Thi Ut and Kajisa, 2006).

4.4.4   Correction of Reanalysis Data

The climate reanalysis data (rainfall, maximum, minimum temperature, and solar radiation) has been corrected using quantile mapping as mentioned in section 4.3.6. The results corresponding to bias-corrected rainfall are shown in this section. The double mass curve technique is used to check the consistency of long-term precipitation data for one selected station in all the four catchments (Searcy et al., 1960). Fig. 4.9 shows double mass curves of the uncorrected and bias-corrected re-analysis data against the observed rainfall for the Baitarani, Ilmenau, Itata and Thubon, catchments, respectively. The aforementioned curves are drawn for 1980 to 2010 for all the catchments except Baitarani (1998-2010) due to observed data constraints. It can be seen from Fig. 4.9 that uncorrected rainfall show different response from NCEP and ERA compared to the observed rainfall in a catchment. This is due to the different spatial resolution as well as the different atmospheric, ocean and land surface models used to estimate the climate variables of the two reanalysis datasets. In addition to this, it is very interesting to see that e.g., ERA has overestimated the rainfall in the Baitarani and Ilmenau catchments, whereas it was underestimated in the other two catchments.

The overall behavior of observed rainfall after the bias correction is reproduced well [Fig. 4.9]. As the correction is done for all the months separately, the program tries to match the overall behavior as well as the amount of bias-corrected rainfall with the observed rainfall. In addition to it, the correction gave a relatively good result describing the seasonal or monthly patterns of the rainfall dataset. This can be seen in almost all the cases depicted in Fig. 4.9. All the bias-corrected datasets are close to the 1:1 line as compared to their respective uncorrected datasets. Apart from the qualitative assessment, quantitative assessment of the bias-corrected ERA and NCEP datasets is also performed (Table 4.4). It can be seen from the statistics that the PBIAS and mean absolute error (MAE) has improved in case of bias-corrected data. In addition to this, it is clear from the analysis that the bias-corrected ERA-interim datasets are more close to observed rainfall than NCEP. It must be mentioned that the bias correction has not worked well for some daily rainfall values, which might influence the final result of the developed SWAT models. Thus, more investigation should be taken into account while analyzing the final model simulation using the reanalysis datasets. In addition to this, it can be seen from Table 4.4 that quantile mapping is unable to reduce the bias to zero. Although the overall bias is always less than $\pm 15\%$ in bias-corrected rainfall datasets.

4.4.5   Forcing Streamflow and Irrigation Simulations with Climate Reanalysis Data

The application of uncorrected and bias-corrected reanalysis data for simulating streamflow is evaluated by using the flow duration curves [Fig. 4.9(a-d)] as well as
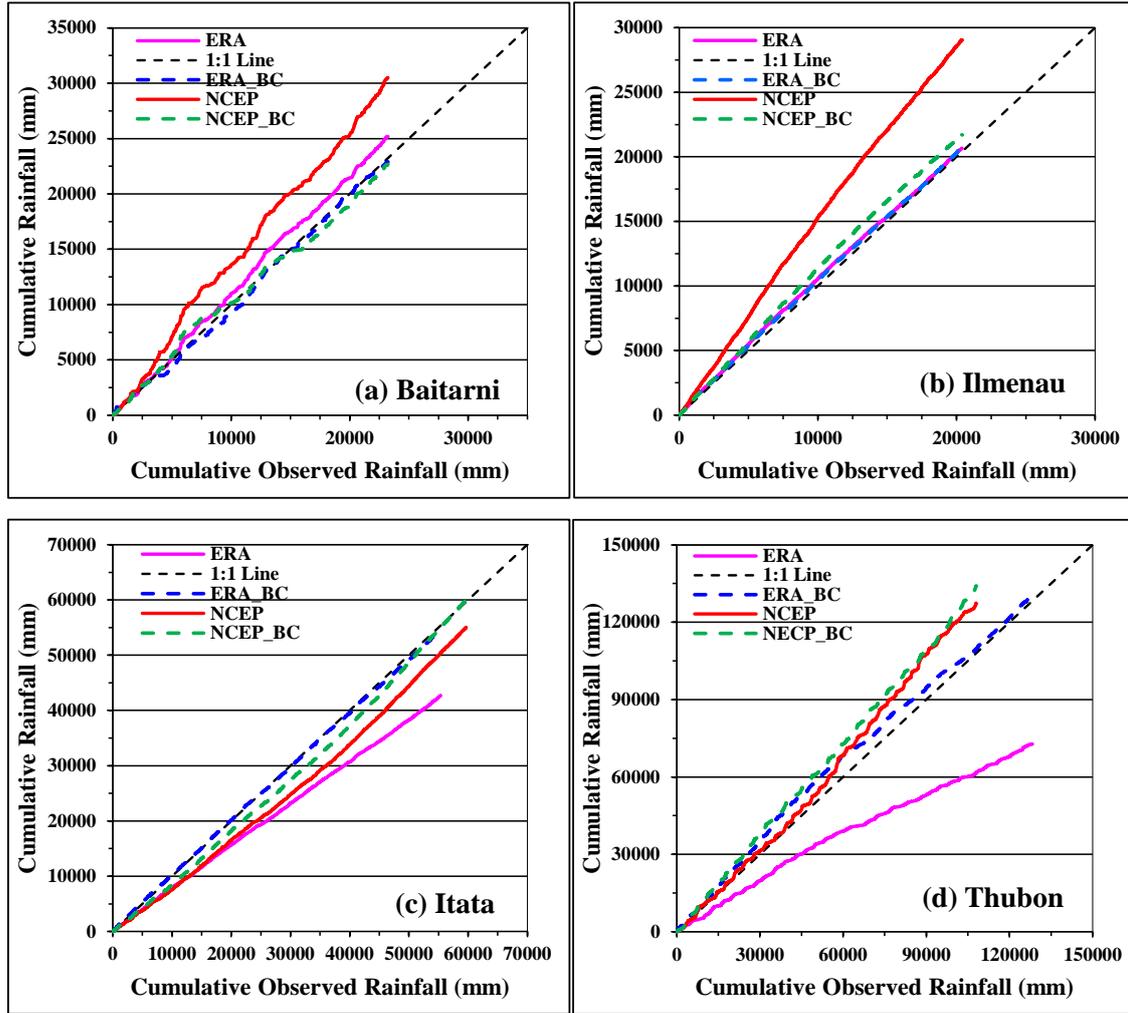
ERA: Raw ERA-interim data, ERA_BC: Bias-corrected ERA-interim, NCEP: Raw NCEP data, and NCEP_BC: Bias-corrected NCEP data.

Figure 4.9: Double mass curve of long-term rainfall data for (a) Baitarani, (b) Ilmenau, (c) Itata, (d) Thubon.

Table 4.4: Statistical evaluation of daily reanalysis rainfall

Sl. No.	Catchment	Statistical indicators (1980-2010)	NCEP	NCEP_BC	ERA	ERA_BC
1.	*Baitarani	PBIAS (%)	-27.28	5.66	-9.44	-1.85
		MAE (daiy, mm)	5.23	4.86	4.7	5
2.	Ilmenau	PBIAS (%)	-42.44	-6.43	-1.32	-1.8
		MAE (daiy, mm)	2.25	1.97	1.4	1.47
3.	Itata	PBIAS (%)	7.74	-0.67	28.39	8.19
		MAE (daiy, mm)	5.32	5.45	7.71	4.19
4.	Thubon	PBIAS (%)	15.21	-5.27	43.32	-1.69
		MAE (daiy, mm)	11.99	12.02	10.67	11.43

Analysis for Baitarani River basin has been carried out from 1998-2010

model evaluation statistics (Table 4.5). In this research, more interest was given to evaluate the low and mean flows as this plays a major role in the irrigation season. It can be seen from the flow duration curves drawn from the four catchments under bias-corrected and uncorrected cases (NCEP and ERA) that the simulated streamflows under bias-corrected climate data are close to the observed streamflows. In addition to this, it is clear from the quantitative assessment conducted on daily time step that the streamflow simulated by using bias-corrected data is usually better when compared to the observed streamflow than the streamflow simulated using uncorrected data (Table 4.5). It can be seen from Table 4.5 that the streamflow simulated by using bias-corrected ERA data (ERA_BC) with PBIAS: –8.61-18.65% and KGE: 0.46-0.67 is better than the streamflow simulated by using bias-corrected NCEP data (ERA_BC), which has PBIAS: 6.54-24.88% and KGE: 0.30-0.72. In addition to this, it can be assessed from the aforementioned table that streamflow simulated by using uncorrected NCEP data does not yield satisfactory results for all the four catchments, whereas the streamflow simulated using uncorrected ERA has acceptable to satisfactory values in Baitarani, Ilmenau and Itata catchments. Therefore, it can be inferred from the results that the uncorrected reanalysis data is highly uncertain to streamflow simulation in all the catchments of this study. However, it can be concluded that bias correction allows a good performance of the hydrological model driven by reanalysis datasets. In addition to this, ERA uncorrected data can also be useful in filling the data gaps of the data-scarce catchments or can be used as a proxy for the catchments where input data is not at all available.

Table 4.5: Statistical evaluation for checking the application of reanalysis datasets for simulating streamflow

Sl. No.	Catchment	Statistical indicators (1984-2000)	NCEP	NCEP_BC	ERA	ERA_BC
1.	*Baitarani	PBIAS (%)	-30.28	24.88	-31.89	-8.61
		KGE	0.37	0.3	0.53	0.46
		R^2	50.22	0.13	0.44	0.27
2.	Ilmenau	PBIAS (%)	-52.99	11.83	40.38	18.65
		KGE	0.36	0.63	0.42	0.622
		R^2 0.47	0.42	0.56	0.45	
3.	Itata	PBIAS (%)	16.35	12.36	31.68	-6.88
		KGE	0.75	0.72	0.49	0.82
		R^2	0.7	0.72	0.76	0.77
4.	Thubon	PBIAS (%)	39.4	6.54	54.04	2.25
		KGE	0.14	0.71	-0.05	0.67
		R^2	0.44	0.57	0.41	0.45

(asterisk) streamflow simulation during 1999-2005.
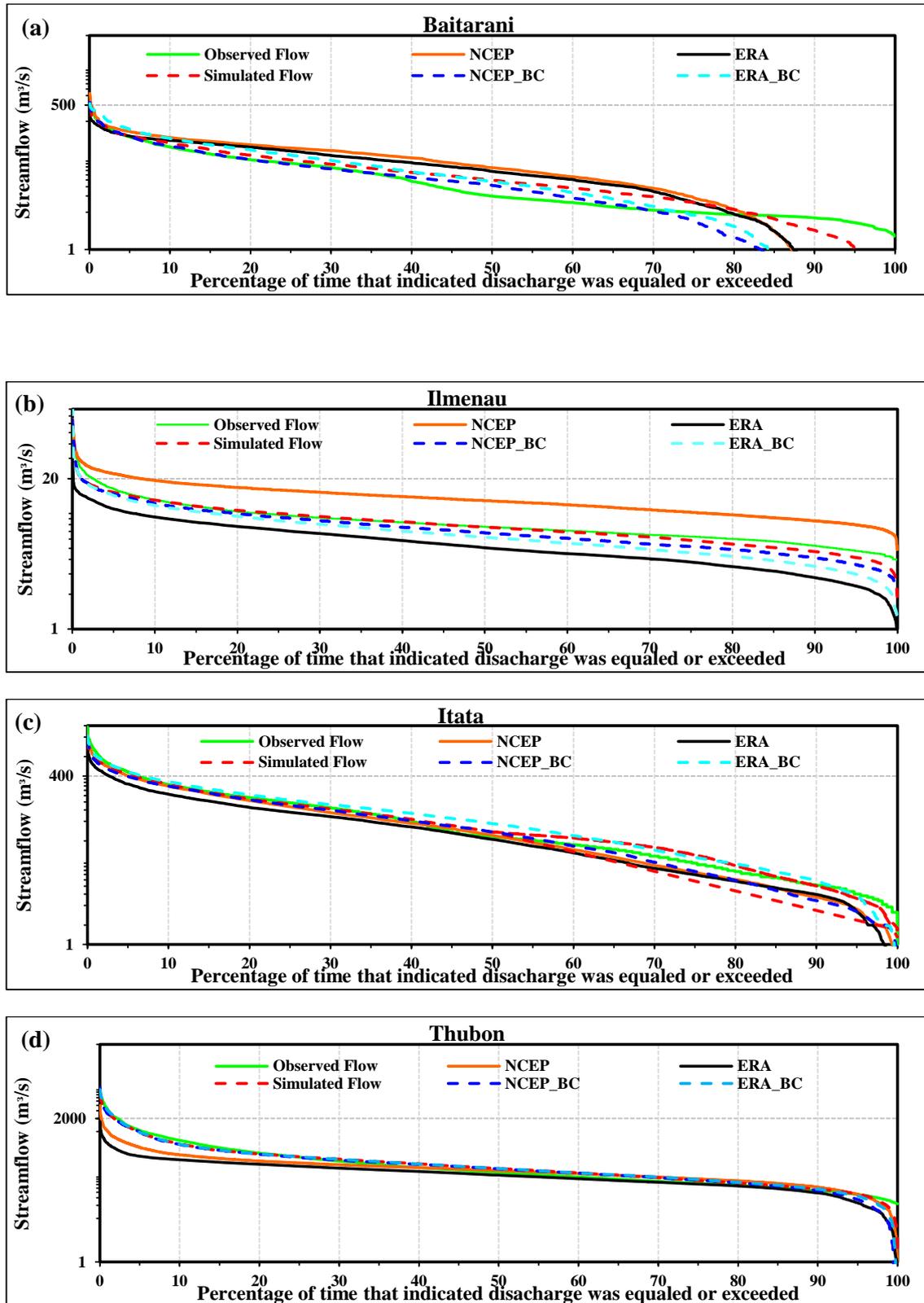
NCEP: streamflow simulated using Raw NCEP data, ERA: streamflow simulated using Raw ERA-interim data, NCEP_BC: streamflow simulated using Bias-corrected NCEP data, and ERA_BC: streamflow simulated using Bias-corrected ERA-interim data.

Figure 4.9: (a-d) Flow duration curves for the calibration period in (a) Baitarani, (b) Ilmenau, (c) Itata, and (d) Thubon catchments.

Apart from evaluating the performance of reanalysis datasets in simulating streamflow in the four catchments, the annual average evapotranspiration and irrigation are also evaluated. As observed irrigation values were not available for all the catchments, the simulated irrigation using observed climate data is compared with the corresponding simulated irrigation using uncorrected and bias-corrected climate reanalysis datasets for the catchments. Double mass curves are drawn for average annual simulated irrigation under observed and reanalysis datasets. In general, it can be seen from Fig. 4.10(a-d) that irrigation simulated by using the bias-corrected data is closer to the 1:1 line as compared to using the uncorrected reanalysis (NCEP and ERA) data in most cases. The percentage deviation in the irrigation simulated using reanalysis data from the simulated irrigation under observed data is shown in Table 4.6.

Table 4.6: Percentage deviation in simulated irrigation under reanalysis weather and observed weather

Sl. No.	Catchment	Statistical indicators	NCEP	NCEP_BC	ERA	ERA_BC
1.	Baitarani	Percent	-27.51	-27.8	6.26	-20.63
2.	Ilmenau	Deviation	-13.8	-14.6	3.24	-5.9
3.	Itata	(%)	-1.62	9.78	20.57	7.86
4.	Thubon		75.66	8.97	61.48	8.89

It can be seen that the long-term average simulated irrigation percent deviation under different cases varies from -27.51 to 75.66%. The aforementioned results are backed by a study performed by Wisser et al. (2008), which states that the error in simulating the irrigation water demand can be as high as $\pm70\%$ at the national scale. In addition to this, it can be seen from the results that the simulated irrigation is sensitive to different weather variables or combination of weather variables in different catchments. As shown in Fig. 4.10, the rainfall in case of the Thubon model (sensitive to rainfall) is overestimated compared to the observed rainfall and this leads to the underestimation of simulated irrigation water demand in NCEP and ERA. However, this is not valid in case of the Baitarani catchment. Furthermore, the annual average simulated irrigation in case of bias-corrected ERA (ERA_BC) is closer to the simulated irrigation under observed data (percent deviation: -7.03 – 8.89%) in almost all the cases except Baitarani (percent deviation: -20.63%).

This deviation in simulated irrigation using bias-corrected weather dataset can be due to the reason that the bias-corrected minimum temperature is not meeting the temporal variability because there is only one temperature gauging station. However, the deviation was acceptable when the model was rerun by only using bias-corrected rainfall and solar radiation. In this case the model gave acceptable results as shown in Fig. 4.10 indicated by ERA_BC* (percent deviation = -7.02%). Additionally, the double mass curves of areal average rainfall, average maximum temperature, and solar radiation are also evaluated during the cropping season against the model simulated annual average evapotranspiration and irrigation for reanalysis datasets. The aforementioned figures confirm the importance of investigating and correcting the bias in temperature and solar radiation as they
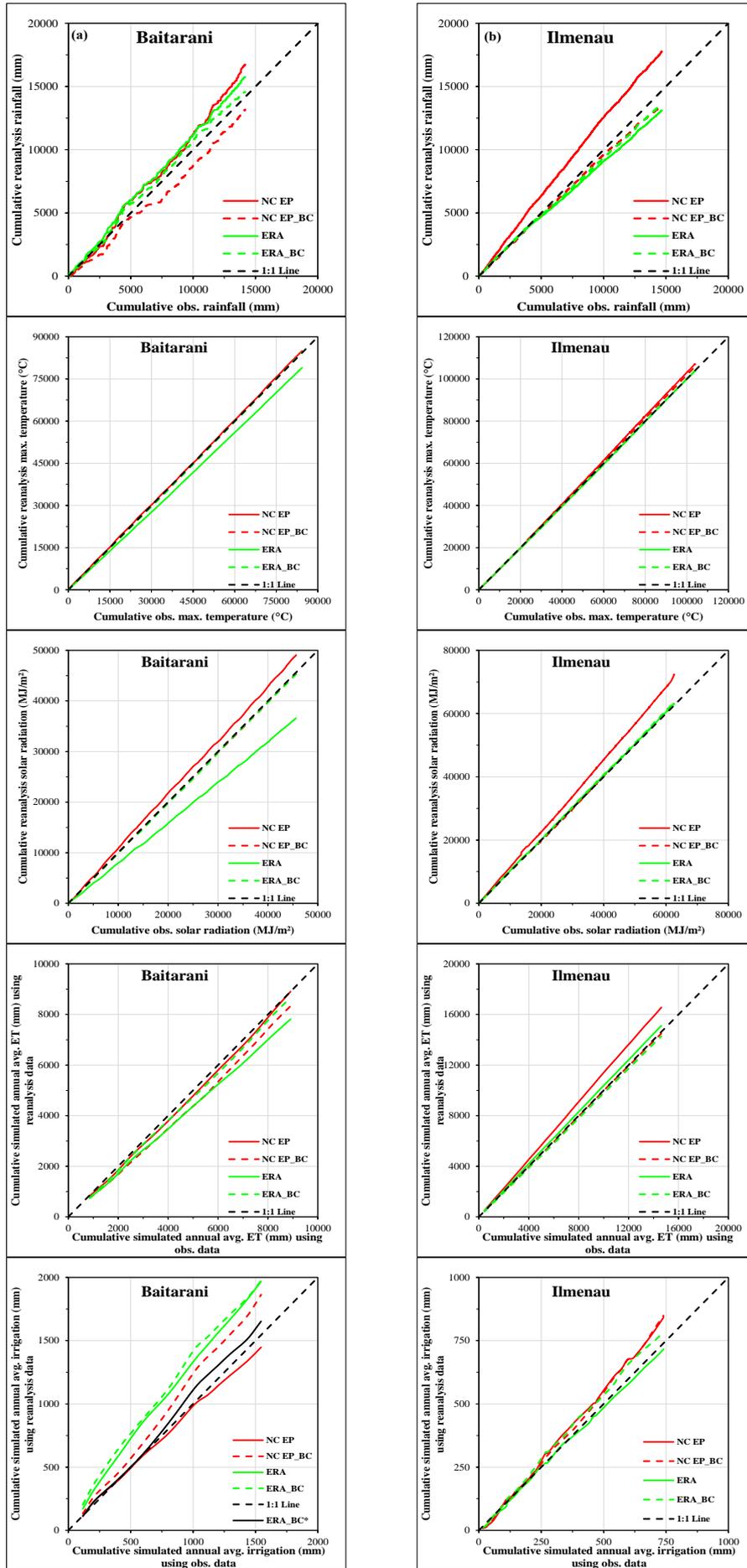
Figure 4.10: (a,b) Double mass curves for different climate variables, simulated annual average ET and irrigation for observed and reanalysis datasets for (a) Baitarani and (b) Ilmenau.
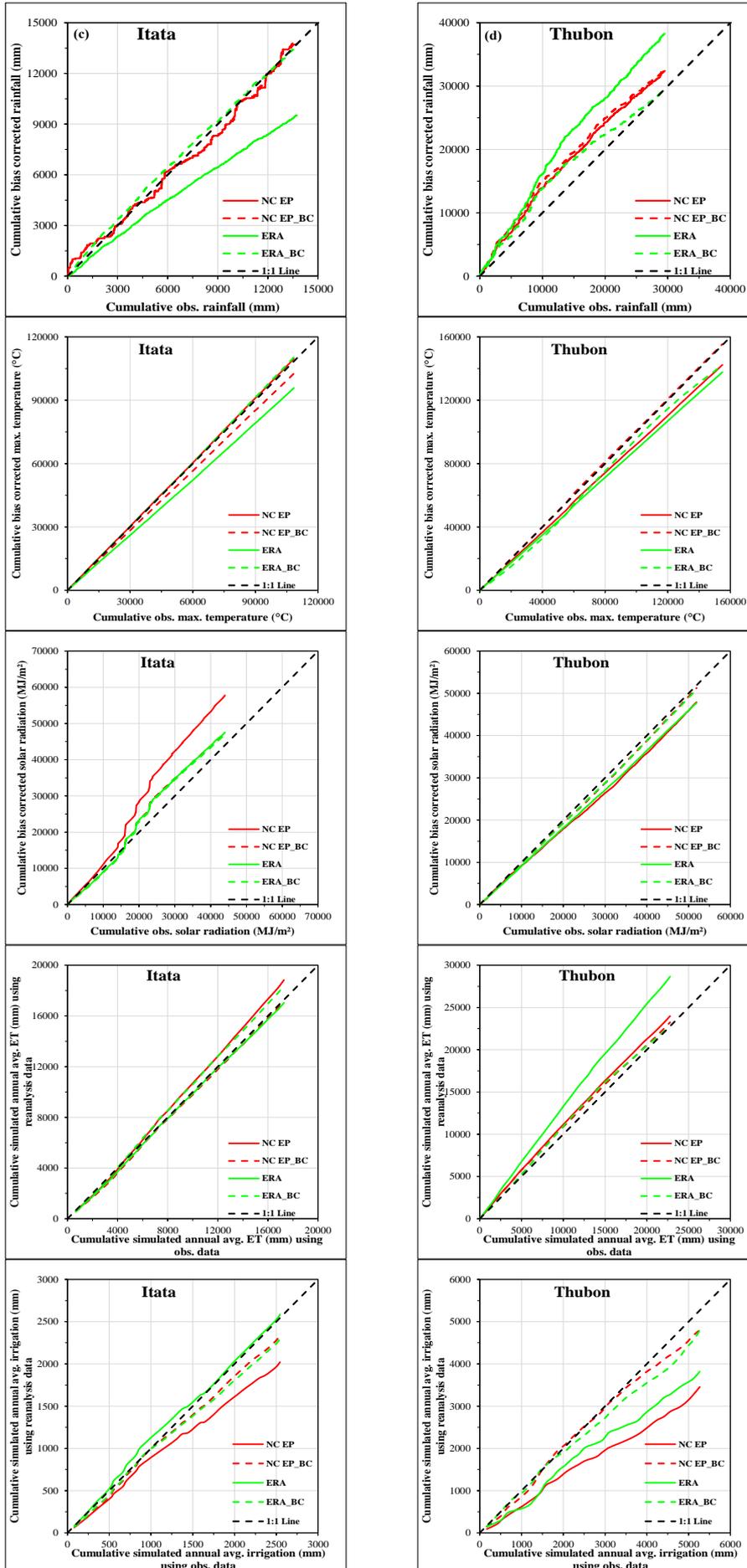
Figure 4.10: (c,d) Double mass curves for different climate variables, simulated annual average ET and irrigation for observed and reanalysis datasets for (c) Itata and (d) Thubon catchments

also play a role in simulation of irrigation water requirement as much as rainfall variability. It can be seen from Fig. 4.10 that the simulated ET is directly related to the overestimation and underestimation of rainfall by reanalysis data compared to the observed rainfall.

Table 4.7 summarizes the findings from the double mass curves of observed areal average rainfall, maximum temperature, and solar radiation during the plant growth period (Fig. 4.9) in order to check the plausibility of the simulated irrigation. The qualitative behavior of the aforementioned climate variables was compared in response to the simulated actual evapotranspiration and irrigation. For rainfall, maximum temperature and solar radiation table show if the variable from reanalysis is higher ($\uparrow$), lower ($\downarrow$) or similar ($\cong$) to the respective observed values in long-term average. For simulated evapotranspiration (ET) and simulated irrigation, the arrows show the results as simulated by SWAT driven with the reanalysis data. The last column of the table indicates the agreement of the simulated irrigation with the expected response. The expectation is based on the climatic feedback mechanisms with the three other variables: overestimation of rainfall can lead to higher ET, because more water is available for actual evapotranspiration, and lower irrigation requirement, as there is more soil water available. Higher temperature and higher solar radiation are expected to have a positive impact on evapotranspiration, which in that case will cause a higher irrigation requirement. It is worth to mention that a clear dependency of a single weather variable to simulated irrigation is difficult to find in all the catchments as the climate variables are interdependent. In addition to this, rainfall is not always the most sensitive climate variable but it always has an impact on ET.

The overall response of the simulated irrigation under different cases is also analyzed using plant and soil water stress. The areal average plant water stress for irrigated crops grown in the respective catchment area is shown in Table 4.8. The overall water stress in different SWAT models forced with reanalysis datasets is more than the water stress during the model developed by using the observed data except in Itata and Thubon catchments. Therefore, the model will apply more water to the crops as it can be seen in case of the Baitarani River basin for all four cases. The aforementioned statement is also supported by the water stress days in case of the Ilmenau catchment. Considering the bias-corrected data to be more close to the observed datasets, the water stress days in models forced with bias-corrected weather input are closer to the ones forced with observed weather input data. In addition to this, the behavior of simulated irrigation using corrected and uncorrected reanalysis in case of Thubon can be easily justified by the water stress days in addition to the rainfall, temperature and solar radiation. As the water stress days in case of bias-corrected reanalysis data is more, therefore the model applies more water, which brings the simulated values closer to the simulated irrigation under observed weather data. In addition to this, the number of water stress days when irrigation is scheduled by the soil water deficit is shown in Table 4.9. It can be assessed from the table that the number of stress days are higher in this case as compared to the plant water stress technique. This justifies more irrigation applied in the second case.

Table 4.7: Plausibility check of simulated irrigation under reanalysis climate compared to the simulated irrigation using observed data

Catchment	Data	Rainfall	Max. Temperature	Solar Radiation	ET	Sim. Irrigation	Agreement
Baitarani	NCEP	↑	≅	↑	≅	≅	As Expected
	NCEP_BC	↓	≅	≅	≅	↑	As Expected
	ERA	↑	↓	↑	↓	↑	Not Expected
	ERA_BC	≅	≅	≅	≅	↑	Not Expected
Ilmenau	NCEP	↑	≅	↑	↑	≅	As Expected
	NCEP_BC	↓	≅	≅	≅	≅	As Expected
	ERA	↓	≅	≅	↑	≅	As Expected
	ERA_BC	↓	≅	≅	≅	≅	As Expected
Itata	NCEP	≅	≅	↑	↑	↑	Not Expected
	NCEP_BC	≅	↓	↑	↓	↓	As Expected
	ERA	↓	↓	↑	↓	≅	As Expected
	ERA_BC	≅	≅	↑	↑	↓	Not Expected
Thubon	NCEP	↑	↓	↓	↑	↓	As Expected
	NCEP_BC	↑	≅	≅	↑	↓	As Expected
	ERA	↑	↓	↓	↑	↓	As Expected
	ERA_BC	↑	↓	≅	↑	↓	As Expected

4.4.6   Optimization of available water resources

Table 4.10 shows the percentage change in the annual average irrigation and yield during deficit irrigation (Scenario: S2) compared to the optimal scenario (Scenario: S1) for all catchments. Only soil water deficit scenarios were used for this analysis, as they were providing more reliable irrigation water amounts as compared to the plant water stress scheduling. It can be seen from the table that the amount of irrigation applied during deficit irrigation is 25-48% less than the optimal irrigation, whereas the overall reduction in average crop yield varies from 0-3.3%. For the Ilmenau catchment, the findings are in a similar range as field experiments carried out by the local agricultural chamber in Hamerstorf, which showed irrigation water savings of 47% by deficit irrigation for winter wheat by a negligible change in yield for winter wheat, whereas for sugar beet 29% of water can be saved on the cost of 6% of yield (Fricke and Riedel, 2016). Therefore, it is clear from all the models that one can use deficit irrigation with small losses in the overall yield. This could be a good adaptation measure in concern of future water scarcity.

Table 4.8: Annual average water stress days for irrigated crops under plant water stress

Sl. No.	Catchment	Observed climate	NCEP	NCEP_BC	ERA	ERA_BC
1.	Baitarani	3.8	6.2	6.1	4.7	5.6
2.	Ilmenau	0.9	1.3	1.3	1.2	1.2
3.	Itata	37.3	28.7	31.4	31	33
4.	Thubon	6.42	5.61	6.36	5.71	5.98

Table 4.9: Annual average water stress days for irrigated crops under soil water deficit

Sl. No.	Catchment	Observed climate	NCEP	NCEP_BC	ERA	ERA_BC
1.	Baitarani	8.2	14.7	12.3	11.3	11.2
2.	Ilmenau	1.7	2.9	2.4	2.6	2.4
3.	Itata	39.4	30.9	33.4	33	34.4
4.	Thubon	6.76	5.63	6.39	5.73	6.02

Table 4.10: Change in annual average irrigation and yield during deficit irrigation compared to optimal irrigation

Catchment	% Change	Observed climate	NCEP	NCEP_BC	ERA	ERA_BC
Baitarani	Irrigation	-37.44	-31.82	-32.7	-33.72	-33.68
	Yield	**-0.06**	**-1.63**	**-0.99**	**-0.48**	**-1.71**
Ilmenau	Irrigation	-43.33	-37.35	-38.5	-39.92	-40.96
	Yield	**-1.22**	**-1.68**	**-2.35**	**-1.69**	**-1.95**
Itata	Irrigation	-30.22	-29.65	-31.47	-40.6	-36.63
	Yield	**-0.75**	**-1.86**	**-1.65**	**-2.27**	**-2.18**
Thubon	Irrigation	-40.36	-48.39	-42.34	-42.25	-42.24
	Yield	**-3.33**	**-0.83**	**-1.82**	**-2.77**	**0**

4.5   Conclusions

This study evaluated the application of SWAT in simulating irrigation water requirement in four different catchments around the globe (Chile, Germany, India, and Vietnam). Modelling results revealed that the SWAT calibration was possible in four meso-scale catchments with good model efficiency (low bias) for streamflow with low percentage deviation in actual evapotranspiration in all the cases. The

automatic irrigation provided plausible results for soil water scheduling in all the catchments with optimal and deficit strategies even if there was no comparison with observed values on that scale. There are indications that irrigation shows systematic overestimation though as reported by other authors before. Plant water stress scheduling shows a significant underestimation of irrigation water requirement in all catchments. The relatively low irrigation values in case of the plant water stress method might be explained by possible errors associated with plant water stress algorithms embedded in the leaf area based crop growth model used by the SWAT. It can be concluded from the results that SWAT's mechanism for irrigation scheduling can be further improved.

The climate variables form NCEP and ERA exhibit different behavior in a catchment. Bias-corrected rainfall, temperature, and solar radiation datasets are more close to their observed counterparts than the uncorrected datasets. It can be inferred from the performance evaluation of reanalysis data that streamflow and irrigation simulated by the model highly depend on input data. Reanalysis datasets were biased in all the four catchments, and in all cases, raw reanalysis data led to serious bias in the estimated evapotranspiration and irrigation requirement. Results showed that rainfall is not always the governing variable in irrigation simulation. Therefore, it is worth to investigate and bias correct the other climate variables. In addition to this, uncertainty exists in the climate reanalysis data; although an attempt has been made to check it via quantile mapping, still there is an acceptable bias in the quantile corrected reanalysis data. It can be deduced that for any given hydrological model not only the input data but also the input data variability plays an important role in the simulation of irrigation in agricultural catchments. Climate change and adaptation studies must take that into account. The results strongly support the application of bias corrections, even if they can be criticized from the meteorological community due to disturbance of the physical consistency of climate variables. However, the relative effects of deficit irrigation strategies on water use and crop yield could be simulated by all datasets.

This study confirms the application of SWAT for regional irrigation studies, which are of high importance for water resources management. With today's improved data availability and computing power, models like SWAT might fill a gap between field-scale models as often used in agriculture and large scale models, whose results have been questioned in other studies due to their large bias when evaluated on smaller scales. In the light of climate change and higher water demand for food production, more attention should be paid on to the simulated irrigation amount at the regional and global scale. Upscaling a regional model, driven by corrected global reanalysis data, might provide a more accurate estimation of irrigation water requirement than the global models due to their over-simplification. Therefore, further research is needed in this direction for improving the global and regional water management.

Acknowledgement

Chapter 5
Model improvement and verification

Abstract

Automatic irrigation in the Soil and Water Assessment Tool (SWAT) is triggered by using plant water stress and soil water deficit irrigation scheduling. Auto-irrigation is important to simulate the catchment's behavior in response to climate change and water management scenarios. However, studies have identified deficiencies in the auto-irrigation algorithms in SWAT as the irrigation water amount simulated under plant water stress scheduling shows a large deviation from the simulated irrigation water amount under soil water deficit scheduling. Therefore, the current research deals with validating and modifying the auto-irrigation scheduling under plant water stress condition using SWAT. The modified SWAT model was evaluated against the Soil-Water-Atmosphere-Plant (SWAP) model as well as observed data for irrigation and crop yield at an experimental field (Hamerstorf, Lower Saxony, Germany) during the 2008-2018 cropping seasons. The two SWAT subroutines .swu and .autoirr were modified. The existing root density distribution function was replaced with the one proposed by Li et al. (1998) and also a dynamic estimation of the plant water uptake compensation factor (EPCO) was incorporated into the modified SWAT. The results revealed that SWAP and modified SWAT were able to simulate the irrigation amount and crop yield with an acceptable bias for all the crops at the experimental site. However, the overall spread of crop yield simulated (11 years) by both the models were less compared to the observed spread for most of the crops. Furthermore, the modified SWAT code was used to simulate the irrigation amount for three different agro-climatic catchments in Germany, India, and Vietnam. Results showed improved irrigation simulation in terms of long-term annual amounts compared to the default SWAT under plant water stress condition.

Keywords: *Root water uptake; Irrigation; Auto-irrigation; SWAT; SWAP*

5.1 Introduction

Plant water uptake plays the main role in water transfer in the soil, plant and atmosphere continuum (Feddes et al., 2001). It is estimated that 65% of the precipitation is returned to the atmosphere via evapotranspiration (ET), which depends on plant water uptake (Oki and Kanae, 2006). Water availability enhances the plant water uptake processes in irrigated agricultural fields. Irrigated agriculture provides an enormous contribution to global food supply and security by producing approximately 40% of food and agricultural commodities on only 20% of the agricultural area (Kadiresan and Khanal, 2018). Hence, the quality of simulations in agricultural water management depends on a good implementation

of root water uptake (Albasha et al., 2015). Water availability and water demand are two important aspects of sustainable water resources management. The increase in water scarcity due to the overuse of limited water resources is a real threat to sustainable water resources development in many parts of the world. Irrigated agriculture is the most relevant consumer of water worldwide. Population growth and climate change will most probably lead to further increasing irrigation water demand (Elliott et al., 2014).

As water is a highly managed commodity in irrigation systems, therefore improving the simulation of root water uptake (RWU) in agro-hydrological models will foster improvements in resource utilization at global, regional and field scales. Research on RWU has resulted in the development of models that vary from conceptual to highly complex physically-based models. Feddes (1982) described one-dimensional water flow in a heterogeneous soil-root system, in which the sink term was integrated over the plant's rooting depth. This model was later improved by Peters (2016), who extended its application to limited aeration and under low water potential conditions. Jarvis (1989) described root water uptake as a function of potential ET and a weighted stress index, which depends on vertical root distribution and water content in the soil. Li et al. (1999) developed an exponential root water extraction function to account for non-uniform root distribution in the soil profile and this was implemented into the Soil-Water-Plant-Atmosphere (SWAP) model.

Jarvis (2011) developed a parsimonious physically-based uptake compensation model that requires fewer parameters than the other empirical approaches. Peters (2016) introduced a constraint to compensate for too high transpiration rates in the empirical model developed by Jarvis (2011). Even though the number of parameters used in the aforementioned models is low, their correct estimation is important for simulating root water uptake. de Willigen et al. (2012) evaluated root water uptake from three soil water flow models of different complexity and revealed that soil physical and root physiological factors are important for root water uptake modeling. Ojha et al. (2009) examined the performance of different root-water extraction models using available data as well as data generated under controlled conditions. The result stresses that the nonlinear parameters in the model can define the nonlinearity in plant water uptake. De Jong van Lier et al. (De Jong van Lier et al.) developed a physically-based root water uptake model containing a compensation mechanism based on the matric flux potential (M) and different root parameters. The proposed reduction function was built into the SWAP model, and predictions were compared to the Feddes model. Results revealed that the developed function can simulate the compensated root water uptake without increasing the number of input parameters or degrading model performance.

Even though RWU is a very small component of the water cycle but it affects one of the most important losses occurring in the system (evapotranspiration, ET) and this makes it sensitive towards the water cycle. In addition, this is a highly complicated and heterogeneous process occurring inside the soil. Macroscopic empirical RWU models are often used in hydrological studies to predict water dynamics through the soil-plant-atmosphere continuum. They have an edge over the other models as

they do not require complete insight into the physical processes of root water uptake thereby eliminating the need for parameters that are difficult to obtain (Ojha et al., 2009). It can be assessed from the literature that RWU in macroscopic models is highly dependent on root density distribution (Albasha et al., 2015) in addition to the soil physical parameters. Daisy (Hansen et al., 2012) and DSSAT (Jones et al., 2003) models use the exponential RWU model for simulating the root water uptake but the model parameters, as well as their equations, are different for different models (Li et al., 2001). SWAP is a one-dimensional, physically-based model, which is used for simulating water, heat and solute transport in saturated and unsaturated zones. It has separate modules for irrigation management and crop growth (WOFOST model, Van Diepen et al., 1989). SWAP provides the user with an option of choosing either linear or physically based root water uptake models (Kroes et al., 2009). In this study, water transport, irrigation management, and crop growth modules of SWAP were used. SWAT (Soil and Water Assessment Tool) uses exponential root water uptake model defined in the EPIC documentation (Sharpley and Williams, 1990; Neitsch et al., 2011) in which root density distribution is a bit simpler as compared to the one discussed by (Li et al., 1999) and (De Jong van Lier et al., 2008).

SWAT has become a popular agro-hydrological model amongst researchers and planners dealing with the simulation of hydrology, agricultural water management and nutrient loads of agricultural watersheds around the world (Neitsch et al., 2011). SWAT provides options for the implementation of scheduled irrigation and auto-irrigation. The latter can be triggered by soil water deficit or by plant water stress. Auto-irrigation is commonly used due to the lack of scheduling data, and it is recommended for the implementation of dynamic irrigation under climate variability or change. Even though SWAT is a widely used model it still has some shortcomings. It has been continuously modified by researchers in the last decades. In this study, the authors focus on the subroutine, which triggers irrigation under plant water stress for automatic irrigation scheduling. There are very few studies that have explored the plant water stress subroutine in SWAT for simulating irrigation water demand for different crops under varying agro-climatic conditions, even though the improvement of the irrigation routines gained more attention in the last years.

Santhi et al. (2005) developed a canal irrigation component in SWAT and validated it for regional planning of an agricultural catchment in Lower Rio Grande Valley, Texas. Dechmi et al. (2012) modified SWAT to correctly simulate the hydrological process in an intensively irrigated catchment located in Spain. Panagopoulos et al. (2014) assessed the cost-effectiveness of different irrigation water management practices in a water-scarce agricultural catchment in Pinios, Greece. Githui et al. (2016) tested different irrigation inputs in SWAT and evaluated them against the observed and simulated flow and ET in an irrigated catchment in Australia. Wei et al. (2018) modified seepage simulation from earthen irrigation systems to improve the simulation of management practices and hydrological processes mainly in-stream flows in an intensively managed agricultural watershed in Colorado, United States. McInerney et al. (2018) evaluated the response of different spatio-temporal irrigation inputs in simulating

streamflow, ET and potential recharge. Marek et al. (2017) used SWAT for simulating the crop yields, crop water use as well as the irrigation required by a semi-arid watershed located in the Texas High Plains, US. The overall results concluded that SWAT's plant growth algorithm is not suitable for simulating the representative cotton yield of the catchment, which could be due to the limitation of auto-irrigation function. Chen et al. (2018) also found that although the SWAT default auto-irrigation triggered by soil water content method provided a reasonable simulation of actual ET, the irrigation amount varied greatly from actual irrigation amount observed in the field. They developed a new management allowable depletion (MAD) based auto-irrigation algorithm in SWAT based on scheduled date and accumulated heat units. In most cases, the irrigation amount simulated by SWAT default auto-irrigation is overestimated compared to the observed values. Chen et al. (2019) evaluated the SWAT-MAD algorithm using field irrigation data based on the FAO-56 irrigation scheduling method for six corn fields in five states of the U.S. The results revealed that the irrigation amount simulated under soil water content auto-irrigation algorithm was overestimated (PBIAS of 32.9% at Clovis site) by the model, whereas in case of plant water demand the model showed an underestimation of 36%. Uniyal et al. (2019) found that the irrigation amount simulated by SWAT using plant water stress is sometimes 2-3 times less than the amount of irrigation simulated by the model under soil water deficit condition. Therefore, there is a need to conduct studies, which test the amount of irrigation simulated by the model as well as the overall crop yield and which propose further improvements in the auto-irrigation routines of SWAT.

With this aim, the objectives of the current research are framed as follows: 1) Improving auto-irrigation in SWAT by changing the root density distribution; 2) validating the proposed model with SWAP and observed data in terms of annual irrigation amount and crop yield at an experimental field (Hamerstorf, Lower Saxony, Germany); 3) evaluating the modified SWAT code at catchment scale by using models from the study of Uniyal et al. (2019) for Baitarani (India, monsoon climate), Thubon (Vietnam, tropical climate) and Wipperau (Germany, humid climate).

5.2 Materials and Methods

5.2.1 Study Area and Data

Data from an experimental field (Fig. 5.1) are used in this study to develop and test the different agro-hydrological models at the field scale. The experimental field is maintained by the agricultural chamber of the Federal State of Lower Saxony in Northern Germany (Landwirtschaftskammer Niedersachsen, LWK). LWK operates different experimental plots in Hamerstorf within the Ilmenau River catchment (Germany). The average annual precipitation of the region was 756 mm from 2007 to 2018, which is distributed throughout the year (humid climate). Weather data was obtained from Deutscher Wetterdienst (DWD).
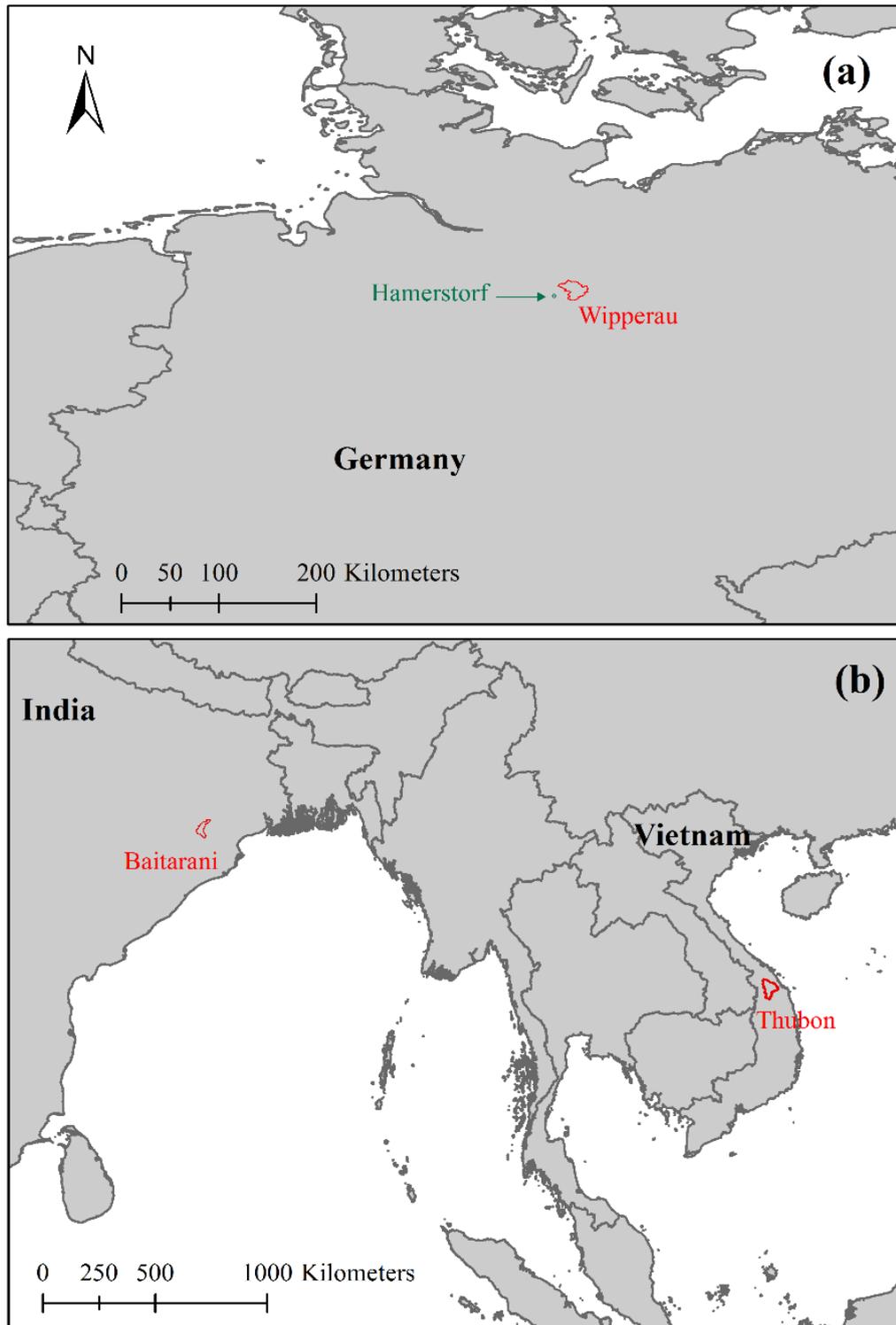
Figure 5.1: Study locations showing the experimental site Hamerstorf (a, in green) and the evaluated catchments Wipperau (a, in red), Baitarani and Thubon (b).

Data analysis revealed that there is considerable variability between years. 2009 and 2018 are hot and dry years compared to the average in terms of average annual maximum temperature (0.4 and 1.15 K) and average annual solar radiation (7 and 34%). In addition, the amount of precipitation received by these two years

was 30-40% less than the average precipitation during the cropping season of winter wheat from 2007-2018. Also, 2007 and 2017 were wet years which received 20-43% more precipitation than their respective average during 2007-2018. The soil in the experimental field is sandy loam with around 80% sand and 15% clay, which makes it a relatively low water-holding soil with high infiltration rates. Soil data were obtained by collecting the soil samples from the experimental field and soil textural analysis was performed in the lab to obtain the soil physical properties and to derive soil hydraulic parameters for the models. The experimental site is used for consultancy purpose in Niedersachsen region for providing irrigation recommendations to farmers on a weekly basis during the cropping season (`https://www.lwk-niedersachsen.de/`). Yearly reports about the experiments were obtained from LWK. These provide information about planting, harvesting, fertilization and irrigation dates for different local crops grown in the experimental field [Corn silage (CSIL), sugar beet (SGBT), potato (POTA), winter wheat (WWHT), etc.]. In addition to this, amounts and scheduling of irrigation (sprinkler) and fertilizer for different crops grown in the experimental field from 2007-2018 were also provided in the reports. Soil's initial condition and information about the preceding crop were also given. The experiments were done under different irrigation scenarios (rainfed, optimal and reduced irrigation), which are also documented in the reports.

5.2.2 Model set up

Design of the model experiment

The physical processes are well defined in a small-scale agricultural model as compared to the catchment scale agro-hydrological model if adequate data is available. As observed field data is available, it was decided to first use a field-scale model (SWAP) to mimic the field conditions and then head towards improving a catchment scale model (SWAT) by using both experimental data and model outputs of the physically-based field-scale model, assuming that they are better and can be used to extend the observed data. SWAP and SWAT were used in this study to simulate the annual irrigation amount as well as crop yield during 2007-2018 at the field scale. The models were developed using the same weather and soil input. For the simulation of the movement of water in the unsaturated soil, SWAT uses a conceptual tipping bucket model whereas SWAP uses the physical Richard's equation. Both SWAT and SWAP use a macroscopic approach to calculate the water uptake by roots. Mineral nitrogen and phosphorus amounts present in the field during 2007 were incorporated into SWAT (.chm file) to depict the initial conditions for nitrogen and phosphorous in the soil profile. Whereas, the SWAP model is initializing the nitrogen concentration from the previous model simulation. The maximum rooting depth of the local soil was taken as 900 mm whereas actual rooting depth of winter wheat was taken 700 mm in SWAT. Crops were planted and harvested by using the planting and harvesting dates provided in the annual reports along with the date and amount of fertilizer application. Both use a temperature sum approach to grow crops but use different crop growth models. Two different irrigation management scenarios were considered 1) scheduled irrigation according to the field experiments and 2) auto-irrigation in both the models. However, in case of automatic irrigation, plant water stress was

used for triggering the irrigation. Plant water stress is defined as the ratio of actual to the potential plant transpiration and for this study, its value is taken as 0.95. The amount of irrigation water applied during an irrigation event was selected as the average amount of irrigation water applied in the field (25 mm) during 2007-2018. Irrigation efficiency was considered as 75%. This includes the total loss that is due to transportation and application. Irrigation water is extracted from the shallow aquifer in the experimental field.

SWAP

In this study, SWAP model version 4.0.1 was used to simulate the interaction of water and crop processes at the field scale. The model was simulated from 2006 – 2018 with 2006 being used as a warm-up period in order to have reliable soil storage at the start of the simulation period. Van Genuchten–Mualem parameters were calculated by using the pedotransfer function published by (Schaap et al., 2001). A separate crop file for corn silage, sugar beet, potato and winter wheat was created using the parameters defined by (Groenendijk et al., 2016). Different SWAP models were created for different crops. The amount of irrigation applied by the model as well as the corresponding yield of a specific crop was compared with the actual field values.

The selection of the SWAP model was done to check whether a field-scale model can simulate the irrigation amount applied to an experimental field. In addition to that, observed irrigation and crop yield data for some additional crops of interest were not available in the experimental field. SWAP was also used to fill the data gaps for SWAT. Therefore, using a physically-based model like SWAP would provide more data points to validate the existing as well as modified SWAT.

SWAT

SWAT (version 2012 revision 664) was used in this study to simulate the soil-water and plant interactions at catchment and field scale. At first, SWAT was developed for the whole Wipperau basin (Fig. 5.1) located in Northern Germany using land use, weather, soil, and elevation data. This is a sub-catchment of the Ilmenau River basin, which shows soil and land-management characteristics close to the Hamerstorf experimental site. It was chosen catchment scale simulations because streamflow of Wipperau is less altered by anthropogenic influence than in the sub-catchment, where the experimental field is placed. Uniyal et al. (2017) can be referred for more information about the catchment characteristics and the model development at the catchment scale. Later, a single HRU (combination of specific land use, soil, and slope) model was analyzed for the experimental site using the input data from the experimental field, like soil properties, weather, crop type, irrigation, and fertilizer amounts, etc. The simulation period was from 2005-2018 with the first three years as a warm-up period. More information about the basic model equations and its processes can be found in (Neitsch et al., 2011).

SWAT has two auto-irrigation algorithms, which vary with the stress identifier 1) plant water demand or 2) soil water deficit. In case of plant water demand, the model

applies a dose of irrigation water on the day, when the ratio of actual transpiration to potential transpiration becomes less than the user defined threshold. For the soil water content irrigation scheduling method, irrigation is triggered when the current water content in the soil profile falls below the field capacity minus the user-defined soil water depletion threshold.

It was seen from the previous study (Uniyal et al., 2019) that very less irrigation amount was simulated by SWAT for WWHT (avg: 25 mm) under plant water stress irrigation scheduling technique, which is not comparable with the annual average irrigation amount applied in the experimental field (avg: 140 mm). Therefore, winter wheat is used as a test crop to check the simulation of crop yield (dry matter) and irrigation amount for experimental field using SWAT and SWAP models and also the improvement in irrigation amount simulated by SWAT using the proposed modifications in this research.

5.2.3 Calibration and Validation of SWAP and SWAT models

Calibration of both the models was performed using the observed yield of winter wheat during 2008-2013, while the rest of the years (2014-2018) were used for model validation. As winter wheat is planted in fall 2007 and harvested in summer 2008, therefore the model comparison was performed from 2008 onwards. Different crop sensitive parameters were used to calibrate SWAP and SWAT under scheduled management practices (irrigation and fertilization).

Table 5.1: Crop parameters used for SWAP model calibration

Parameter	Calibrated value
TSUMEA (temperature sum from emergence to anthesis, °C)	1200/*750/**1300
TSUMAM (temperature sum from anthesis to maturity, °C)	1000
TSUMEMEOPT (temperature sum needed for crop emergence, °C)	70
CVO (efficiency of conversion into storage organs)	0.85
DVSNLT (development stage above which no crop nitrogen uptake does occur)	1.5
FRNX (optimal N concentration as fraction of maximum N concentration)	0.4/*0.35/**0.35
BLAI (maximum potential leaf area index, m^2/m^2)	6
WSYF [lower limit of harvest index, $(kg/ha)/(kg/ha)$]	0.4
$BIO_E[radiation use efficiency,(kg/ha)/(MJ/m^2)]$	35
HVST [Harvest index for optimal growing conditions]	0.5

*Corresponds to the parameter values used in 2017 and ** corresponds to the one used in 2018.*

Crop parameters in SWAP were sensitive towards extreme weather conditions in the year 2017 (wet) and 2018 (dry and hot) compared to the average conditions during 2008-2016. Therefore, in this case, SWAP was calibrated and validated in

two different ways 1) using same parameters for all the years 2) using different parameters for 2017 and 2018 based on precipitation and temperature during the cropping season using winter wheat as the crop (Table 5.1).

Most of the parameters values were taken from the crop-specific simulation parameters report for the European community (Boons-Prins et al., 1993). The light use efficiency was set to 0.65. As in both the years (2017 and 2018), more water was present in the field due to rain or irrigation, which reduced the nitrogen concentration available to plant, therefore optimal nitrogen concentration ratio FRNX was reduced from 0.4 to 0.35. In addition, the temperature sum from emergence to anthesis TSUMEA was taken 750 in 2017 and 1300 in 2018, as the average temperature was less in 2017 compared to 2018.

5.2.4 Modification of SWAT for auto-irrigation

It was seen from this study that the irrigation amount simulated by the model under plant water stress condition is less compared to the actual amount of water applied to the experimental field. However, the amount of water applied in the experimental field is close to the irrigation amount simulated by SWAT under soil water deficit irrigation scheduling method. This was further discussed in detail by (Uniyal et al., 2019). Therefore, it is very important to diagnose the amount of water stress simulated by the model under plant water stress irrigation scheduling. The water stress factor ($WSTRS$) used in this method is the ratio of actual root water uptake (U_p) to the potential transpiration (E_p). The irrigation trigger mechanism depends on the actual plant need (actual transpiration) and potential transpiration. SWAT assumes actual transpiration as equal to the root water uptake. The amount of irrigation simulated by the model completely depends on the stress factor. Therefore, by using Eqn. 5.1 it can be generalized as follows:

$$wstr = f(U_p, E_p) \tag{5.1}$$

Potential transpiration E_p is calculated by using the Penman-Monteith equation (Allen et al., 1998). On the other hand, the root water uptake is calculated by using the plant growth module from the EPIC model (Sharpley and Williams, 1990).

This can be further improved by modifying the module. The existing exponential equation used in the model for calculating the potential root water uptake is defined as follows:

$$U_{Pl} = \frac{E_{Pi}}{1 - exp(\lambda)} \left(1 - exp\left[-\lambda \left(\frac{Z_l}{RZ} \right) \right] \right) - (1 - EPCO) \left(1 - exp\left[-\lambda \left(\frac{Z_l}{RZ} \right) \right] \right)$$
$$- EPCO \sum_{k=1}^{l-1} u_k$$

$$\tag{5.2}$$

where is U_{Pl} the potential root water uptake from layer l (mm/d), is potential transpiration (mm/d), is the water use distribution parameter, $EPCO$ is plant

uptake compensation factor Zl is the current rooting depth (mm) and RZ is the maximum rooting depth (mm).

The irrigation simulated by the model can be improved 1) by calibration, 2) modifying the code. 1) The existing SWAT model can be calibrated for two important parameters (λ and $EPCO$), which control the actual root water uptake. $EPCO$'s default value is 0.95. The water distribution parameter λ depends on soil characteristics. Its high value denotes high water uptake near the surface and very low water uptake in the lower half of the root zone. By default, this value is set to 10, which means the roots extract a high amount of water from the near-surface to fulfill the transpiration demand of the plant. Calibration can only be done if the observed irrigation amount is known otherwise it will be difficult to calibrate the parameters. At first, the models were calibrated for winter wheat using the field observed schedules of irrigation and fertilizer. Later on, the developed models were simulated using the auto-irrigation under plant water stress condition and then the simulated irrigation from SWAP and SWAT was validated with the experimental irrigation amounts.

2) Modifications of SWAT are developed and validated based on the data of the experimental field as described below. Later on, the modified model can be used to simulate irrigation amounts with higher confidence in the catchments where observed irrigation amounts are unknown. RWU depends primarily on root density distribution and soil physical properties. Therefore, in this case, root density distribution and dynamic estimation of the plant uptake compensation factor is incorporated into the modified SWAT (called SWAT_m in this paper).

Root density distribution

The existing mathematical description of root density distribution (Eq. 5.3) can be replaced by an equation (Eq. 5.4) defined by Li et al. (1999) to improve the simulated irrigation amount. The new equation is an enhanced version of the existing equation and the parameters involved in this equation are all readily available in the model database. The root water extraction models using the enhanced root density distribution function performed better than other models in some studies (Li et al., 1999, 2001).

$$\text{Root density distribution} = \frac{E_{Pi}}{1 - exp(\lambda)} \left(1 - exp\left[-\lambda \left(\frac{Z_l}{RZ} \right) \right] \right) \qquad (5.3)$$

$$\text{Root density distribution} = \frac{ln\left[\frac{1+exp(-bZ_1)}{1+exp(-bZ_2)} \right] + 0.5[exp(-bZ_1) - exp(-bZ_2)]}{ln[\frac{2}{1+exp(-bRZ)}] + 0.5[1 - exp(-bRZ)]} \qquad (5.4)$$

Where, Z_1 and Z_2 are the depths, up to which the root water extraction has to be calculated, b is the extinction coefficient, which governs the percentage of root water supplied by the top 10% of the root zone.

Dynamic estimation of plant water uptake compensation factor

The $EPCO$, a root growth stress factor depends on different stress factors, namely soil strength, temperature, and aluminum toxicity. The aforementioned stresses depend on soil properties. The lowest of these three stresses governs $EPCO$ (Sharpley and Williams, 1990). In this study, two stresses are considered for estimating the dynamic value for $EPCO$ namely soil stress (SS_l) and temperature stress ($TMPRS$). Due to the lack of basic data required to calculate the stress due to aluminum toxicity for the experimental field and with no information regarding aluminum toxicity, the authors have not considered this stress in the study area. The equations used for calculating the soil strength stress factor are as follows:

$$SS_l = 0.1 + \frac{0.9BD_l}{BD_l + exp([bt_1 + bt_2 BD_l)} \qquad (5.5)$$

This stress mainly depends upon bulk density, texture, field capacity and soil water content (Eavis, 1972; Monteith and Banath, 1965; Taylor et al., 1966; Sharpley and Williams, 1990). Where SS_l is the soil strength factor in layer l, BD is the wet bulk density of soil (t/m3), bt_1 and bt_2 are the parameters that depends on soil texture. There are specific equations to calculate the variables and parameters required for this equation, which are discussed in detail in the EPIC manual (Sharpley and Williams, 1990). Additionally, a new sub-routine (SSL) is added to the code for calculating soil strength factor (SS_i). Furthermore, the TMPRS is calculated by using the code already present in SWAT (Neitsch et al., 2011; Arnold et al., 2012). Therefore,

$$EPCO = Min(SS_l, TMPRS) \qquad (5.6)$$

In addition, a management scenario proposed by (Chen et al., 2018) was also added to the model. In this, the whole plant growth cycle is divided into three stages, initial (0-0.35), mid-season (0.35-0.75) and late season (0.75-1.0). The ratio of accumulated heat units was used to define these crop stages in the model. Irrigation was triggered in the model based on different stresses defined for these stages (Chen et al., 2018). In general, the stress for the initial and the late season is assigned as (0.95-0.5). For the mid-season stage (0.6-0.4) as a crop can withstand stress during this stage without much reduction in the yield (Allen et al., 1998). This code is implemented (hardcoded) in the autoirr.f module of the SWAT model (rev664).

Irrigation scheme efficiency

This section deals with the improvement in the implementation of application and conveyance efficiency in SWAT. In the original version of SWAT (rev664 source) the irrigation amount simulated by the model during an irrigation event is calculated by subtracting the surface runoff loss during the process. However, in actual practice water is applied to the field first and after that, the runoff losses occur during an irrigation event. Therefore, the amount of water applied should be equal to the amount of water going into the soil plus the amount of water lost from the field due to surface runoff. Additionally, the amount of water extracted from the source should

be equal to the amount of water applied by the model during irrigation application (water going into the soil plus the surface runoff) divided by the application efficiency (this includes losses during transportation as well as during application). These corrections have been implemented into the irrigation.f and autoirr.f modules of the modified SWAT model. Later, the SWAT_m was used to simulate the irrigation amount and crop yield (dry matter) for the rest of the crops (CSIL, POTA, and SGBT). The SWAT simulated results were then evaluated against the observed and SWAP simulated irrigation amount and crop yields using statistical indicators and box plots to validate the proposed modifications.

Lastly, SWAT_m was applied to three different catchments to test the modified code at the catchment scale. The effective parameters used for catchment scale models were derived from the most common parameter upscaling approach used in distributed hydrological modeling. This approach assumes that the processes, equations, and data from the smaller scale are also applicable at a larger scale. It is assumed that the effective parameters from field/plot scale, when used for regional scale hydrological models, would reproduce the mean response of the system observed at regional or catchment scale (Refsgaard et al., 2016). This assumption was justified by Refsgaard (1997) and Henriksen et al. (2003) whereas it was rejected by Beven (1995).

5.3 Results and Discussion

5.3.1 Model Performance with scheduled irrigation

This section comprises of the results comparing the simulated annual crop yield (dry matter) by SWAP and SWAT using field observed irrigation and fertilizer scheduling with a) observed yield from the experimental field at Hamerstorf (Obs_Field) and b) agricultural census data for the Uelzen region (Census_Ulz) during 2008-2018. Fig. 5.2 shows the observed and simulated yield of winter wheat under given irrigation and fertilizer amounts. Census_Ulz is the agricultural census data of the Federal State of Lower Saxony, which is reported by the farmers via an online platform. Due to a wide range of soil fertility and the presence of rainfed agriculture, the larger scale yield is expected to be lower than the one on the highly managed experimental field. SWAP_C1 is the calibrated yield simulated by using the same crop parameters for the entire period of interest, whereas SWAP_C2 uses different crop parameters for 2017 and 2018 as they were extreme years.

Calibration results of WWHT simulated by SWAP revealed 7.2% underestimation for both SWAP_C1 and SWAP_C2. Whereas, validation results were better in case of SWAP_C2 (3.31%) compared to SWAP_C1 (PBIAS: 38.2%). This is due to the fact that SWAP is not able to simulate crop yield in two extreme years to a satisfactory level (2017 and 2018). This justifies the use of weather-dependent crop parameters in SWAP as it is sensitive to temperature e.g., the model performance in SWAP_C2 is improved compared to the SWAP_C1 in terms of overall variability. In addition, SWAT model is also under-estimating the model performance during both calibration and validation period with PBIAS 3.3% and 13.8%, respectively. It can be inferred from Fig. 5.2 that the simulated yields from

both the models are not able to match the overall spread of WWHT from the observed yield compared to the long-term mean. This qualitative analysis is also supported by the quantitative analysis, which revealed the underestimation of simulated yield by 5.64% and 6.15% from SWAP and SWAT during 2008-2018, respectively. Furthermore, the simulated WWHT yield from SWAT and SWAP matches well with Census_Ulz in terms of their overall spread and mean. This is due to less uncertainty or averaging effects at the district scale compared to field scale. The overall underestimation in case of SWAT is attributed to some warm years (2015 and 2018), for which the considered model has bad model performance in simulating yield.
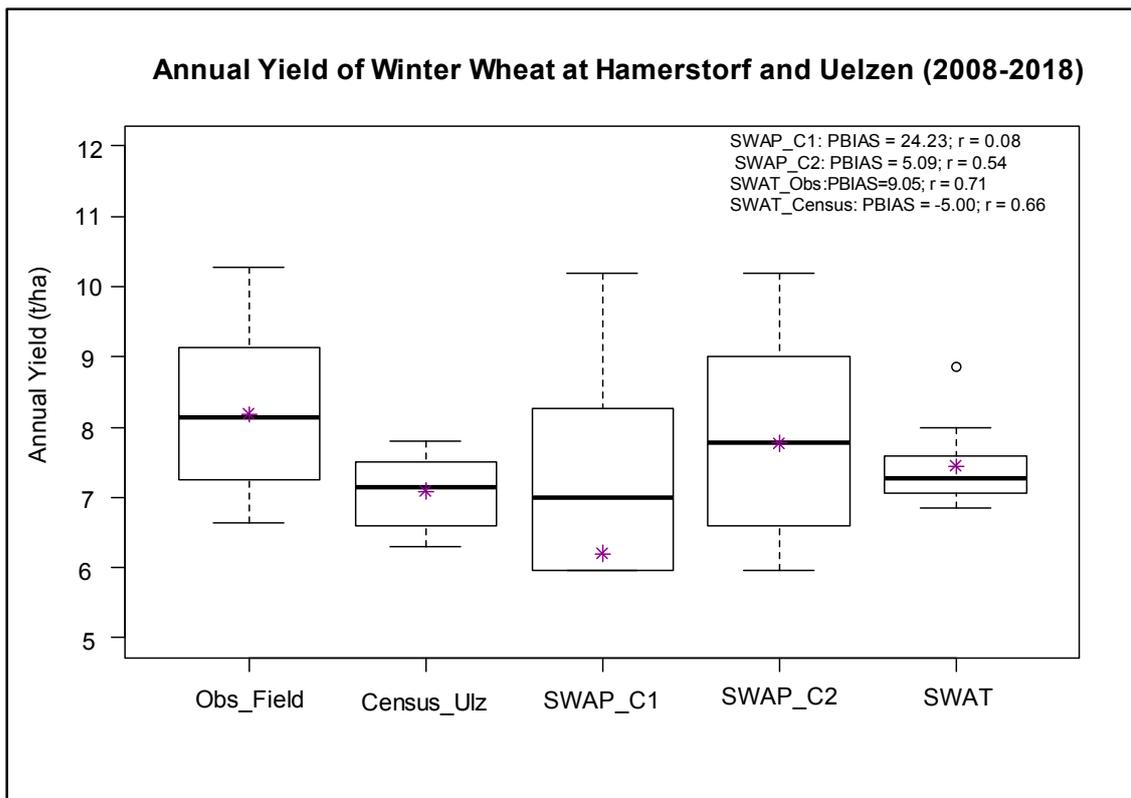
Obs_Field: denotes the observed crop yield data from Hamerstorf; Census_Ulz: denotes crop yield from agricultural census data for the Uelzen region; SWAP_C1: denotes the simulated yield using SWAP model under stationary parameters; SWAP_C2: denotes the simulated yield using SWAP model under non-stationary parameters; SWAT: denotes the simulated yield using SWAT model under stationary parameters.

Figure 5.2: Comparison of SWAP and SWAT simulated yield of WWHT under scheduled irrigation and fertilizer amounts with the observed yield from Hamerstorf and the census data of Uelzen during 2008-2018.

The overall deviation in winter wheat in these years is 15.29% whereas it is 3.19% in the rest of the years. In addition to this, the overall difference in the long-term means from both the models is close to 0.5 t/ha compared to the long-term average of the observed yield during 2008-2018. The model simulated yields and error ranges are backed by a study done in Europe (Abbaspour et al., 2015). It is obvious from the boxplots (Fig. 5.2) that the variability of the observed yield from

the experimental field is better represented by SWAP, whereas SWAT represents the overall yield's distribution better for the regional census data of Uelzen compared to the experimental field. These results comply with the target scale of application of the two models used.

5.3.2   Model Performance under Auto-irrigation

Fig. 5.3 shows the range of annual irrigation simulated by models using plant water stress triggering under auto-irrigation scheduling along with the observed irrigation amount applied in the field. SWAT_UC shows the irrigation amount simulated by SWAT model under default plant water stress auto-irrigation condition without calibration of and *EPCO*. In addition, SWAT denotes the irrigation amount simulated after calibrating the model using (2) and *EPCO* (0.6) parameter whereas, SWAT_m shows the simulated irrigation from the modified SWAT model. SWAT_m uses a dynamic value of *EPCO*, which is calculated internally by the model and also it doesn't use .

*Obs_Field: denotes the observed crop yield data from Hamerstorf; Census_Ulz: denotes crop yield from agricultural census data for the Uelzen region; SWAP_C1: denotes the simulated yield using SWAP model under stationary parameters; SWAP_C2: denotes the simulated yield using SWAP model under non-stationary parameters; SWAT: denotes the simulated yield using SWAT model under stationary parameters.
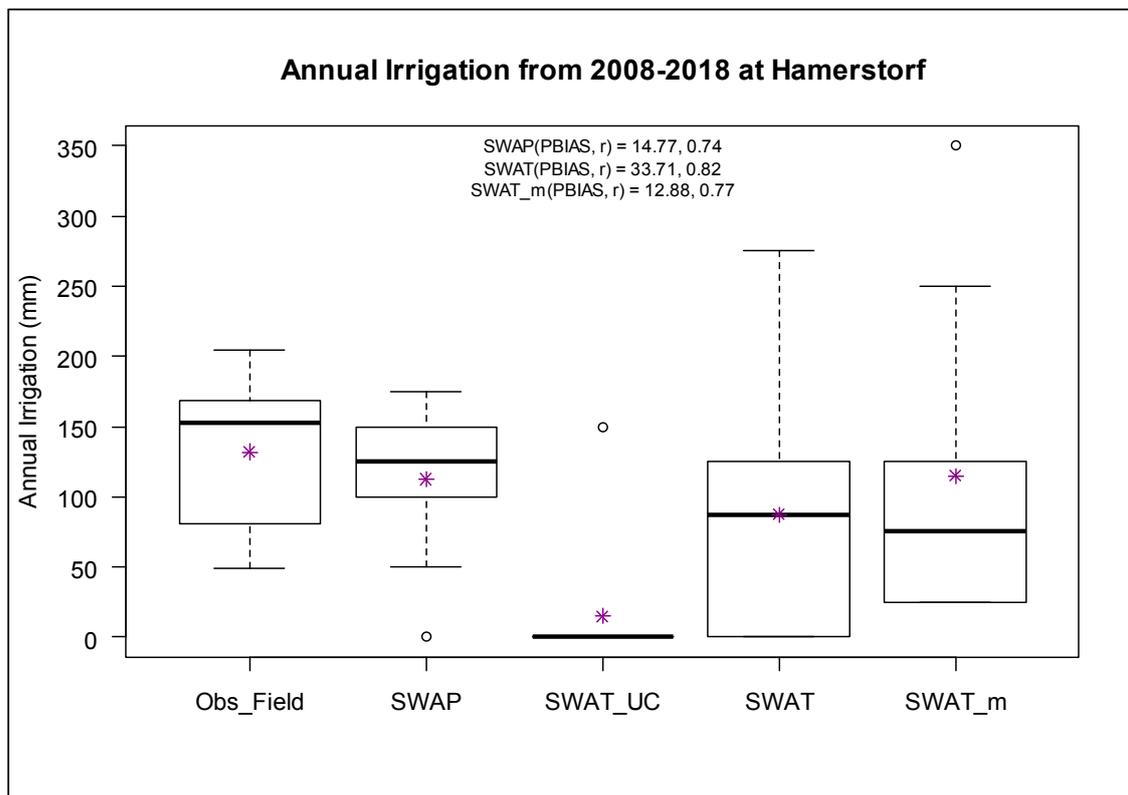
Figure 5.3: Comparison of observed and auto-irrigated annual irrigation from SWAP and SWAT models during 2008-2018 at Hamerstorf.

It can be seen from the results that the overall spread and mean is well replicated by

SWAP as compared to both the SWAT cases. The irrigation amount from SWAT and SWAT_m is relatively good compared to observed and SWAP in simulating the mean annual irrigation amount than the one simulated by uncalibrated SWAT (SWAT_UC). But still one can see a huge uncertainty in irrigation simulation in terms of higher annual variability and a general underestimation. The one by one comparison of simulated irrigation from SWAP and SWAT revealed that the overall model response to an extreme dry year (2018) is not well represented. In 2018 SWAP simulated 175 mm and SWAT models simulated irrigation values ranging from 250-350 mm whereas in 2017, which was a wet year, all the models simulated either zero or 25 mm of irrigation which is close. One can see a general overestimation in 2018 from all the different SWAT models, e.g., even though the irrigation amount is zero in case of SWAT_UC in all the years but still it has 125 mm of irrigation amount simulated in 2018. This reveals that there is more stress in SWAT in 2018 compared to other years specifically due to high observed temperature.

The statistical indicators PBIAS and correlation (r) are also used to evaluate the simulated irrigation amount. It can be seen from the results that both the models are underestimating the irrigation amount, SWAT by 34% and SWAP by 11%. It should be noted that the one by one matching of observed and simulated irrigation is not possible. Therefore, the bias from the field values is acceptable for simulated irrigation (Chen et al., 2018) as well as crop yield (Abbaspour, 2011). This can be justified by several reasons: 1) the irrigation amount as applied in the experimental field was based on the combination of previous day's weather conditions along with the forecast of future weather and soil water deficit as well as the condition of the plant (plant water stress); 2) the irrigation amount applied in one irrigation event in both the models during an irrigation event is the same but in field conditions it varies from year to year and also varies within a year. However, based on the qualitative and quantitative analysis, it can be inferred that simulated irrigation amount from SWAP, SWAT and SWAT_m is in a good range (Chen et al., 2018).
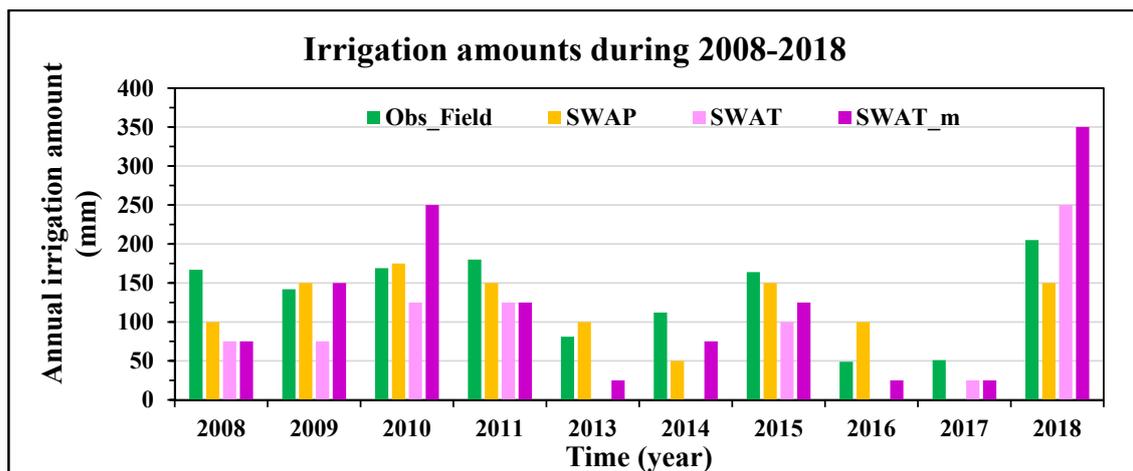
Figure 5.4: Observed and simulated irrigation amounts for Winter wheat at Hamerstorf.

In addition, Fig. 5.4 shows the year-wise comparison of irrigation amounts simulated by SWAP and different SWAT models under plant water demand

irrigation scheduling technique against the observed irrigation amounts applied in the field. It can be seen from the figure that the overall response of observed and modified SWAT is better (SWAT_m) compared to the irrigation amounts simulated by the calibrated SWAT model (SWAT). However, the overall variability is better matched in case of SWAP simulated irrigation amounts. This might be due to the reason that SWAT sometimes irrigates out of season (Chen et al., 2019). The higher amount can be related to more frequent triggering. Furthermore, the observed amounts applied in the experimental field were restricted in extreme years like 2018 due to overuse of water rights.
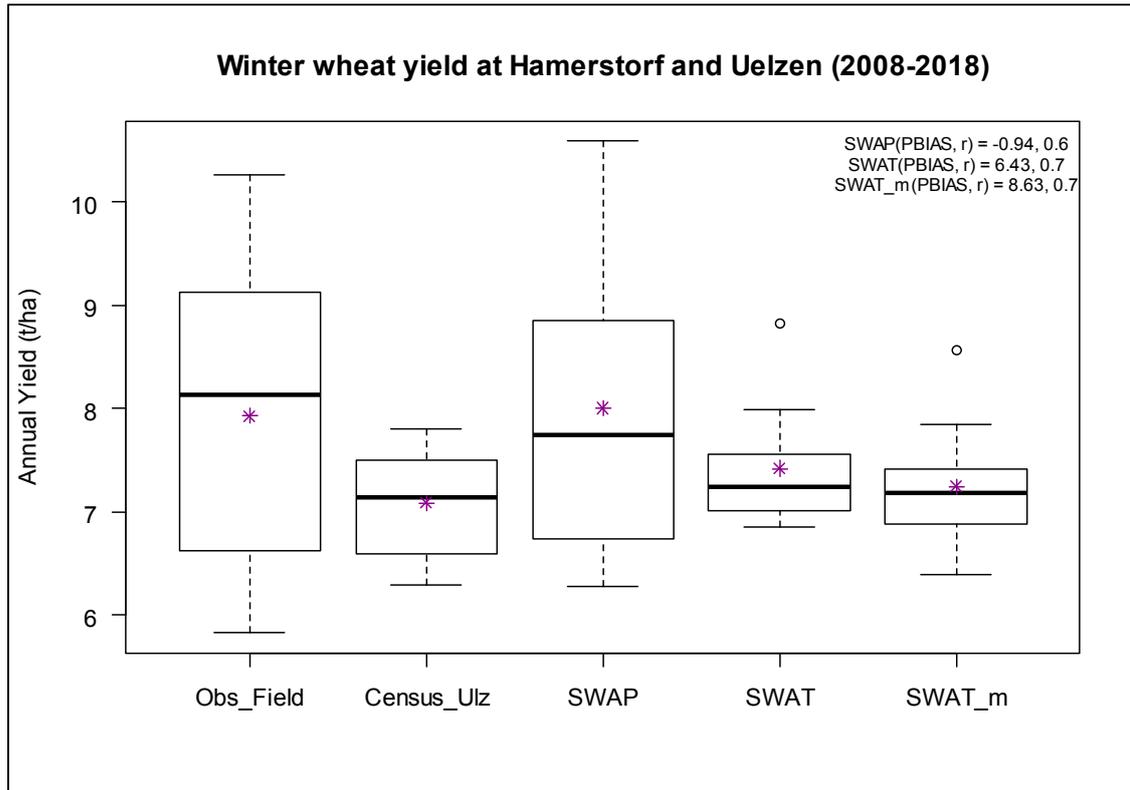
*Obs_Field: denotes the observed crop yield data from Hamerstorf; Census_Ulz: denotes crop yield from agricultural census data for the Uelzen region; SWAP: denotes the simulated yield using SWAP model under non-stationary parameters; SWAT: denotes the simulated yield using SWAT model; SWAT_m: denotes the simulated yield using modified SWAT.

Figure 5.5: Comparison of observed yield in Hamerstorf and census data from Uelzen with simulated annual yield (calibrated SWAP and SWAT) under auto-irrigation during 2008-2018.

Fig. 5.5 shows the boxplot comparison of observed (Obs_Field and Obs_Ulz) and simulated (SWAP, SWAT and SWAT_m) WWHT during 2008-2018 at Hamerstorf. In this, the auto-irrigation scheduling under plant water stress condition was used. The overall distribution and crop yield are mostly reduced compared to the yield simulated in Fig. 5.2. It can be seen from figure that the overall range of WWHT yield simulated by different SWAT models is nearly the same. It can be concluded from this result that water stress is not the dominant stress affecting the crop yield

as the same crop parameters were used in two cases (SWAT and SWAT_m, Fig. 5.2 and Fig.5.5). The long-term mean as well as PBIAS (6.2 - 8.8%) and r (0.6 - 0.7) is in accordance with the observed yield of WWHT at Hamerstorf and the overall prediction uncertainty is less in model simulated results. In addition, the mean and median of simulated yield from all the models are close to the observed yield of winter wheat in the Uelzen district.

Other crops

Evaluation of annual irrigation amount and yield simulated by SWAT_m and SWAP for corn silage (CSIL), sugar beet (SGBT), and potato (POTA) was also performed for the experimental field.
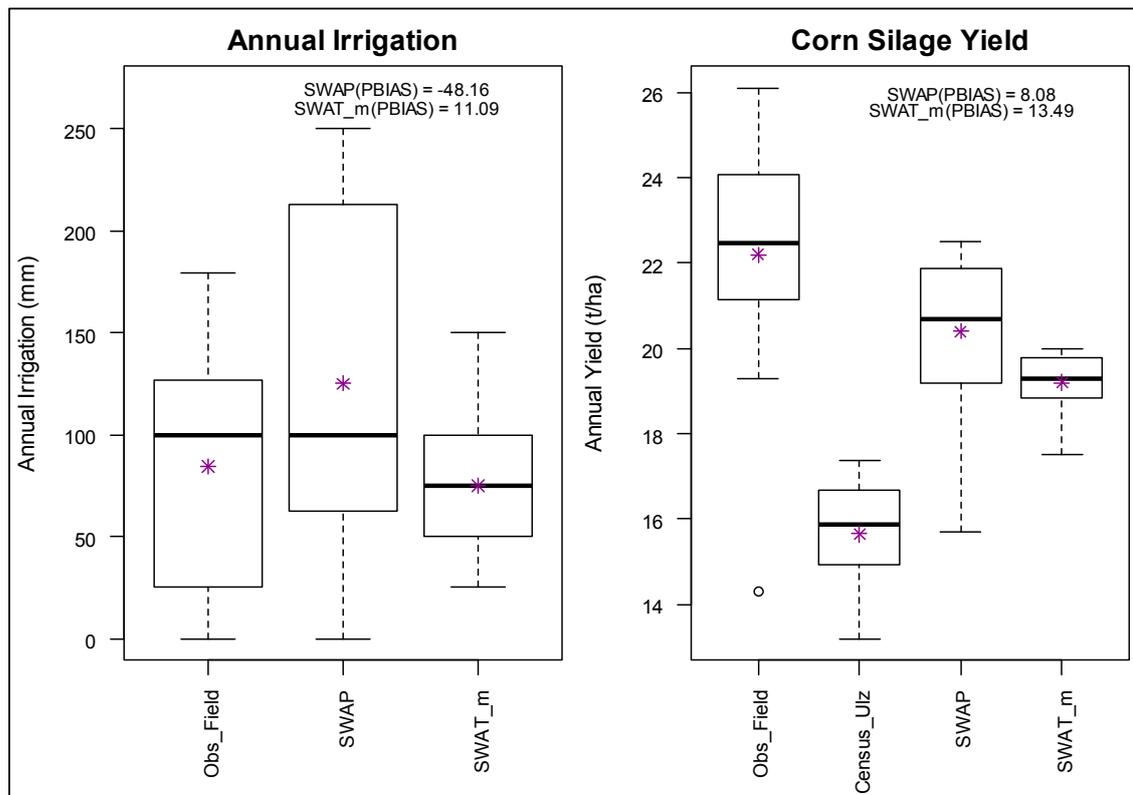
*Obs_Field: denotes the observed crop yield/irrigation amounts data from Hamerstorf; SWAP: denotes the simulated yield/irrigation amounts using SWAP model under non-stationary parameters; SWAT_m: denotes the simulated yield/ irrigation amounts using modified SWAT; Census_Ulz: denotes crop yield from agricultural census data for the Uelzen region.

Figure 5.6: Comparison of observed (Hamerstorf and Uelzen) and simulated annual irrigation and CSIL yield under auto-irrigation in calibrated SWAP and SWAT models during 2007-2018.

It should be noted that in the case of these crops, same values of crop parameters were used for calibration and validation from 2008-2013 and 2014-2018, respectively. Fig. 5.6 shows the boxplots of annual irrigation and yield (dry matter) from CSIL. It is assessed from the boxplots that the mean annual

irrigation simulated by SWAP (125 mm) and SWAT_m (75 mm) are close to the observed mean (84 mm). Quantitative analysis revealed an overestimation of simulated irrigation in case of SWAP by 48% and underestimation in case of SWAT_m by 11%. The simulated yield from both the models is matching well with each other (difference: 0.17%) as compared to the observed yield. In addition, their overall spread and mean is not matching well with the observed yield (PBIAS: 8.6-8.7%). This could be attributed to the crop model parameters for CSIL.

Apart from CSIL, Figs. 5.7-5.8 show the comparative evaluation of simulated irrigation amount and crop yield for SGBT and POTA, respectively. It can be seen from Figs. 5.7-5.8 that the simulated irrigation is underestimated in case of SGBT (PBIAS: 15.15-15.20%) while it is overestimated in case of POTA (PBIAS: –29.96 to –14.7%). For both the crops the overall spread and annual average mean of simulated irrigation, the amount is matching relatively well when compared to WWHT and CSIL.

Obs_Field: denotes the observed crop yield/irrigation amounts data from Hamerstorf; SWAP: denotes the simulated yield/irrigation amounts using SWAP model under non-stationary parameters; SWAT_m: denotes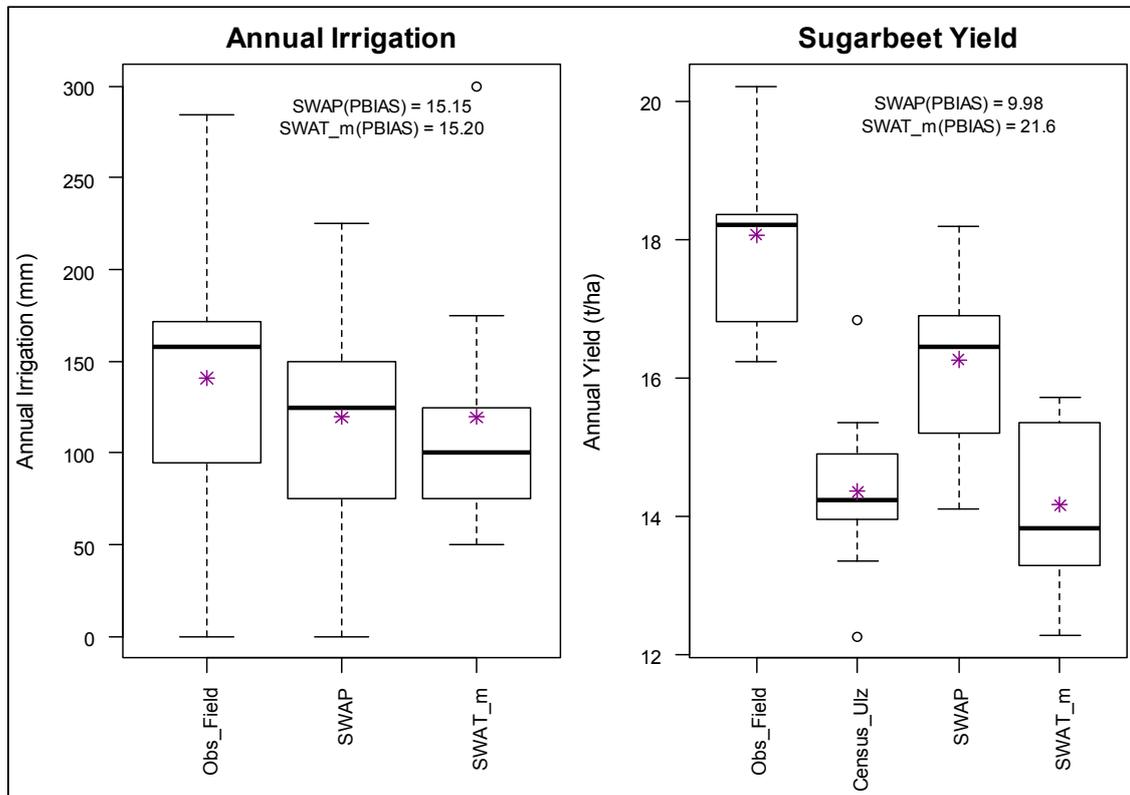 the simulated yield/ irrigation amounts using modified SWAT; Census_Ulz: denotes crop yield from agricultural census data for the Uelzen region.

Figure 5.7: Comparison of observed (Hamerstorf and Uelzen) and simulated annual irrigation and SGBT yield under auto-irrigation in calibrated SWAP and SWAT models during 2007-2018.

A general trend is observed in simulating crop yield using SWAP and SWAT_m,

which revealed that the simulated yield is always underestimated for all the crops. It should be noted that the mean and spread of crop yield from the Uelzen district is less compared to Hamerstorf (Figs. 5.6-5.8). This is expected because not all fields in this region are irrigated and some soils show a poorer quality (sandy soil) compared to the one in the experimental field (loamy sand). In case of all crops, the overall spread simulated by SWAP and SWAT_m is covering the observed yield estimated from the Uelzen district.

Obs_Field: denotes the observed crop yield/irrigation amounts data from Hamerstorf; SWAP: denotes the simulated yield/irrigation amounts using SWAP model under non-stationary parameters; SWAT_m: denotes the simulated yield/ irrigation amounts using modified SWAT; Census_Ulz: denotes crop yield from agricultural census data for the Uelzen region.

Figure 5.8: Comparison of observed (Hamerstorf and Uelzen) and simulated annual irrigation and POTA yield under auto-irrigation in calibrated SWAP and SWAT models during 2007-2018.

5.3.3 Verification of SWAT_m at the catchment scale

The SWAT_m was tested for three different catchments with different agro-climatic conditions namely, Baitarani, Thubon, and Wipperau (Fig. 5.1). Fig. 5.9 shows the annual average irrigation amount simulated for the Wipperau catchment during 2007-2018 for different crops. Here, Obs_Field is the observed irrigation applied in Hamerstorf field given for comparison purpose, SWAT_p is the irrigation amount simulated by SWAT under plant water stress auto-irrigation setting, whereas SWAT_m is the simulated irrigation amount using the SWAT_m during auto-irrigation. SWAT_s and SWAT_s_m are the irrigation amounts simulated by

original and modified SWAT under soil water deficit auto-irrigation setting. This is given to check if there is any feedback between the modifications with the soil moisture deficit auto-irrigation routine. The boxplots from SWAT_s and SWAT_s_m show that less irrigation is applied with the new code. This difference can be explained by the difference in ET (2%) due to the changes in the root density distribution. This has an effect on the transpiration calculated by the model, and thus on soil moisture and the triggering of auto-irrigation. The overall difference reduction in mean annual irrigation in case of SWAT_s_m varies from 9 to 10% compared to SWAT_s. The overall irrigation amount in case of CSIL, SGBT, and WWHT have significantly increased as compared to the one simulated by SWAT_p model. Furthermore, simulated irrigation amount for POTA is more in case of SWAT_p and SWAT_m compared to the ones applied in the field but the overall spread is less than the amount applied in the field.
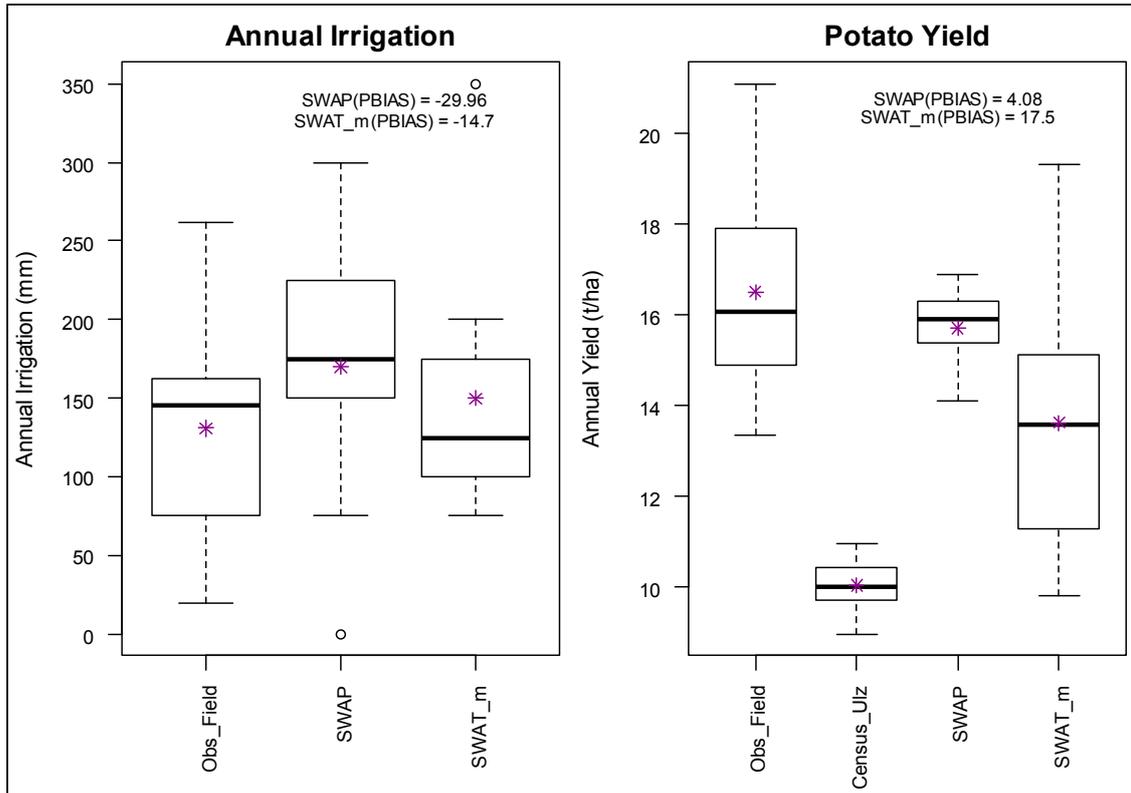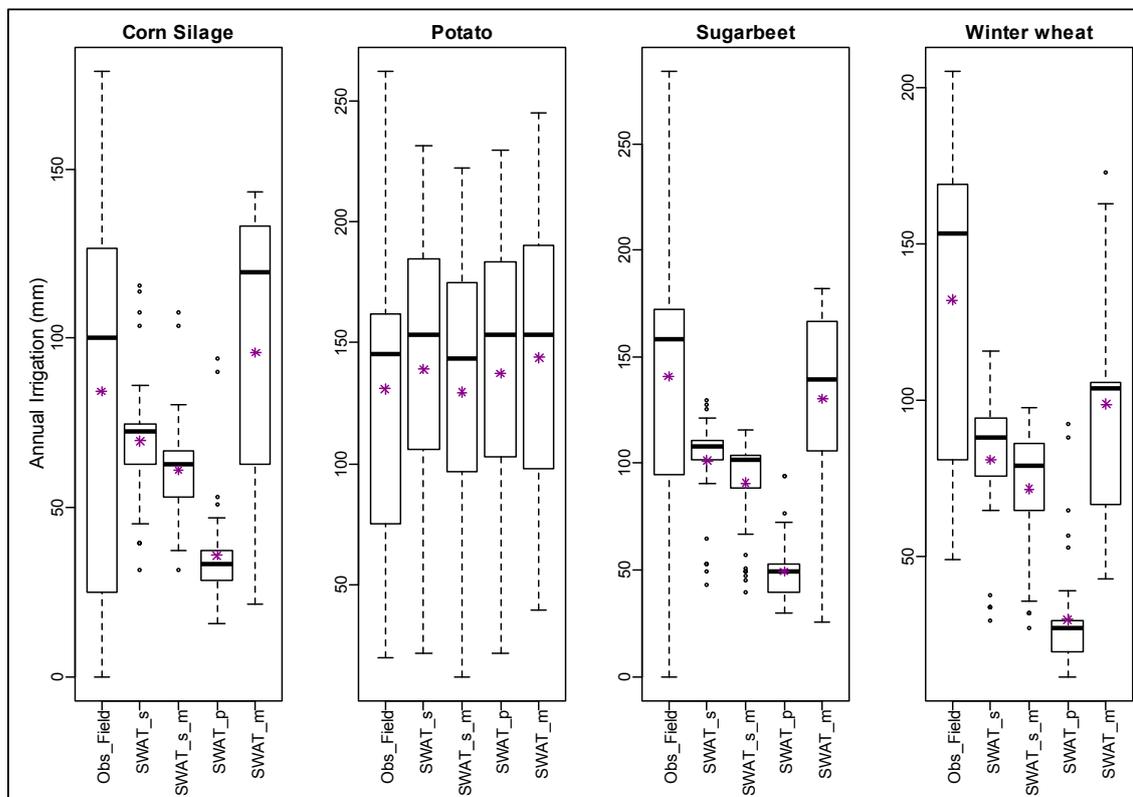

Obs_Field: denotes the observed irrigation amounts from Hamerstorf; SWAT_s: denotes the simulated irrigation amounts using SWAT model under default soil water stress irrigation scheduling method; SWAT_s_m: denotes the simulated irrigation amounts using modified SWAT model under default soil water stress irrigation scheduling method; SWAT_p: denotes the simulated irrigation amounts using SWAT model under default plant water demand irrigation scheduling method; SWAT_m: denotes the simulated irrigation amounts using modified SWAT model under modified plant water scheduling method.

Figure 5.9: Comparison of SWAT simulated irrigation with the observed irrigation amount from the experimental field.

Here, Obs_Field is used as a reference as there is no other observed data for the whole Wipperau catchment. It can be assessed from the results that although Obs_Field

cannot be directly compared with SWAT_p and SWAT_m but its overall spread and mean will provide useful insight to evaluate the modified SWAT.

Fig. 5.10 shows the annual average irrigation amounts simulated under plant water stress (SWAT_p) and soil water deficit (SWAT_s) irrigation along with the modified SWAT (SWAT_m) under plant water stress irrigation scheduling condition for Baitarani and Thubon catchments during 2000-2010. As the observed irrigation amounts are not available in these catchments, therefore, irrigation amounts simulated by model under soil water deficit condition (SWAT_s) is assumed to be close to the local conditions of the catchments by comparing the simulated irrigation amounts with the literature and expert opinions. In addition, the results reveal a clear improvement in terms of the annual average mean of irrigation amounts simulated using SWAT_m and SWAT_s models. As more water is applied in case of SWAT_m therefore it is expected that it will affect ET because more water is available for the plant to transpire. The results showed a slight increase in catchment's ET varying from 0.10 (Wipperau) to 1.10% (Baitarni) and increase in total aquifer recharge from 1.25% (Thubon) to 9.57% (Wipperau).
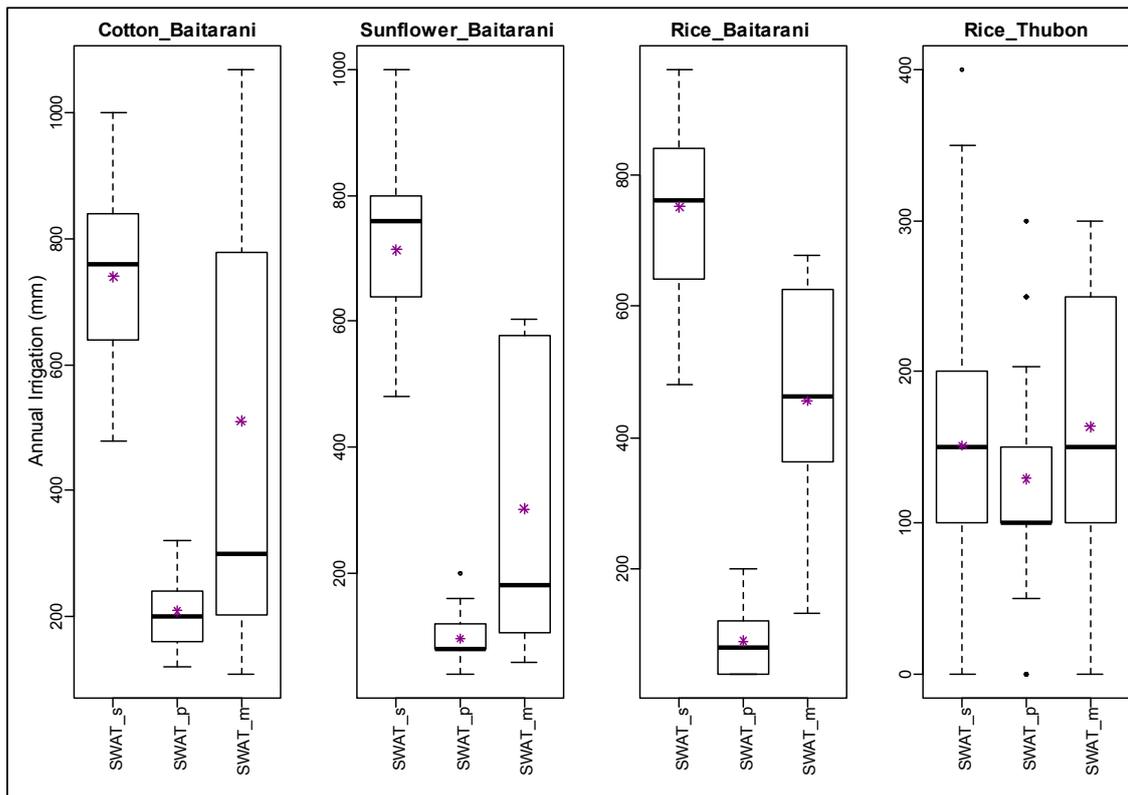
SWAT_s: denotes the simulated irrigation amounts using SWAT model under default soil water stress irrigation scheduling method; SWAT_p: denotes the simulated irrigation amounts using SWAT model under default plant water demand irrigation scheduling method; SWAT_m: denotes the simulated irrigation amounts using modified SWAT model under modified plant water scheduling method.

Figure 5.10: Comparison of SWAT simulated irrigation from Baitarani catchment, India and Thubon catchment, Vietnam during 2000-2010.

5.4 Conclusions

Irrigation scheduling methods help to improve the simulation of irrigation water demand by agro-hydrological models. The current study modified the SWAT code in improving the irrigation water demand simulated using plant water stress during 2007-2018 for an experimental site (Hamerstorf) in Lower Saxony, Germany. A field scale model (SWAP) was also used to simulate the irrigation amount and the crop yield from this experimental field. SWAP and SWAT were calibrated for simulating crop yield of corn silage, sugar beet, potato, and winter wheat. The results revealed that the calibrated models were able to simulate the annual irrigation amount and crop yield with acceptable bias. However, there is uncertainty in model parameters during calibration.

The proposed modification revealed that root density distribution and dynamic compensation factor play an important role in quantifying the plant water stress in the model during auto-irrigation mode. It can be seen from the modified SWAT model that root density distribution, soil strength, and temperature are affecting the actual root water uptake. The verification of the modified SWAT model at catchment scale was performed. It can be concluded from the results that the overall simulation of irrigation amount was improved with only a minor impact on the simulated annual yield of different crops, catchment's annual average ET and total aquifer recharge. In general, this study has provided a good insight into the process affecting auto-irrigation in the case of plant water stress condition. In addition, there is minor effect of the modified code on the soil water deficit irrigation scheduling method. Therefore, the findings of this study will help researchers to get more consistent irrigation amounts simulated by SWAT auto-irrigation scheduling techniques, and thus reduce the uncertainties associated with the simulation of irrigation water demand by SWAT, in particular when observed values are not available as it is the case for climate change predictions.

It can be seen from the results that improvement can be done in the plant growth modules used by both the models. In addition, the use of non-stationary crop parameters is encouraged as SWAP was not able to simulate crop yield in extreme years. Both the models show good capabilities of mimicking the past and current irrigation amounts but they are limited in terms of operational predictions as the weather of the season is not known a priori. This limitation can be overcome by using model parameter ensembles or by updating the model once the seasonal weather characteristics become clear.

Follow-up studies could be done to combine the SWAT subroutines modified by different authors to build new irrigation routines for the next generation of SWAT code, e.g. Chen et al. (2018) for irrigation soil water deficit scheduling under management allowed depletion. The current model distributes the same amount of water to the entire HRU area; however, this is not true in actual practice. Therefore, aspects such as model code modifications for applying non-uniform distribution of irrigation water can be part of future research. In addition, aluminum toxicity could be incorporated in the model, which authors have neglected for this study. Future research in irrigation simulation should implement model parameter uncertainty

analyses for hydrological models. In addition to that, the model uncertainty can be dealt with using the model ensemble for simulating irrigation amounts at field and catchment scale.

Acknowledgement

Chapter 6
Conclusions and Outlook

SWAT is an open-source software widely used in simulating the impact of different management practices on hydrology, sediment, fertilizer load in agricultural catchments around the world at a regional scale. Crop irrigation management is a complex and difficult task in which three questions need to be answered:
(i) How much water should be applied?
(ii) When should it be applied?
(iii) How should it be applied?

Irrigation scheduling is conventionally based on experience, soil water balance calculations, crop growth simulation models, soil water measurements, or on sensing the plant's response to water deficits using remote sensing data sets. In order to obtain this knowledge, a hydrological model should first estimate the soil moisture content satisfactorily only then a reliable irrigation water demand can be simulated by the model. With this aim, the present study first evaluated the application of SWAT in simulating soil moisture against remote sensing data and field data for two different catchments in Northern Germany and later on irrigation water demand under four different agro-climatic regions in the world (Chile, Germany, India, and Vietnam) were carried out.

For soil moisture estimation the calibrated and validated SWAT model was used to derive parameter uncertainty bands in simulating soil moisture under different soils and crops during irrigation season of 2016. The results reveal that parameter uncertainty varies with crop and soil but it frames the observed soil moisture values. However, there might be considerable model structural uncertainty due to the oversimplification of soil water equations in SWAT which uses a cascade of tipping bucket approach. In addition to this, the substantial variability in the observed soil moisture data cannot be neglected.

Landsat derived temperature, NDVI and TVDI were converted into soil moisture by using several regression models. Regression models were trained by using the TDR measurements. The best regression model in terms of mean and least overall deviation from the observed soil moisture was used for further analysis. This study reveals that in data-scarce conditions, the soil moisture extracted from Landsat could be used as a good indicator to evaluate the spatio-temporal dynamics of soil moisture simulated by using hydrological models. The observed soil moisture data from the field is necessarily required to calibrate the spatial maps obtained from the Landsat. Both soil moisture data sources have their own shortcomings. Due to time and financial constraints, observed data is available from very few moisture monitoring stations whereas, remote sensing requires clear sky on the day when the satellite is passing through the study area which is not usual in a humid climate.

There is a huge difference in the scale and resolution of soil moisture data procured from the three different sources (field, hydrological model, remote sensing) in terms of space and time. In addition to this, the SWAT model provides the

average value of soil moisture of the upper 30 cm of the soil profile, whereas TDR gives the average soil moisture value for approximately the upper 16 cm of the soil profile. However, Landsat provides soil moisture of the top few centimeters of the soil profile only. In addition, this study found that the Landsat images could be used to modify the SWAT soil parameters by investigating a consistent behavior of spatial soil moisture patterns. The modification was confirmed by a higher resolution soil map and by field investigations. Furthermore, using the results of this analysis, the hydrological model can be rectified and applied with higher confidence in simulating soil moisture. This research has helped to improve the knowledge about large scale spatio-temporal dynamics of soil moisture at finer resolution in a humid country. It could be beneficial for arid or semi-arid countries as the number of days with clear sky throughout the year is higher, and there is irrigation demand during the entire growing season. This is further verified by the spread and behavior of soil moisture which is better matching during the dry season from all the sources in this study. Additionally, the Landsat extracted soil moisture can also be used for recalibrating the hydrological model with the aim of reducing uncertainty in simulated soil moisture estimates.

For Irrigation water demand, the SWAT model was evaluated for simulating irrigation water requirement in four different agro-climatic catchments around the world (Chile, Germany, India, and Vietnam). Modelling results revealed that the SWAT model was calibrated with good model efficiency (low bias) for streamflow with low percentage deviation in ET in all the cases. Two different irrigation scheduling techniques were used to simulate irrigation water demand simulated by SWAT namely soil water deficit and plant water stress. The automatic irrigation provided plausible results for soil water deficit irrigation scheduling in all the catchments with optimal and deficit strategies even if there was no comparison with observed values on that scale. There are indications that irrigation shows systematic overestimation though. Plant water stress scheduling shows significant underestimation of irrigation water requirement in all catchments. This can be justified by less plant water stress days. It can be concluded from the results that SWAT's mechanism for irrigation scheduling can be further improved.

The effect of reanalysis climate data on different water balance components was also evaluated for the four catchments. It was seen from the results that different climate variables form NCEP and ERA exhibit different behaviors in a given catchment. Bias-corrected rainfall, temperature, and solar radiation datasets are more close to their observed counterparts than the uncorrected datasets. The model simulation with bias-corrected reanalysis data showed that the input weather is highly sensitive to streamflow and irrigation simulated by the model. Unbiased reanalysis data led to serious bias in the estimated ET and irrigation requirement. Results showed that it is worth correcting the bias of the other climate variables as rainfall is not always the governing variable in irrigation simulation. As climate reanalysis data are uncertain, an attempt has been made to check it via quantile mapping but still there is an acceptable bias in the quantile corrected reanalysis data. The results strongly favour the use of bias-corrected data in hydrological modelling studies. It can be concluded that in hydrological modelling not only the input data but also its variability plays an important role. Therefore, climate change and adaptation

studies must take this into account.

It was concluded from the previous study that SWAT needs modification in its plant water demand irrigation scheduling technique. There was a gap in the irrigation water amounts simulated by SWAT for some crops varying from 2-4 times more in case of soil water deficit compared to the plant water stress (especially for Wipperau and Ilmenau, Germany). Therefore, the SWAT code was modified to improve the irrigation water demand simulated using plant water stress during 2007-2018 for an experimental site (Hamerstorf) in Lower Saxony, Germany. A field scale model, SWAP was also used to simulate the irrigation amount and the crop yield from this experimental field. Both the models were calibrated for simulating crop yield. The results revealed that the calibrated models were satisfactorily able to simulate the annual irrigation amount and crop yield. However, the model parameter uncertainty still persisted during calibration.

The proposed modification revealed that root density distribution and dynamic compensation factor play an important role in quantifying the plant water stress in the model during auto-irrigation mode. It can be seen from the modified SWAT model that root density distribution, soil strength, and temperature are affecting the actual root water uptake. The verification of the modified SWAT model to a catchment scale model was performed. It can be concluded from the results that the overall simulation of irrigation amount was improved with no or minor impact on the annual yield of different crops, catchment's annual average ET and total aquifer recharge. In general, this study has provided a good insight into the process affecting auto-irrigation in the case of plant water stress condition. In, addition, there is a minor effect of modified code on the other irrigation scheduling technique in SWAT, i.e., soil water deficit. Therefore, the findings of this study will help researchers to get more consistent irrigation amounts simulated by both auto-irrigation scheduling techniques. This will reduce the uncertainties associated with the simulation of irrigation water demand by SWAT, in particular when observed values are not available as it is the case for climate change predictions.

The aforementioned studies confirm that the application of SWAT for regional irrigation studies is of high importance for water resource management. With today's improved data availability and computing power, models like SWAT might fill a gap between field scale models as often used in agriculture and large scale models, whose results have been questioned in other studies due to their large bias when evaluated on smaller scales. In case of soil moisture estimation, further research could be done to improve the level of precision in terms of depth. This would involve extended modelling as well as soil moisture measurement at the field scale. SWAT also provides daily estimates of soil moisture at finer resolution, which can be used for continuous simulation and forecasting of soil moisture. Possible fields of application are planning and design of large scale irrigation systems and irrigation control schemes, investigations about the impact of climate change on soil moisture and irrigation scheduling. In addition, after reliable irrigation estimates at regional and field scale, further research is needed to upscale crop yield and irrigation water demand for improving the global and regional water management. Different follow-up studies could be done to combine the

SWAT subroutines modified by different authors to build new irrigation routines for the next generation of SWAT code. In addition, the application of non-uniform distribution of irrigation water can be part of future research.

To secure a more complete picture of future water vulnerabilities, it is necessary to consider the interactions among climate change and variability, surface and groundwater hydrology, water engineering, and human systems, including societal adaptations to water scarcity. However, to enable crop models to be more useful in understanding adaptations such as irrigation or crop insurance, crop models need improvement in regards to their estimates of crop water use. There is a need to rethink, how we can achieve more crop per drop. Including the effects of inter-annual variability in meteorological forcing on soil moisture variability might be subject of future research. In addition, to be more specific the use of non-stationary crop parameters is encouraged as SWAP was not able to simulate crop yield in extreme years. Both the models show good capabilities of mimicking the past and current irrigation amounts but they are limited in terms of operational predictions as the weather is unknown. This limitation can be overcome by using model parameter ensembles or by updating the model once the seasonal weather characteristics become clear. Improved understanding of these processes is needed for the transformation of point-scale measurements and parameters to scales required for regional scale hydrological modeling. As there is considerable uncertainty in absolute irrigation water demand simulated by hydrological models (Webber et al., 2016), an ensemble modelling approach will be beneficial in simulating the overall variability. The parameter, model structural uncertainty, weather and soil data uncertainty should be taken into consideration while simulating irrigation water demand and soil moisture using hydrological models. This will help researchers to address uncertainties in irrigation prediction at regional scale e.g., in the context of climate change prediction or regional irrigation consulting. The findings of the three studies and the follow-up studies can also be used for predicting and monitoring agricultural droughts at a regional scale. Another benefit of using remote sensing estimates of soil moisture is its ability to characterize drought.

Bibliography

Abbaspour, K. C. (2011). Swat-cup4: Swat calibration and uncertainty programs–a user manual. *Swiss Federal Institute of Aquatic Science and Technology, Eawag.*

Abbaspour, K. C., Rouholahnejad, E., Vaghefi, S., Srinivasan, R., Yang, H., and Kløve, B. (2015). A continental-scale hydrology and water quality model for europe: Calibration and uncertainty of a high-resolution large-scale swat model. *Journal of Hydrology*, 524:733–752.

Abrahamsen, P. and Hansen, S. (2000). Daisy: an open soil-crop-atmosphere system model. *Environmental modelling & software*, 15(3):313–330.

Al-Najar, H. (2011). The integration of fao-cropwat model and gis techniques for estimating irrigation water requirement and its application in the gaza strip. *Natural Resources*, 2(03):146.

Albasha, R., Mailhol, J.-C., and Cheviron, B. (2015). Compensatory uptake functions in empirical macroscopic root water uptake models–experimental and numerical analysis. *Agricultural Water Management*, 155:22–39.

Alemayehu, T., Griensven, A. v., Woldegiorgis, B. T., and Bauwens, W. (2017). An improved swat vegetation growth module and its evaluation for four tropical ecosystems. *Hydrology and Earth System Sciences*, 21(9):4449–4467.

Allen, R., Irmak, A., Trezza, R., Hendrickx, J. M., Bastiaanssen, W., and Kjaersgaard, J. (2011). Satellite-based et estimation in agriculture using sebal and metric. *Hydrological Processes*, 25(26):4011–4027.

Allen, R. G., Pereira, L. S., Raes, D., Smith, M., et al. (1998). Crop evapotranspiration-guidelines for computing crop water requirements-fao irrigation and drainage paper 56. *Fao, Rome*, 300(9):D05109.

Andarzian, B., Bannayan, M., Steduto, P., Mazraeh, H., Barati, M., Barati, M., and Rahnama, A. (2011). Validation and testing of the aquacrop model under full and deficit irrigated wheat production in iran. *Agricultural Water Management*, 100(1):1–8.

Arnold, J., Allen, P., Muttiah, R., and Bernhardt, G. (1995). Automated base flow separation and recession analysis techniques. *Groundwater*, 33(6):1010–1018.

Arnold, J., Bieger, K., White, M., Srinivasan, R., Dunbar, J., and Allen, P. (2018). Use of decision tables to simulate management in swat+. *Water*, 10(6):713.

Arnold, J. G., Moriasi, D. N., Gassman, P. W., Abbaspour, K. C., White, M. J., Srinivasan, R., Santhi, C., Harmel, R., Van Griensven, A., Van Liew, M. W., and Kannan, N. (2012). Swat: Model use, calibration, and validation. *Transactions of the ASABE*, 55(4):1491–1508.

Arnold, J. G., Srinivasan, R., Muttiah, R. S., and Williams, J. R. (1998). Large area hydrologic modeling and assessment part i: model development 1. *JAWRA Journal of the American Water Resources Association*, 34(1):73–89.

Barr, A. G., Kite, G., Granger, R., and Smith, C. (1997). Evaluating three evapotranspiration methods in the slurp macroscale hydrological model. *Hydrological processes*, 11(13):1685–1705.

Bastiaanssen, W. G., Menenti, M., Feddes, R., and Holtslag, A. (1998). A remote sensing surface energy balance algorithm for land (sebal). 1. formulation. *Journal of hydrology*, 212:198–212.

Bastiaanssen, W. G., Molden, D. J., and Makin, I. W. (2000). Remote sensing for irrigated agriculture: examples from research and possible applications. *Agricultural water management*, 46(2):137–155.

Bastola, S. and Misra, V. (2014). Evaluation of dynamically downscaled reanalysis precipitation data for hydrological application. *Hydrological Processes*, 28(4):1989–2002.

Bell, K. R., Blanchard, B., Schmugge, T., and Witczak, M. (1980). Analysis of surface moisture variations within large-field sites. *Water Resources Research*, 16(4):796–810.

Beven, K. (1995). Linking parameters across scales: subgrid parameterizations and scale dependent hydrological models. *Hydrological Processes*, 9(5-6):507–525.

Beven, K. and Binley, A. (1992). The future of distributed models: model calibration and uncertainty prediction. *Hydrological processes*, 6(3):279–298.

Boons-Prins, E., De Koning, G., and Van Diepen, C. (1993). Crop-specific simulation parameters for yield forecasting across the european community. Technical report, CABO-DLO [etc.].

Brocca, L., Melone, F., Moramarco, T., and Morbidelli, R. (2009). Antecedent wetness conditions based on ers scatterometer data. *Journal of Hydrology*, 364(1-2):73–87.

Brocca, L., Melone, F., Moramarco, T., Wagner, W., Naeimi, V., Bartalis, Z., and Hasenauer, S. (2010). Improving runoff prediction through the assimilation of the ascat soil moisture product. *Hydrology and Earth System Sciences*, 14(10):1881–1893.

Bruinsma, J. (2017). *World agriculture: towards 2015/2030: an FAO study.* Routledge.

Bryant, K., Benson, V., Kiniry, J., Williams, J., and Lacewell, R. (1992). Simulating corn yield response to irrigation timings: Validation of the epic model. *Journal of Production Agriculture*, 5(2):237–242.

Cabelguenne, M., Debaeke, P., Puech, J., and Bosc, N. (1997). Real time irrigation management using the epic-phase model and weather forecasts. *Agricultural water management*, 32(3):227–238.

Carlson, T. N., Gillies, R. R., and Perry, E. M. (1994). A method to make use of thermal infrared temperature and ndvi measurements to infer surface soil water content and fractional vegetation cover. *Remote sensing reviews*, 9(1-2):161–173.

Carlson, T. N., Gillies, R. R., and Schmugge, T. J. (1995). An interpretation of methodologies for indirect measurement of soil water content. *Agricultural and forest meteorology*, 77(3-4):191–205.

Chen, F., Crow, W. T., Starks, P. J., and Moriasi, D. N. (2011). Improving hydrologic predictions of a catchment model via assimilation of surface soil moisture. *Advances in Water Resources*, 34(4):526–536.

Chen, H., Zhang, W., Wang, K., and Fu, W. (2010). Soil moisture dynamics under different land uses on karst hillslope in northwest guangxi, china. *Environmental Earth Sciences*, 61(6):1105–1111.

Chen, Y., Marek, G., Marek, T., Brauer, D., and Srinivasan, R. (2017). Assessing the efficacy of the swat auto-irrigation function to simulate irrigation, evapotranspiration, and crop response to management strategies of the texas high plains. *Water*, 9(7):509.

Chen, Y., Marek, G., Marek, T., Gowda, P., Xue, Q., Moorhead, J., Brauer, D., Srinivasan, R., and Heflin, K. (2019). Multisite evaluation of an improved swat irrigation scheduling algorithm for corn (zea mays l.) production in the us southern great plains. *Environmental Modelling & Software*, 118:23–34.

Chen, Y., Marek, G. W., Marek, T., Brauer, D. K., and Srinivasan, R. (2018). Improving swat auto-irrigation functions for simulating agricultural irrigation management using long-term lysimeter field data. *Environmental modelling & software*, 99:25–38.

Christensen, J. H., Boberg, F., Christensen, O. B., and Lucas-Picher, P. (2008). On the need for bias correction of regional climate change projections of temperature and precipitation. *Geophysical Research Letters*, 35(20).

Conrad, C., Colditz, R. R., Dech, S., Klein, D., and Vlek, P. L. (2011). Temporal segmentation of modis time series for improving crop classification in central asian irrigation systems. *International Journal of Remote Sensing*, 32(23):8763–8778.

Corradini, C. (2014). Soil moisture in the development of hydrological processes and its determination at different spatial scales. *Journal of Hydrology*, 516:1–5.

Cuenca, R., Ciotti, S., and Hagimoto, Y. (2013). Application of landsat to evaluate effects of irrigation forbearance. *Remote Sensing*, 5(8):3776–3802.

Danner, C. L., McKinney, D. C., Teasley, R. L., and Sandoval-Solis, S. (2006). Documentation and testing of the weap model for the rio grande/bravo basin. Technical report, Center for Research in Water Resources, University of Texas at Austin.

De Jong van Lier, Q., Van Dam, J., Metselaar, K., De Jong, R., and Duijnisveld, W. (2008). Macroscopic root water uptake distribution using a matric flux potential approach. *Vadose Zone Journal*, 7(3):1065–1078.

de Willigen, P., van Dam, J. C., Javaux, M., and Heinen, M. (2012). Root water uptake as simulated by three soil water flow models. *Vadose Zone Journal*, 11(3).

Dechmi, F., Burguete, J., and Skhiri, A. (2012). Swat application in intensive irrigation systems: Model modification, calibration and validation. *Journal of Hydrology*, 470:227–238.

Dee, D. P., Uppala, S., Simmons, A., Berrisford, P., Poli, P., Kobayashi, S., Andrae, U., Balmaseda, M., Balsamo, G., Bauer, d. P., et al. (2011). The era-interim reanalysis: Configuration and performance of the data assimilation system. *Quarterly Journal of the royal meteorological society*, 137(656):553–597.

DeLiberty, T. L. and Legates, D. R. (2003). Interannual and seasonal variability of modelled soil moisture in oklahoma. *International Journal of Climatology: A Journal of the Royal Meteorological Society*, 23(9):1057–1086.

Diaz, J. R., Weatherhead, E., Knox, J., and Camacho, E. (2007). Climate change impacts on irrigation water requirements in the guadalquivir river basin in spain. *Regional Environmental Change*, 7(3):149–159.

Doorenbos, J. and Pruitt, W. (1977). 0.(1977). guidelines for predicting crop water requirements. *FAO Irrigation and Drainage Paper*, 24:15–20.

Droogers, P. and Bastiaanssen, W. (2002). Irrigation performance using hydrological and remote sensing modeling. *Journal of Irrigation and Drainage Engineering*, 128(1):11–18.

Droogers, P. and Kite, G. (2002). Remotely sensed data used for modelling at different hydrological scales. *Hydrological Processes*, 16(8):1543–1556.

Dubey, S. K. and Sharma, D. (2018). Assessment of climate change impact on yield of major crops in the banas river basin, india. *Science of The Total Environment*, 635:10–19.

Eavis, B. (1972). Soil physical conditions affecting seedling root growth. *Plant and soil*, 36(1-3):613–622.

Eitzinger, J., Trnka, M., Hösch, J., Žalud, Z., and Dubrovskỳ, M. (2004). Comparison of ceres, wofost and swap models in simulating soil water content during growing season under different soil conditions. *Ecological Modelling*, 171(3):223–246.

Elliott, J., Deryng, D., Müller, C., Frieler, K., Konzmann, M., Gerten, D., Glotter, M., Flörke, M., Wada, Y., Best, N., Eisner, S., Fekete, B. M., Folberth, C., Foster, I., Gosling, S. N., Haddeland, I., Khabarov, N., Ludwig, F., Masaki, Y., Olin, S., Rosenweig, A. C., Satoh, Y., Schmid, E., Stacke, T., Tang, Q., and Dominik, W. (2014). Constraints and potentials of future irrigation water availability on agricultural production under climate change. *Proceedings of the National Academy of Sciences*, 111(9):3239–3244.

Entekhabi, D., Njoku, E. G., O'Neill, P. E., Kellogg, K. H., Crow, W. T., Edelstein, W. N., Entin, J. K., Goodman, S. D., Jackson, T. J., Johnson, J., et al. (2010). The soil moisture active passive (smap) mission. *Proceedings of the IEEE*, 98(5):704–716.

Essou, G. R., Brissette, F., and Lucas-Picher, P. (2017). Impacts of combining reanalyses and weather station data on the accuracy of discharge modelling. *Journal of hydrology*, 545:120–131.

Esteve, P., Varela-Ortega, C., Blanco-Gutiérrez, I., and Downing, T. E. (2015). A hydro-economic model for the assessment of climate change impacts and adaptation in irrigated agriculture. *Ecological Economics*, 120:49–58.

Fang, Q., Ma, L., Yu, Q., Ahuja, L., Malone, R., and Hoogenboom, G. (2010). Irrigation strategies to improve the water use efficiency of wheat–maize double cropping systems in north china plain. *Agricultural Water Management*, 97(8):1165–1174.

Feddes, R. A. (1982). *Simulation of field water use and crop yield*. Pudoc.

Feddes, R. A., Hoff, H., Bruen, M., Dawson, T., De Rosnay, P., Dirmeyer, P., Jackson, R. B., Kabat, P., Kleidon, A., Lilly, A., and Pitman, A. J. (2001). Modeling root water uptake in hydrological and climate models. *Bulletin of the American meteorological society*, 82(12):2797–2810.

Feng, Z., Liu, D., and Zhang, Y. (2007). Water requirements and irrigation scheduling of spring maize using gis and cropwat model in beijing-tianjin-hebei region. *Chinese Geographical Science*, 17(1):56–63.

Firoz, A., Nauditt, A., Fink, M., and Ribbe, L. (2018). Quantifying human impacts on hydrological drought using a combined modelling approach in a tropical river basin in central vietnam. *Hydrology and Earth System Sciences*, 22(1):547.

Foley, J. A., Ramankutty, N., Brauman, K. A., Cassidy, E. S., Gerber, J. S., Johnston, M., Mueller, N. D., O'Connell, C., Ray, D. K., and West, P. C. (2011). Solutions for a cultivated planet. *Nature*, 478(7369):337.

Fricke, E. and Riedel, A. (2016). Versuchsbericht 2016. *Fachverband Feldbewässerung, Uelzen*, pages 1–8.

Fu, Q., Yang, L., Li, H., Li, T., Liu, D., Ji, Y., Li, M., and Zhang, Y. (2019). Study on the optimization of dry land irrigation schedule in the downstream songhua river basin based on the swat model. *Water*, 11(6):1147.

García-Vila, M. and Fereres, E. (2012). Combining the simulation crop model aquacrop with an economic model for the optimization of irrigation management at farm level. *European Journal of Agronomy*, 36(1):21–31.

Gardner, W. and Kirkham, D. (1952). Determination of soil moisture by neutron scattering. *Soil Science*, 73(5):391–402.

Geerts, S. and Raes, D. (2009). Deficit irrigation as an on-farm strategy to maximize crop water productivity in dry areas. *Agricultural Water Management*, 96(9):1275 – 1284.

George, B., Shende, S., and Raghuwanshi, N. (2000). Development and testing of an irrigation scheduling model. *Agricultural water management*, 46(2):121–136.

Gharbia, S. S., Smullen, T., Gill, L., Johnston, P., and Pilla, F. (2018). Spatially distributed potential evapotranspiration modeling and climate projections. *Science of the Total Environment*, 633:571–592.

Gheysari, M., Mirlatifi, S. M., Homaee, M., Asadi, M. E., and Hoogenboom, G. (2009). Nitrate leaching in a silage maize field under different irrigation and nitrogen fertilizer rates. *Agricultural water management*, 96(6):946–954.

Githui, F., Thayalakumaran, T., and Selle, B. (2016). Estimating irrigation inputs for distributed hydrological modelling: a case study from an irrigated catchment in southeast australia. *Hydrological processes*, 30(12):1824–1835.

Glenn, E. P., Doody, T. M., Guerschman, J. P., Huete, A. R., King, E. A., McVicar, T. R., Van Dijk, A. I., Van Niel, T. G., Yebra, M., and Zhang, Y. (2011). Actual evapotranspiration estimation by ground and remote sensing methods: the australian experience. *Hydrological Processes*, 25(26):4103–4116.

Godwin, D. (1990). *A user's guide to CERES Wheat, V2. 10*, volume 2. International Fertilizer Development Center.

Goetz, S. (1997). Multi-sensor analysis of ndvi, surface temperature and biophysical variables at a mixed grassland site. *International Journal of remote sensing*, 18(1):71–94.

Grayson, R. B. and Western, A. W. (1998). Towards areal estimation of soil water content from point measurements: time and space stability of mean response. *Journal of Hydrology*, 207(1-2):68–82.

Griensven, A. v., Ndomba, P., Yalew, S., and Kilonzo, F. (2012). Critical review of swat applications in the upper nile basin countries. *Hydrology and Earth System Sciences*, 16(9):3371–3381.

Groenendijk, P., Boogaard, H., Heinen, M., Kroes, J., Supit, I., and de Wit, A. (2016). Simulation nitrogen-limited crop growth with swap/wofost: process descriptions and user manual. Technical report, Wageningen Environmental Research.

Gruhier, C., Rosnay, P. d., Hasenauer, S., Holmes, T., De Jeu, R., Kerr, Y., Mougin, E., Njoku, E., Timouk, F., Wagner, W., and Zribi, M. (2009). Soil moisture active and passive microwave products: intercomparison and evaluation over a sahelian site. *Hydrology and Earth System Sciences*.

Gupta, H. V., Kling, H., Yilmaz, K. K., and Martinez, G. F. (2009). Decomposition of the mean squared error and nse performance criteria: Implications for improving hydrological modelling. *Journal of hydrology*, 377(1-2):80–91.

Gurr, C. (1962). Use of gamma rays in measuring water content and permeability in unsaturated columns of soil. *Soil Science*, 94(4):224–229.

Hai, L. T. (2003). The organization of the liberalized rice market in vietnam.

Han, E., Merwade, V., and Heathman, G. C. (2012). Implementation of surface soil moisture data assimilation with watershed scale distributed hydrological model. *Journal of hydrology*, 416:98–117.

Hansen, S., Abrahamsen, P., Petersen, C. T., and Styczen, M. (2012). Daisy: Model use, calibration, and validation. *Transactions of the ASABE*, 55(4):1317–1333.

He, J., Cai, H., and Bai, J. (2013). Irrigation scheduling based on ceres-wheat model for spring wheat production in the minqin oasis in northwest china. *Agricultural Water Management*, 128:19–31.

Heng, L. K., Hsiao, T., Evett, S., Howell, T., and Steduto, P. (2009). Validating the fao aquacrop model for irrigated and water deficient field maize. *Agronomy Journal*, 101(3):488–498.

Henriksen, H. J., Troldborg, L., Nyegaard, P., Sonnenborg, T. O., Refsgaard, J. C., and Madsen, B. (2003). Methodology for construction, calibration and validation of a national hydrological model for denmark. *Journal of Hydrology*, 280(1-4):52–71.

Houngbo, G. F. (2018). The united nations world water development report 2018: nature-based solutions for water.

Houser, P. R., Shuttleworth, W. J., Famiglietti, J. S., Gupta, H. V., Syed, K. H., and Goodrich, D. C. (1998). Integration of soil moisture remote sensing and hydrologic modeling using data assimilation. *Water Resources Research*, 34(12):3405–3420.

Huisman, J. A., Hubbard, S. S., Redman, J. D., and Annan, A. P. (2003). Measuring soil water content with ground penetrating radar. *Vadose Zone Journal*, 2(4):476–491.

Hundal, S. S. and Kaur, P. (1997). Application of the ceres-wheat model to yield predictions in the irrigated plains of the indian punjab. *The Journal of Agricultural Science*, 129(1):13–18.

Hwang, S., Graham, W. D., Geurink, J. S., and Adams, A. (2014). Hydrologic implications of errors in bias-corrected regional reanalysis data for west central florida. *Journal of hydrology*, 510:513–529.

Iglesias, A., Rosenzweig, C., and Pereira, D. (2000). Agricultural impacts of climate change in spain: developing tools for a spatial analysis. *Global Environmental Change*, 10(1):69–80.

Jackson, T. J. (1993). Iii. measuring surface soil moisture using passive microwave remote sensing. *Hydrological Processes*, 7(2):139–152.

Jackson, T. J., Chen, D., Cosh, M., Li, F., Anderson, M., Walthall, C., Doriaswamy, P., and Hunt, E. R. (2004). Vegetation water content mapping using landsat data derived normalized difference water index for corn and soybeans. *Remote Sensing of Environment*, 92(4):475–482.

Jarvis, N. (1989). A simple empirical model of root water uptake. *Journal of Hydrology*, 107(1-4):57–72.

Jarvis, N. (2011). Simple physics-based models of compensatory plant water uptake: Concepts and eco-hydrological consequences. *Hydrology and Earth System Sciences*, 15(11):3431–3446.

Jensen, C. R., Battilani, A., Plauborg, F., Psarras, G., Chartzoulakis, K., Janowiak, F., Stikic, R., Jovanovic, Z., Li, G., Qi, X., Liu, F., Jacobsen, S., and Andersen, M. N. (2010). Deficit irrigation based on drought tolerance and root signalling in potatoes and tomatoes. *Agricultural Water Management*, 98(3):403–413.

Jha, M. K. (2012). Quantifying soil moisture distribution at a watershed scale. In *Soil Health and Land Use Management*. IntechOpen.

Jiang, J., Feng, S., Huo, Z., Zhao, Z., and Jia, B. (2011). Application of the swap model to simulate water–salt transport under deficit irrigation with saline water. *Mathematical and Computer Modelling*, 54(3):902–911.

Jiang, Y., Xu, X., Huang, Q., Huo, Z., and Huang, G. (2015). Assessment of irrigation performance and water productivity in irrigated areas of the middle heihe river basin using a distributed agro-hydrological model. *Agricultural water management*, 147:67–81.

Jiang, Y., Xu, X., Huang, Q., Huo, Z., and Huang, G. (2016a). Optimizing regional irrigation water use by integrating a two-level optimization model and an agro-hydrological model. *Agricultural water management*, 178:76–88.

Jiang, Y., Zhang, L., Zhang, B., He, C., Jin, X., and Bai, X. (2016b). Modeling irrigation management for water conservation by dssat-maize model in arid northwestern china. *Agricultural Water Management*, 177:37–45.

Joh, H.-K., Lee, J.-W., Park, M.-J., Shin, H.-J., Yi, J.-E., Kim, G.-S., Srinivasan, R., and Kim, S.-J. (2011). Assessing climate change impact on hydrological components of a small forest watershed through swat calibration of evapotranspiration and soil moisture. *Transactions of the ASABE*, 54(5):1773–1781.

Jones, J., Hoogenboom, G., Porter, C., Boote, K., Batchelor, W., Hunt, L., and Ritchie, J. (2003). The dssat cropping system model european journal of agronomy.

Joshi, P. and Agnihotri, A. (1984). An assessment of the adverse effects of canal irrigation in india. *Indian Journal of Agricultural Economics*, 39(902-2018-2320).

Kadiresan, K. and Khanal, P. R. (2018). Rethinking irrigation for global food security. *Irrigation and drainage*, 67(1):8–11.

Kalma, J., Bates, B., and Woods, R. (1995). Predicting catchment-scale soil moisture status with limited field measurements. *Hydrological processes*, 9(3-4):445–467.

Karuku, G., Gachene, C., Karanja, N., Cornelis, W., and Verplancke, H. (2014). Use of cropwat model to predict water use in irrigated tomato production at kabete, kenya. *E. Afr. agric. For. J.(2014)*, 80(3):175–183.

Kim, N. W. and Lee, J. (2010). Enhancement of the channel routing module in swat. *Hydrological Processes: An International Journal*, 24(1):96–107.

Kite, G. (1998). Manual for the slurp hydrological model. *NHRI, saskatoon, Canada*.

Kite, G. and Droogers, P. (2000). Comparing evapotranspiration estimates from satellites, hydrological models and field data. *Journal of Hydrology*, 229(1-2):3–18.

Kroes, J., Van Dam, J., Groenendijk, P., Hendriks, R., and Jacobs, C. (2009). Swap version 3.2. theory description and user manual. Technical report, Alterra.

Lam, Q., Schmalz, B., and Fohrer, N. (2011). The impact of agricultural best management practices on water quality in a north german lowland catchment. *Environmental monitoring and assessment*, 183(1-4):351–379.

Leroux, D. J., Pellarin, T., Vischel, T., Cohard, J.-M., Gascon, T., Gibon, F., Mialon, A., Galle, S., Peugeot, C., and Seguis, L. (2016). Assimilation of smos soil moisture into a distributed hydrological model and impacts on the water cycle variables over the ouémé catchment in benin. *Hydrology and Earth System Sciences*, 20(7):2827–2840.

Li, D., Liang, Z., Li, B., Lei, X., and Zhou, Y. (2019). Multi-objective calibration of mike she with smap soil moisture datasets. *Hydrology Research*, 50(2):644–654.

Li, K., Boisvert, J., and Jong, R. D. (1999). An exponential root-water-uptake model. *Canadian Journal of soil science*, 79(2):333–343.

Li, K., De Jong, R., Boisvert, J., and Stott, D. (2001). Comparison of root-water-uptake models. In *Sustaining the Global Farm: Selected Papers from the 10th Int. Soil Conservation Organization Meeting*, pages 1112–1117. Purdue University and USDA-ARS National Soil Erosion Research Laboratory . . . .

Li, M., Ma, Z., and Du, J. (2010). Regional soil moisture simulation for shaanxi province using swat model validation and trend analysis. *Science China Earth Sciences*, 53(4):575–590.

Li, S., Liang, W., Zhang, W., and Liu, Q. (2016). Response of soil moisture to hydro-meteorological variables under different precipitation gradients in the yellow river basin. *Water resources management*, 30(6):1867–1884.

Liang, H., Hu, K., Batchelor, W. D., Qi, Z., and Li, B. (2016). An integrated soil-crop system model for water and nitrogen management in north china. *Scientific reports*, 6:25755.

Liding, C., Zhilin, H., Jie, G., Fu, B., and Huang, Y. (2007). The effect of land cover/vegetation on soil water dynamic in the hilly area of the loess plateau. *China*, 70(2):200–208.

Liu, J., Williams, J. R., Zehnder, A. J., and Yang, H. (2007). Gepic–modelling wheat yield and crop water productivity with high resolution on a global scale. *Agricultural systems*, 94(2):478–493.

Lobell, D. B. and Ortiz-Monasterio, J. I. (2006). Evaluating strategies for improved water use in spring wheat with ceres. *Agricultural water management*, 84(3):249–258.

López, P. L., Sutanudjaja, E. H., Schellekens, J., Sterk, G., and Bierkens, M. F. (2017). Calibration of a large-scale hydrological model using satellite-based soil moisture and evapotranspiration products. *Hydrology and Earth System Sciences*, 21(6):3125–3144.

Loukas, A. and Vasiliades, L. (2014). Streamflow simulation methods for ungauged and poorly gauged watersheds. *Natural Hazards and Earth System Sciences*, 14(7):1641–1661.

Ma, Y., Feng, S., Huo, Z., and Song, X. (2011). Application of the swap model to simulate the field water cycle under deficit irrigation in beijing, china. *Mathematical and Computer Modelling*, 54(3-4):1044–1052.

Maier, N. and Dietrich, J. (2016). Using swat for strategic planning of basin scale irrigation control policies: a case study from a humid region in northern germany. *Water Resources Management*, 30(9):3285–3298.

Mapfumo, E., Chanasyk, D. S., and Willms, W. D. (2004). Simulating daily soil water under foothills fescue grazing with the soil and water assessment tool model (alberta, canada). *Hydrological processes*, 18(15):2787–2800.

Marek, G. W., Gowda, P. H., Evett, S. R., Baumhardt, R. L., Brauer, D. K., Howell, T. A., Marek, T. H., and Srinivasan, R. (2016). Estimating evapotranspiration for dryland cropping systems in the semiarid texas high plains using swat. *JAWRA Journal of the American Water Resources Association*, 52(2):298–314.

Marek, G. W., Gowda, P. H., Marek, T. H., Porter, D. O., Baumhardt, R. L., and Brauer, D. K. (2017). Modeling long-term water use of irrigated cropping rotations in the texas high plains using swat. *Irrigation Science*, 35(2):111–123.

Maxmen, A. (2018). As cape town water crisis deepens, scientists prepare for'day zero'. *Nature*, 554(7690).

McInerney, D., Mark, T., Dmitri, K., Faith, G., Thabo, T., Min, L., and George, K. (2018). The importance of spatiotemporal variability in irrigation inputs for hydrological modeling of irrigated catchments. *Water Resources Research*, 54(9):6792–6821.

Mehta, V. K., Haden, V. R., Joyce, B. A., Purkey, D. R., and Jackson, L. E. (2013). Irrigation demand and supply, given projections of climate and land-use change, in yolo county, california. *Agricultural water management*, 117:70–82.

Meinardus, A., Griggs, R., Benson, V., and Williams, J. (2001). Epic. the texas a&m blackland research and extension center, temple, tx.

Meyles, E., Williams, A., Ternan, L., and Dowd, J. (2003). Runoff generation in relation to soil moisture patterns in a small dartmoor catchment, southwest england. *Hydrological Processes*, 17(2):251–264.

Milzow, C., Krogh, P. E., and Bauer-Gottwein, P. (2011). Combining satellite radar altimetry, sar surface soil moisture and grace total storage changes for hydrological model calibration in a large poorly gauged catchment. *Hydrology and Earth System Sciences*, 15(6):1729–1743.

Mohanty, B. P., Skaggs, T. H., and Famiglietti, J. S. (2000). Analysis and mapping of field-scale soil moisture variability using high-resolution, ground-based data during the southern great plains 1997 (sgp97) hydrology experiment. *Water Resources Research*, 36(4):1023–1031.

Molden, D. (2013). *Water for food water for life: A comprehensive assessment of water management in agriculture.* Earthscan, London, U.K.

Monteith, N. and Banath, C. (1965). The effect of soil strength on sugarcane root growth. *Trop. Agric*, 42:293–296.

Moran, M., Clarke, T., Inoue, Y., and Vidal, A. (1994). Estimating crop water deficit using the relation between surface-air temperature and spectral vegetation index. *Remote sensing of environment*, 49(3):246–263.

Moriasi, D. N., Arnold, J. G., Van Liew, M. W., Bingner, R. L., Harmel, R. D., and Veith, T. L. (2007). Model evaluation guidelines for systematic quantification of accuracy in watershed simulations. *Transactions of the ASABE*, 50(3):885–900.

Mu, Q., Zhao, M., and Running, S. W. (2013). Modis global terrestrial evapotranspiration (et) product (nasa mod16a2/a3). *Algorithm Theoretical Basis Document, Collection*, 5.

Muller, E. and Décamps, H. (2001). Modeling soil moisture–reflectance. *Remote Sensing of Environment*, 76(2):173 – 180.

Muñoz, E., Arumí, J. L., Wagener, T., Oyarzún, R., and Parra, V. (2016). Unraveling complex hydrogeological processes in andean basins in south-central chile: An integrated assessment to understand hydrological dissimilarity. *Hydrological Processes*, 30(26):4934–4943.

Muttiah, R. S. and Wurbs, R. A. (2002). Scale-dependent soil and climate variability effects on watershed water balance of the swat model. *Journal of hydrology*, 256(3-4):264–285.

Nam, D. H., Udo, K., and Mano, A. (2013). Assessment of future flood intensification in central vietnam using a super-high-resolution climate model output. *Journal of Water and Climate Change*, 4(4):373–389.

Narasimhan, B., Srinivasan, R., Arnold, J., and Di Luzio, M. (2005). Estimation of long-term soil moisture using a distributed parameter hydrologic model and verification using remotely sensed data. *Transactions of the ASAE*, 48(3):1101–1113.

Nay-Htoon, B., Tung Phong, N., Schlüter, S., and Janaiah, A. (2013). A water productive and economically profitable paddy rice production method to adapt water scarcity in the vu gia-thu bon river basin, vietnam. *Journal of Natural Resources and Development*, 3(1):58–65.

Nayak, A. B. (2006). An analysis using liss iii data for estimating water demand for rice cropping in parts of hirakud command area, orissa, india. ITC.

Neitsch, S. L., Arnold, J. G., Kiniry, J. R., and Williams, J. R. (2011). Soil and water assessment tool theoretical documentation version 2009. Technical report, Texas Water Resources Institute.

Niehoff, D., Fritsch, U., and Bronstert, A. (2002). Land-use impacts on storm-runoff generation: scenarios of land-use change and simulation of hydrological response in a meso-scale catchment in sw-germany. *Journal of hydrology*, 267(1-2):80–93.

Nielsen, D. R., Biggar, J. W., and Erh, K. T. (1973). Spatial variability of field-measured soil-water properties. *Hilgardia*, 42(7):215–259.

Nihoul, J. C., Zavialov, P. O., and Micklin, P. P. (2012). *Dying and dead seas climatic versus anthropic causes*, volume 36. Springer Science & Business Media.

Ojha, C., Prasad, K., Shankar, V., and Madramootoo, C. (2009). Evaluation of a nonlinear root-water uptake model. *Journal of irrigation and drainage engineering*, 135(3):303–312.

Oki, T. and Kanae, S. (2006). Global hydrological cycles and world water resources. *science*, 313(5790):1068–1072.

O'Neill, P., Entekhabi, D., Njoku, E., and Kellogg, K. (2010). The nasa soil moisture active passive (smap) mission: Overview. In *2010 IEEE International Geoscience and Remote Sensing Symposium*, pages 3236–3239. IEEE.

Ongley, E. D. (2000). The yellow river: managing the unmanageable. *Water International*, 25(2):227–231.

Ozdogan, M., Yang, Y., Allez, G., and Cervantes, C. (2010). Remote sensing of irrigated agriculture: Opportunities and challenges. *Remote sensing*, 2(9):2274–2304.

Paloscia, S., Pettinato, S., Santi, E., Notarnicola, C., Pasolli, L., and Reppucci, A. (2013). Soil moisture mapping using sentinel-1 images: Algorithm and preliminary validation. *Remote Sensing of Environment*, 134:234–248.

Panagopoulos, Y., Makropoulos, C., Gkiokas, A., Kossida, M., Evangelou, L., Lourmas, G., Michas, S., Tsadilas, C., Papageorgiou, S., Perleros, V., Drakopoulou, S., and Mimikou, M. (2014). Assessing the cost-effectiveness of irrigation water management practices in water stressed agricultural catchments: the case of pinios. *Agricultural water management*, 139:31–42.

Parajka, J., Naeimi, V., Blöschl, G., Wagner, W., Merz, R., and Scipal, K. (2006). Assimilating scatterometer soil moisture data into conceptual hydrologic models at the regional scale. *Hydrology and Earth System Sciences Discussions*, 10(3):353–368.

Park, J.-Y., Ahn, S.-R., Hwang, S.-J., Jang, C.-H., Park, G.-A., and Kim, S.-J. (2014). Evaluation of modis ndvi and lst for indicating soil moisture of forest areas based on swat modeling. *Paddy and water environment*, 12(1):77–88.

Pauwels, V. R., Hoeben, R., Verhoest, N. E., and De Troch, F. P. (2001). The importance of the spatial patterns of remotely sensed soil moisture in the improvement of discharge predictions for small-scale basins through data assimilation. *Journal of Hydrology*, 251(1-2):88–102.

Pawar, G., Kale, M., and Lokhande, J. (2017). Response of aquacrop model to different irrigation schedules for irrigated cabbage. *Agricultural Research*, 6(1):73–81.

Peachey, E. J. (2004). The aral sea basin crisis and sustainable water resource management in central asia. *JOURNAL OF PUBLIC AND INTERNATIONAL AFFAIRS-PRINCETON-*, 15:1–20.

Peel, M. C., Finlayson, B. L., and McMahon, T. A. (2007). Updated world map of the köppen-geiger climate classification. *Hydrology and earth system sciences discussions*, 4(2):439–473.

Peña-Arancibia, J. L., Mainuddin, M., Kirby, J. M., Chiew, F. H., McVicar, T. R., and Vaze, J. (2016). Assessing irrigated agriculture's surface water and groundwater consumption by combining satellite remote sensing and hydrologic modelling. *Science of the Total Environment*, 542:372–382.

Pervez, M. S. and Brown, J. F. (2010). Mapping irrigated lands at 250-m scale by merging modis data and national agricultural statistics. *Remote Sensing*, 2(10):2388–2412.

Peters, A. (2016). Modified conceptual model for compensated root water uptake–a simulation study. *Journal of hydrology*, 534:1–10.

Phogat, V., Mahadevan, M., Skewes, M., and Cox, J. W. (2012). Modelling soil water and salt dynamics under pulsed and continuous surface drip irrigation of almond and implications of system design. *Irrigation Science*, 30(4):315–333.

Piani, C., Haerter, J., and Coppola, E. (2010a). Statistical bias correction for daily precipitation in regional climate models over europe. *Theoretical and Applied Climatology*, 99(1-2):187–192.

Piani, C., Weedon, G., Best, M., Gomes, S., Viterbo, P., Hagemann, S., and Haerter, J. (2010b). Statistical bias correction of global simulated daily precipitation and temperature for the application of hydrological models. *Journal of hydrology*, 395(3-4):199–215.

Plesca, I., Timbe, E., Exbrayat, J.-F., Windhorst, D., Kraft, P., Crespo, P., Vaché, K. B., Frede, H.-G., and Breuer, L. (2012). Model intercomparison to explore catchment functioning: Results from a remote montane tropical rainforest. *Ecological Modelling*, 239:3–13.

Polanco, E. I., Fleifle, A., Ludwig, R., and Disse, M. (2017). Improving swat model performance in the upper blue nile basin using meteorological data integration and subcatchment discretization. *Hydrology and Earth System Sciences*, 21(9):4907–4926.

Poveda, G., Waylen, P. R., and Pulwarty, R. S. (2006). Annual and inter-annual variability of the present climate in northern south america and southern mesoamerica. *Palaeogeography, Palaeoclimatology, Palaeoecology*, 234(1):3–27.

Rabiee, Z., Honar, T., and Kazemi, A. (2013). Optimal, simultaneous land and water allocation under resource limitation conditions, using soil water balance (case study of doroudzan dam irrigation and drainage network). *Journal of Irrigation and Drainage Engineering*, 05015008(8):1–10.

Rafiei Emam, A., Kappas, M., Linh, N., and Renchin, T. (2017). Hydrological modeling and runoff mitigation in an ungauged basin of central vietnam using swat model. *Hydrology*, 4(1):16.

Rajib, M. A., Merwade, V., and Yu, Z. (2016). Multi-objective calibration of a hydrologic model using spatially distributed remotely sensed/in-situ soil moisture. *Journal of hydrology*, 536:192–207.

Rallo, G., Agnese, C., Minacapilli, M., and Provenzano, G. (2012). Comparison of swap and fao agro-hydrological models to schedule irrigation of wine grapes. *Journal of Irrigation and Drainage Engineering*, 138(7):581–591.

Refsgaard, J., Jakonsen, R., Hansen, A., Hojberg, A., Zurek, A., Rozanski, K., Witczak, S., Wachniew, Donnely, C., Capell, R., Bartosova, Strömqvist, J., Wörman, A., and Moren, I. (2016). *Upscaling Methodologies, SOILS2SEA DELIVERABLE NO. 3.2.* Geological Survey of Denmark and Greenland.

Refsgaard, J. C. (1997). Parameterisation, calibration and validation of distributed hydrological models. *Journal of hydrology*, 198(1-4):69–97.

Richards, L. and Gardner, W. (1936). Tensiometers for measuring the capillary tension of soil water. *Journal of the American Society of Agronomy*.

Rinaldi, M. (2001). Application of epic model for irrigation scheduling of sunflower in southern italy. *Agricultural Water Management*, 49(3):185–196.

Rockström, J. and Falkenmark, M. (2000). Semiarid crop production from a hydrological perspective gap between potential and actual yields. *Critical Reviews in Plant Science*, 19(4):319–346.

Rodell, M., Velicogna, I., and Famiglietti, J. S. (2009). Satellite-based estimates of groundwater depletion in india. *Nature*, 460(7258):999.

Romaguera, M., Krol, M. S., Salama, M., Hoekstra, A. Y., and Su, Z. (2012). Determining irrigated areas and quantifying blue water use in europe using remote sensing meteosat second generation (msg) products and global land data assimilation system (gldas) data. *Photogrammetric Engineering & Remote Sensing*, 78(8):861–873.

Rosegrant, M. W., Ringler, C., and Zhu, T. (2009). Water for agriculture: maintaining food security under growing scarcity. *Annual review of Environment and resources*, 34:205–222.

Saha, S., Moorthi, S., Pan, H.-L., Wu, X., Wang, J., Nadiga, S., Tripp, P., Kistler, R., Woollen, J., Behringer, D., Liu, H., Stokes, D., Grumbine, R., Gayno, G., Wang, J., Hou, Y., Chuang, H., Juang, H., Sela, J., Iredell M, Treadon, R., Kleist, D., Delst, P., Keyser, D., Derber, J., Ek, M., Meng, J., Wei, H., Yang, R., Lord, S., Dool, H., Kumar, A., Wang, W., Long, C., Chelliah, M., Xue, Y., Huang, B., Schemm, J., Ebisuzaki, W., Lin, R., Xie, P., Chen, M., Zhou, S., Higgins, W., Zou, C., Liu, Q., Chen, Y., Han, Y., Cucurull, L., Reynolds, R, R. G., and Goldberg, M. (2010). The ncep climate forecast system reanalysis. *Bulletin of the American Meteorological Society*, 91(8):1015–1058.

Sandholt, I., Rasmussen, K., and Andersen, J. (2002). A simple interpretation of the surface temperature/vegetation index space for assessment of surface moisture status. *Remote Sensing of environment*, 79(2-3):213–224.

Santhi, C., Muttiah, R., Arnold, J., and Srinivasan, R. (2005). A gis-based regional planning tool for irrigation demand assessment and savings using swat. *Transactions of the ASAE*, 48(1):137–147.

Scanlon, B., Jolly, I., Sophocleous, M., and Zhang, L. (2007). Global impacts of conversions from natural to agricultural ecosystems on water resources: Quantity versus quality. *Water Resources Research*, 43(3):1–18.

Scanlon, B. R., Faunt, C. C., Longuevergne, L., Reedy, R. C., Alley, W. M., McGuire, V. L., and McMahon, P. B. (2012). Groundwater depletion and sustainability of irrigation in the us high plains and central valley. *Proceedings of the national academy of sciences*, 109(24):9320–9325.

Schaap, M. G., Leij, F. J., and Van Genuchten, M. T. (2001). Rosetta: A computer program for estimating soil hydraulic parameters with hierarchical pedotransfer functions. *Journal of hydrology*, 251(3-4):163–176.

Schmugge, T. (1978). Remote sensing of surface soil moisture. *Journal of Applied Meteorology*, 17(10):1549–1557.

Schmugge, T., Gloersen, P., Wilheit, T., and Geiger, F. (1974). Remote sensing of soil moisture with microwave radiometers. *Journal of Geophysical Research*, 79(2):317–323.

Schmugge, T., Jackson, T., and McKim, H. (1980). Survey of methods for soil moisture determination. *Water Resources Research*, 16(6):961–979.

Schulla, J. and Jasper, K. (2007). Model description wasim-eth. *Institute for Atmospheric and Climate Science, Swiss Federal Institute of Technology, Zürich.*

Schultz, G. A. (1988). Remote sensing in hydrology. *Journal of Hydrology*, 100(1-3):239–265.

Scott, C. A., Bastiaanssen, W. G. M., and ud Din Ahmad, M. (2003). Mapping root zone soil moisture using remotely sensed optical imagery. *Journal of Irrigation and Drainage Engineering*, 129(5):326–335.

Searcy, J. K., Hardison, C. H., and Langbein, W. B. (1960). *Double-mass Curves: Manual of Hydrology: Part 1. General Surface-water Techniques.* US Government Printing Office.

Seidel, S., Werisch, S., Schütze, N., and Laber, H. (2017). Impact of irrigation on plant growth and development of white cabbage. *Agricultural water management*, 187:99–111.

Seidel, S. J., Werisch, S., Barfus, K., Wagner, M., Schütze, N., and Laber, H. (2016). Field evaluation of irrigation scheduling strategies using a mechanistic crop growth model. *Irrigation and Drainage*, 65(2):214–223.

Seneviratne, S. I., Corti, T., Davin, E. L., Hirschi, M., Jaeger, E. B., Lehner, I., Orlowsky, B., and Teuling, A. J. (2010). Investigating soil moisture–climate interactions in a changing climate: A review. *Earth-Science Reviews*, 99(3-4):125–161.

Shafiei, M., Ghahraman, B., Saghafian, B., Davary, K., Pande, S., and Vazifedoust, M. (2014). Uncertainty assessment of the agro-hydrological swap model application at field scale: A case study in a dry region. *Agricultural Water Management*, 146:324 – 334.

Sharpley, A. and Williams, J. (1990). Epic-erosion/productivity impact calculator: 1. *Model documentation.*

Shelia, V., Šimøunek, J., Boote, K., and Hoogenbooom, G. (2018). Coupling dssat and hydrus-1d for simulations of soil water dynamics in the soil-plant-atmosphere system. *Journal of Hydrology and Hydromechanics*, 66(2):232–245.

Shen, Y., Li, S., Chen, Y., Qi, Y., and Zhang, S. (2013). Estimation of regional irrigation water requirement and water supply risk in the arid region of northwestern china 1989–2010. *Agricultural Water Management*, 128:55–64.

Shrestha, S., Deb, P., and Bui, T. T. T. (2016). Adaptation strategies for rice cultivation under climate change in central vietnam. *Mitigation and Adaptation Strategies for Global Change*, 21(1):15–37.

Siebert, S., Döll, P., Hoogeveen, J., Faures, J. M., Frenken, K., and Feick, S. (2000). Development and validation of the global map of irrigation areas. *Hydrology and Earth System Sciences Discussions*, 2(4):1299–1324.

Singh, R., Kroes, J., Van Dam, J., and Feddes, R. (2006). Distributed ecohydrological modelling to evaluate the performance of irrigation system in sirsa district, india: I. current water management and its productivity. *Journal of Hydrology*, 329(3-4):692–713.

Sivapalan, M., Takeuchi, K., Franks, S., Gupta, V., Karambiri, H., Lakshmi, V., Liang, X., McDonnell, J., Mendiondo, E., and O'connell, P. (2003). Iahs decade on predictions in ungauged basins (pub), 2003–2012: Shaping an exciting future for the hydrological sciences. *Hydrological sciences journal*, 48(6):857–880.

Sloan, P. G. and Moore, I. D. (1984). Modeling subsurface stormflow on steeply sloping forested watersheds. *Water Resources Research*, 20(12):1815–1822.

Smith, M. (1992). *CROPWAT: A computer program for irrigation planning and management*. Number 46. Food & Agriculture Org.

Stammerjohn, S. E., Martinson, D. G., Smith, R. C., and Iannuzzi, R. A. (2008). Sea ice in the western antarctic peninsula region: Spatio-temporal variability from ecological and climate change perspectives. *Deep Sea Research Part II: Topical Studies in Oceanography*, 55(18-19):2041–2058.

Steduto, P., Hsiao, T. C., Raes, D., and Fereres, E. (2009). Aquacrop—the fao crop model to simulate yield response to water: I. concepts and underlying principles. *Agronomy Journal*, 101(3):426–437.

Steele, D. D., Thoreson, B. P., Hopkins, D. G., Clark, B. A., Tuscherer, S. R., and Gautam, R. (2015). Spatial mapping of evapotranspiration over devils lake basin with sebal: application to flood mitigation via irrigation of agricultural crops. *Irrigation science*, 33(1):15–29.

Stehr, A., Debels, P., Arumi, J. L., Romero, F., and Alcayaga, H. (2009). Combining the soil and water assessment tool (swat) and modis imagery to estimate monthly flows in a data-scarce chilean andean basin. *Hydrological sciences journal*, 54(6):1053–1067.

Stricevic, R., Cosic, M., Djurovic, N., Pejic, B., and Maksimovic, L. (2011). Assessment of the fao aquacrop model in the simulation of rainfed and supplementally irrigated maize, sugar beet and sunflower. *Agricultural Water Management*, 98(10):1615–1621.

Sun, H.-Y., Liu, C.-M., Zhang, X.-Y., Shen, Y.-J., and Zhang, Y.-Q. (2006). Effects of irrigation on water balance, yield and wue of winter wheat in the north china plain. *Agricultural Water Management*, 85(1):211 – 218.

Sun, L., Seidou, O., Nistor, I., Goïta, K., and Magagi, R. (2016). Simultaneous assimilation of in situ soil moisture and streamflow in the swat model using the extended kalman filter. *Journal of Hydrology*, 543:671–685.

Surendran, U., Sushanth, C., Mammen, G., and Joseph, E. (2017). Fao-cropwat model-based estimation of crop water need and appraisal of water resources for sustainable water resource management: Pilot study for kollam district-humid tropical region of kerala, india. *Current Science (00113891)*, 112(1).

Tang, Q., Peterson, S., Cuenca, R. H., Hagimoto, Y., and Lettenmaier, D. P. (2009). Satellite-based near-real-time estimation of irrigated crop water consumption. *Journal of Geophysical Research: Atmospheres*, 114(D5).

Tavakoli, M. and De Smedt, F. (2013). Validation of soil moisture simulation with a distributed hydrologic model (wetspa). *Environmental earth sciences*, 69(3):739–747.

Taylor, H. M., Roberson, G. M., and Parker Jr, J. J. (1966). Soil strength-root penetration relations for medium-to coarse-textured soil materials. *Soil science*, 102(1):18–22.

Teixeira, A. d. C., Bastiaanssen, W., Ahmad, M., and Bos, M. (2009). Reviewing sebal input parameters for assessing evapotranspiration and water productivity for the low-middle sao francisco river basin, brazil: Part a: Calibration and validation. *agricultural and forest meteorology*, 149(3-4):462–476.

Teuling, A. J. and Troch, P. A. (2005). Improved understanding of soil moisture variability dynamics. *Geophysical Research Letters*, 32(5).

Teutschbein, C. and Seibert, J. (2010). Regional climate models for hydrological impact studies at the catchment scale: a review of recent modeling strategies. *Geography Compass*, 4(7):834–860.

Thenkabail, P. S., Biradar, C. M., Noojipady, P., Dheeravath, V., Li, Y., Velpuri, M., Gumma, M., Gangalakunta, O. R. P., Turral, H., Cai, X., Vithanage, J., Schull, M. A., and Dutta, R. (2009). Global irrigated area map (giam), derived from remote sensing, for the end of the last millennium. *International Journal of Remote Sensing*, 30(14):3679–3733.

Thi Ut, T. and Kajisa, K. (2006). The impact of green revolution on rice production in vietnam. *The Developing Economies*, 44(2):167–189.

Thrasher, B., Maurer, E. P., Duffy, P. B., and McKellar, C. (2012). Bias correcting climate model simulated daily temperature extremes with quantile mapping.

Timm, L. C., Pires, L. F., Roveratti, R., Arthur, R. C. J., Reichardt, K., Oliveira, J. C. M. d., and Bacchi, O. O. S. (2006). Field spatial and temporal patterns of soil water content and bulk density changes. *Scientia Agricola*, 63(1):55–64.

Topp, G. C., Davis, J. L., and Annan, A. P. (1980). Electromagnetic determination of soil water content: Measurements in coaxial transmission lines. *Water Resources Research*, 16(3):574–582.

Tourian, M., Elmi, O., Chen, Q., Devaraju, B., Roohi, S., and Sneeuw, N. (2015). A spaceborne multisensor approach to monitor the desiccation of lake urmia in iran. *Remote Sensing of Environment*, 156:349–360.

Tromp-van Meerveld, H. and McDonnell, J. (2006). On the interrelations between topography, soil depth, soil moisture, transpiration rates and species distribution at the hillslope scale. *Advances in Water Resources*, 29(2):293–310.

Tung, Y.-K. (2011). Uncertainty and reliability analysis in water resources engineering. *Journal of Contemporary Water Research and Education*, 103(1):13–21.

Udias, A., Pastori, M., Malago, A., Vigiak, O., Nikolaidis, N. P., and Bouraoui, F. (2018). Identifying efficient agricultural irrigation strategies in crete. *Science of the Total Environment*, 633:271–284.

Uniyal, B. and Dietrich, J. (2019a). Dataset: Soil moisture measuring campaign ilmenau 2016/2017. soil moisture data published, `https://doi.org/10.25835/0036557`.

Uniyal, B. and Dietrich, J. (2019b). Modifying automatic irrigation in swat for plant water stress scheduling. *Agricultural Water Management*, 223(105714):1–12.

Uniyal, B., Dietrich, J., Vasilakos, C., and Ourania, T. (2017). Evaluation of swat simulated soil moisture at catchment scale by field measurements and landsat derived indices. *Agricultural Water Management*, 193:55–70.

Uniyal, B., Dietrich, J., Vu, N. Q., Jha, M. K., and Arumi, J. L. (2019). Simulation of regional irrigation requirement with swat in different agro-climatic zones driven by observed climate and two reanalysis datasets. *Science of Total Environment*, 649:846–865.

Van Dam, J., Huygen, J., Wesseling, J., Feddes, R., Kabat, P., Van Walsum, P., Groenendijk, P., and Van Diepen, C. (1997). Theory of swap version 2.0; simulation of water flow, solute transport and plant growth in the soil-water-atmosphere-plant environment. Technical report, DLO Winand Staring Centre.

Van Diepen, C. v., Wolf, J., Van Keulen, H., and Rappoldt, C. (1989). Wofost: a simulation model of crop production. *Soil use and management*, 5(1):16–24.

Van Niel, T. and McVicar, T. (2004). Current and potential uses of optical remote sensing in rice-based irrigation systems: a review. *Australian Journal of Agricultural Research*, 55(2):155–185.

Varis, O., Kajander, T., and Lemmelä, R. (2004). Climate and water: from climate models to water resources management and vice versa. *Climatic Change*, 66(3):321–344.

Vazifedoust, M., Van Dam, J., Bastiaanssen, W., and Feddes, R. (2009). Assimilation of satellite data into agrohydrological models to improve crop yield forecasts. *International Journal of Remote Sensing*, 30(10):2523–2545.

Vereecken, H., Huisman, J., Pachepsky, Y., Montzka, C., Van Der Kruk, J., Bogena, H., Weihermüller, L., Herbst, M., Martinez, G., and Vanderborght, J. (2014). On the spatio-temporal dynamics of soil moisture at the field scale. *Journal of Hydrology*, 516:76–96.

Vereecken, H., Kamai, T., Harter, T., Kasteel, R., Hopmans, J., and Vanderborght, J. (2007). Explaining soil moisture variability as a function of mean soil moisture: A stochastic unsaturated flow perspective. *Geophysical Research Letters*, 34(22).

Verma, A. K. and Jha, M. K. (2015). Evaluation of a gis-based watershed model for streamflow and sediment-yield simulation in the upper baitarani river basin of eastern india. *Journal of Hydrologic Engineering*, 20(6):C5015001.

Vervoort, R. W., Miechels, S. F., van Ogtrop, F. F., and Guillaume, J. H. (2014). Remotely sensed evapotranspiration to calibrate a lumped conceptual model: Pitfalls and opportunities. *Journal of hydrology*, 519:3223–3236.

Vidal, I., Longeri, L., and Hétier, J. M. (1999). Nitrogen uptake and chlorophyll meter measurements in spring wheat. *Nutrient Cycling in Agroecosystems*, 55(1):1–6.

Vivoni, E. R., Rango, A., Anderson, C. A., Pierini, N. A., Schreiner-McGraw, A. P., Saripalli, S., and Laliberte, A. S. (2014). Ecohydrology with unmanned aerial vehicles. *Ecosphere*, 5(10):1–14.

Wada, Y., Wisser, D., Eisner, S., Flörke, M., Gerten, D., Haddeland, I., Hanasaki, N., Masaki, Y., Portmann, F. T., Stacke, T., Tessler, Z., and Schewe, J. (2013). Multimodel projections and uncertainties of irrigation water demand under climate change. *Geophysical Research Letters*, 40(17):4626–4632.

Walker, J. P., Willgoose, G. R., and Kalma, J. D. (2001). One-dimensional soil moisture profile retrieval by assimilation of near-surface observations: a comparison of retrieval algorithms. *Advances in Water Resources*, 24(6):631–650.

Walker, W., Prajamwong, S., Allen, R., and Merkley, G. (1995). Usu command area decision support model—cadsm. *Crop-water-simulation models in practice. Wageningen Pers, Wageningen*, pages 231–271.

Wanders, N., Karssenberg, D., Roo, A. d., De Jong, S., and Bierkens, M. (2014). The suitability of remotely sensed soil moisture for improving operational flood forecasting. *Hydrology and Earth System Sciences*, 18(6):2343–2357.

Wang, X., Xie, H., Guan, H., and Zhou, X. (2007). Different responses of modis-derived ndvi to root-zone soil moisture in semi-arid and humid regions. *Journal of hydrology*, 340(1-2):12–24.

Wang, X. L., Swail, V. R., and Zwiers, F. W. (2006). Climatology and changes of extratropical cyclone activity: Comparison of era-40 with ncep–ncar reanalysis for 1958–2001. *Journal of Climate*, 19(13):3145–3166.

Wang, Y., Chen, Y., and Peng, S. (2011). A gis framework for changing cropping pattern under different climate conditions and irrigation availability scenarios. *Water resources management*, 25(13):3073–3090.

Webber, H., Gaiser, T., Oomen, R., Teixeira, E., Zhao, G., Wallach, D., Zimmermann, A., and Ewert, F. (2016). Uncertainty in future irrigation water demand and risk of crop failure for maize in europe. *Environmental Research Letters*, 11(7):074007.

Wei, M.-Y. (1995). Soil moisture: Report of a workshop held in tiburon, california, 25-27 january 1994. In *NASA conference publication (USA)*. NASA Headquarters.

Wei, X., Bailey, R. T., and Tasdighi, A. (2018). Using the swat model in intensively managed irrigated watersheds: Model modification and application. *Journal of Hydrologic Engineering*, 23(10):1–17.

Wessolek, G., K. M. R. M. (2009). *Bodenökologie und Bodengenese.* Technische UniversitätBerlin,.

Western, A. W., Grayson, R. B., Blöschl, G., Willgoose, G. R., and McMahon, T. A. (1999). Observed spatial organization of soil moisture and its relation to terrain indices. *Water resources research*, 35(3):797–810.

Williams, J., Jones, C., Kiniry, J., and Spanel, D. A. (1989a). The epic crop growth model. *Transactions of the ASAE*, 32(2):497–0511.

Williams, J., Jones, C., Kiniry, J., and Spanel, D. A. (1989b). The epic crop growth model. *Transactions of the ASAE*, 32(2):497–0511.

Williams, J. R. (1990). The erosion-productivity impact calculator (epic) model: a case history. *Philosophical Transactions of the Royal Society of London. Series B: Biological Sciences*, 329(1255):421–428.

Wisser, D., Frolking, S., Douglas, E. M., Fekete, B. M., Vörösmarty, C. J., and Schumann, A. H. (2008). Global irrigation water demand: Variability and uncertainties arising from agricultural and climate data sets. *Geophysical Research Letters*, 35(24):1–5.

Wittenberg, H. (2003). Effects of season and man-made changes on baseflow and flow recession: case studies. *Hydrological Processes*, 17(11):2113–2123.

Wittenberg, H. (2015). Groundwater abstraction for irrigation and its impacts on low flows in a watershed in northwest germany. *Resources*, 4(3):566–576.

Woznicki, S. A., Nejadhashemi, A. P., and Parsinejad, M. (2015). Climate change and irrigation demand: Uncertainty and adaptation. *Journal of Hydrology: Regional Studies*, 3:247–264.

Xie, X. and Cui, Y. (2011). Development and test of swat for modeling hydrological processes in irrigation districts with paddy rice. *Journal of Hydrology*, 396(1-2):61–71.

Xin, J., Tian, G., Liu, Q., and Chen, L. (2006). Combining vegetation index and remotely sensed temperature for estimation of soil moisture in china. *International Journal of Remote Sensing*, 27(10):2071–2075.

Zappa, M. and Gurtz, J. (2003). Simulation of soil moisture and evapotranspiration in a soil profile during the 1999 map-riviera campaign. *Hydrology and Earth System Sciences Discussions*, 7(6):903–919.

Zaussinger, F., Dorigo, W., Gruber, A., Tarpanelli, A., Filippucci, P., and Brocca, L. (2019). Estimating irrigation water use over the contiguous united states by combining satellite and reanalysis soil moisture data. *Hydrology and Earth System Sciences*, 23(2):897–923.

Zhang, C., Liu, J., Shang, J., and Cai, H. (2018). Capability of crop water content for revealing variability of winter wheat grain yield and soil moisture under limited irrigation. *Science of the Total Environment*, 631:677–687.

Zhang, D. and Zhou, G. (2016). Estimation of soil moisture from optical and thermal remote sensing: A review. *Sensors*, 16(8):1308.

Zhang, Y., Chiew, F. H., Zhang, L., and Li, H. (2009). Use of remotely sensed actual evapotranspiration to improve rainfall–runoff modeling in southeast australia. *Journal of Hydrometeorology*, 10(4):969–980.

Zhu, T., Ringler, C., and Rosegrant, M. W. (2018). Viewing agricultural water management through a systems analysis lens. *Water Resources Research*.

Zreda, M., Desilets, D., Ferré, T. P. A., and Scott, R. L. (2008). Measuring soil moisture content non-invasively at intermediate spatial scale using cosmic-ray neutrons. *Geophysical Research Letters*, 35(21):1–5.

Zucco, G., Brocca, L., Moramarco, T., and Morbidelli, R. (2014). Influence of land use on soil moisture spatial–temporal variability and monitoring. *Journal of hydrology*, 516:193–199.

Zuo, D., Xu, Z., Peng, D., Song, J., Cheng, L., Wei, S., Abbaspour, K. C., and Yang, H. (2015). Simulating spatiotemporal variability of blue and green water resources availability with uncertainty analysis. *Hydrological Processes*, 29(8):1942–1955.

Zwart, S. J. and Bastiaanssen, W. G. (2007). Sebal for detecting spatial variation of water productivity and scope for improvement in eight irrigated wheat systems. *Agricultural water management*, 89(3):287–296.